SEDIMENTOLOGY OF THE BASAL STODDART FORMATION

(UPPER MISSISSIPPIAN) IN THE AREA OF

JOSEPHINE FIELD, NORTHWEST ALBERTA

LICENCE TO McMASTER UNIVERSITY

This _____ Thesis _____ has been written
           [Thesis, Project Report, etc.]

by _____ Robert Blair Hrabi _____ for
           [Full Name(s)]
Undergraduate course number ___ 4K6 ___ at McMaster
University under the supervision/direction of _____
_____ Dr. R. G. Walker _____ .

In the interest of furthering teaching and research, I/we
hereby grant to McMaster University:

1. The ownership of __2__ copy(ies) of this
    work;
2. A non-exclusive licence to make copies of
    this work, (or any part thereof) the
    copyright of which is vested in me/us, for
    the full term of the copyright, or for so
    long as may be legally permitted. Such
    copies shall only be made in response to a
    written request from the Library or any
    University or similar institution.

I/we further acknowledge that this work (or a surrogate
copy thereof) may be consulted without restriction by any
interested person.

_____   _____
Signature of Witness,   Signature of Student
Supervisor

April 28, 1987
date

(This Licence to be bound with the work)

SEDIMENTOLOGY OF THE BASAL STODDART FORMATION

(UPPER MISSISSIPPIAN) IN THE AREA OF

JOSEPHINE FIELD, NORTHWEST ALBERTA

by

ROBERT BLAIR HRABI

A Thesis

Submitted to the Department of Geology

in Partial Fulfillment of the Requirements

for the Degree

Honours Bachelor of Science

McMaster University

April, 1987

Honours Bachelor of Science   McMaster University

(Geology)   Hamilton, Ontario

TITLE: Sedimentology of the basal Stoddart Formation

        (Upper Mississippian) in the area of

        Josephine Field, northwest Alberta

AUTHOR: Robert Blair Hrabi

SUPERVISOR: Dr. R. G. Walker

NUMBER OF PAGES: ix, 115

ABSTRACT

A sedimentogical and petrological examination of the basal sands of the Stoddart Formation in the area of Josephine field has been undertaken. The determination of the depositiional environment and the history of sedimentation of the basal Stoddart sands are the objectives of this study.

The thick sands at the base of the Stoddart Formation which have a blocky gamma ray response consist of fine-grained sandstone dominated by angle of repose cross-bedding. The sedimentary structures, stratification types, composition and facies relationships of these sands indicate that they are of a coastal aeolian origin.

The compositional, textural and surface texture characteristics of these sands were studied under petrographic, cathodolumenescent and scanning electron microscopes. Observations indicate that the above criteria can be used to support the interpretation of an aeolian origin for the cross-bedded sands of the basal Stoddart Formation.

The sands of the basal Stoddart show rapid transitions between sub-aerial and marine environments. These rapid changes are believed to be caused by sudden sea level fluctuations resulting from movement of reactivated faults in the Peace River arch area.

ACKNOWLEDGEMENTS

TABLE OF CONTENTS

LIST OF FIGURES

LIST OF PLATES

LIST OF TABLES

CHAPTER ONE

INTRODUCTION

1.1 Statement of Problem and Objectives

This thesis represents the result of an integrated facies and petrologic study of the basal deposits of the Stoddart Formation (terminology of Rutgers, 1958 and Macauley et al., 1964) of Mississippian (Chesterian) age. The study was done in the area of Josephine Field, N.W. Alberta (Township 83, Range 9, West 6) (Figure 1.1) which was discovered in March and April of 1974 (11-17-83-9W6 well) and has initial established reserves of 1562 million cubic metres gas and 3000 cubic metres oil.

The basal portion of the Stoddart Formation generally consists of a thick sequence of green to black fissile shale, overlain by interfingered shale, siltstones and mature, quartzose to calcareous sandstones. The mature quartzose sands at the base of the formation produce substantial quantities of gas and minor amounts of oil in the Peace River area of N.W. Alberta and N.E. British Columbia.

Two problems are associated with these sands: the first is that the sand bodies show rapid lateral variability and discontinuity, making correlation and economic exploration of these sands very difficult; and secondly, no detailed sedimentological study, defining environment of deposition

Figure 1.1   Location of Josephine Field area in
              northwest Alberta near Peace River.

LOCATION MAP

STUDY AREA

Alberta

Edmonton o

o Calgary

0 _____ 250km

Josephine Field

T84

T83

T82

RIO

RO9

RO8W6
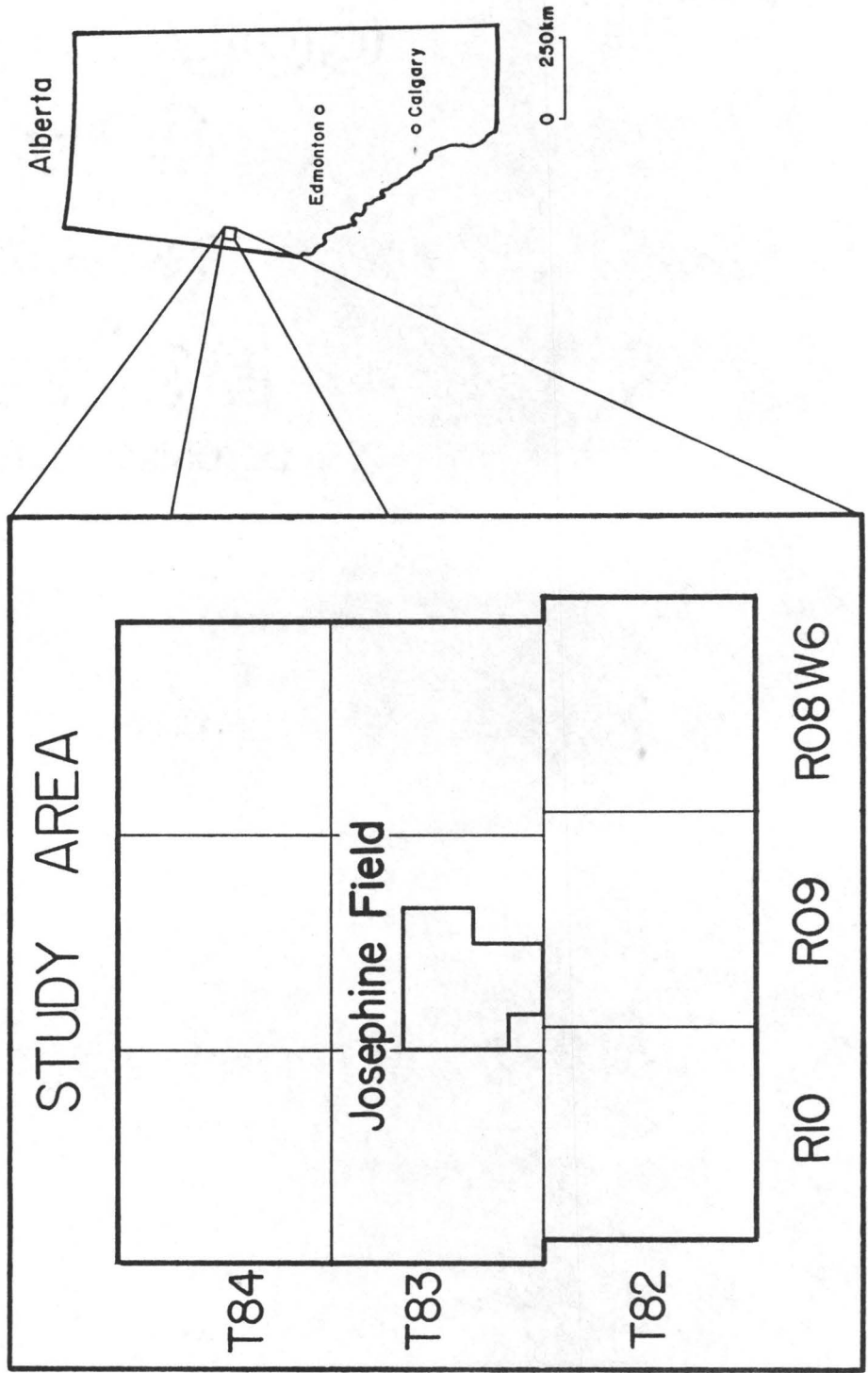
or sedimentation patterns within the basal portions of the Stoddart Formation, has ever been published.

Fourteen cores and all petrophysical logs (60) were examined within the nine townships including and surrounding the Josephine Field in Township 83, Range 9, West 6. This compact area had the advantage of allowing an integrated approach to the study as opposed to separate petrologic and environmental studies.

The primary aim of this project is to describe and interpret the facies of the basal portion of the Stoddart Formation, to assimilate these into an overall depositional environment and to describe the changes in sedimentation through time. This will be accomplished by interpreting the facies and facies sequences present in the core within the study area. These interpretations will be used to characterize the gamma ray log response within individual facies and facies sequences so that the interpretation of sedimentary environment can be extended to parts of the study area where core control is non-existent. In addition, various lithologies in the basal portion of the Stoddart Formation were observed under petrographic microscope, cathodoluminescent microscope and scanning electron microscope, to determine if any evidence was present to substantiate the environmental interpretation.

The secondary aim of the project is to apply the
interpretations made to the problem of understanding the
lateral facies transitions, so that better correlation of the
different facies can be made in the future. It is hoped that
this will also improve the ability to locate
stratigraphically trapped hydrocarbon reservoirs in the main
sands of the basal Stoddart Formation. Additional work of a
similar nature must be done in nearby fields in order to
reconstruct the overall paleogeography of the Peace River
area during the Mississippian Chester period. It might then
be possible to determine if the movements of the Peace River
Arch had any affect on the deposition of the main quartzose
sands and thus the distribution of hydrocarbons in this area.

1.2 Geologic and Tectonic Setting

The Mississippian-Pennsylvanian Stoddart Formation is a
small part of a thick Paleozoic succession of carbonates,
shales and mature sandstones. The general patterns of
sedimentation of the Paleozoic section have been governed by
repeatedly renewed faults and differential movement of the
basement (Sikabonyi and Rodgers, 1959) which was active
during sedimentation.

To the south, the Mississippian through Middle Triassic
lithological assemblage of the Rocky Mountain Belt is

interpreted to have been deposited in a relatively stable shelf-slope environment (Monger et al., 1972) with a continental margin generally shown to have a NNW-SSE trend (Monger et al., 1972). A large part of the northern half of the West Canadian Basin was a shallow basin surrounded by three prominent, block faulted, positive features: the Peace River uplift; the Fort Nelson uplift and the Tathlina Lake uplift.

The area in which this study was carried out is situated on the north-west flank of the Peace River Arch. Until the Upper Devonian, the Arch was a low lying positive landmass characterized by a system of fault scarps and folds similar to those of the Canadian Shield (Lavoie, 1958). During the Upper Devonian, Wabamun sediments onlapped the landmass and eventually covered it.

The tectonic regime slowly changed during deposition of the Banff Formation and Rundle Group. Lavoie (1958) believed that the increase in thickness of the Banff Formation and Rundle Group over the Peace River Arch was due to slow subsidence along reactivated basement faults. Sikabonyi and Rodgers (1959) believe that the difference in thickness is due to fault induced erosion occurring after deposition of these sediments. The fact that the transition from Debolt Formation carbonates (top of Rundle Group) changes from conformable in the Peace River area to unconformable farther to the east (Halbertsma, 1959) corresponding with the

decrease in isopach thickness indicates the thickness change is a result of erosional rather than depositional variations.

Lavoie (1958) felt that faulting prior to and during Stoddart Formation deposition is the major cause of the tremendous variation in the Stoddart Formation thickness, and that it is highly unlikely that faulting and subsequent erosion occurred after deposition of this unit. Most other workers (Macauley, 1958; Rutgers, 1958; Halbertsma, 1959; Sikabonyi and Rodgers, 1959; Macauley et al., 1964) believe that a major unconformity and erosion surface exists at the Stoddart Group-Belloy Formation boundary from which thousands of feet of section were removed in some areas. The Permian Belloy sediments were then deposited on this peneplained surface.

In general, subsurface studies of the Carboniferous indicate a relatively stable, shallow basin environment (Macauley et al., 1964) from late Devonian until late Mississippian. The deposition of the Stoddart Group marks an abrupt change in sedimentation. Initially, fine marine clastics conformably overlie the Debolt carbonates. Periods of regression and transgression are indicated by repeated introduction of coarse clastic facies within the Kiskatinaw interval. A return to shallow marine basinal conditions is indicated only in the uppermost Taylor Flat carbonate interval of the Stoddart Formation (Macauley et al., 1964).

1.3 Stratigraphy and Biostratigraphy

The Stoddart Formation was first named by Rutgers (1958) who included all rocks from the Mississippian Debolt carbonates below to the then named Permo-Pennsylvanian beds. In the type section (Pacific Fort St. John No. 23 gas well; 3-29-83-18W6), Rutgers (1958) divided the formation into two informal members; a lower predominantly clastic section and an upper carbonate section. No age determinations could be done on the fossil fragments found in the unit. Rutgers, basing his conclusions on the stratigraphic position of the unit between beds of relatively certain age, believed the Stoddart Formation was Mississippian or younger and at least older than Triassic and possibly pre-Pennsylvanian.

Halbertsma (1959) raised the Stoddart to group status and defined three formations within this group. In ascending order, the Golata is dominantly shale, the Kiskatinaw is a mixed sand and shale unit and the uppermost Taylor Flat is a carbonate unit. Halbertsma (1959) also published the first faunal determinations from this section which were substantiated by later work (Halbertsma and Staplin, 1960). The ages determined for the sections were based largely on plant spores. In summary, the Golata was found to be Mississippian (Chesterian). Chesterian plant spores were also found close to the base of the Kiskatinaw. Pennsylvanian plant spores were found in the middle of the Taylor Flat interval, and the Permo-Pennsylvanian beds,

renamed the Belloy Formation (Halbertsma, 1959), contained
Permian plant spores.

Halbertsma and Staplin (1960) felt that the Taylor Flat-
Kiskatinaw boundary was unconformable and represented the
Mississippian-Pennsylvanian time break. Macauley (1958) and
Rutgers (1958) both believed this was only a facies contact.
Halbertsma (1961) later proposed that the Floral Group be
established to include the Kiskatinaw and Golata Formations,
as the contact between the two was difficult to define in
many areas. The Formational nomenclature of the Peace River
area is given in Figure 1.2.

In the area of this study, the basal sand which defines
the Kiskatinaw-Golata boundary is laterally discontinuous and
the transition from Kiskatinaw to Taylor Flat has extensive
interfingering of carbonates and clastics and is arbitrarily
defined in a number of areas. In addition, the exact
position of the Mississsippian-Pennsylvanian contact has not
been determined despite Halbertsma and Staplin's belief that
the Kiskatinaw-Taylor Flat transition represented this time
break. Therefore, the Golata-Kiskatinaw-Taylor Flat
subdivisions of Halbertsma (1959) do not possess the
necessary mapping qualities to be recognized as formations
and can only be considered as facies or members of the
Stoddart Formation. Macauley et al. (1964) recognize these
drawbacks in giving the Stoddart group status. They leave
the Stoddart as a formation but realizing the common use of

Figure 1.2   Comparison of Formational nomenclature

of Late Paleozoic sediments, Peace

River area, northwest Alberta.

MACAULEY ET AL. (1964) AND THIS THESIS			RUTGERS (1958)		HALBERTSMA AND STAPLIN (1960)			HALBERTSMA (1961)		
PERMIAN		BELLOY FORMATION	PERMIAN	'PERMO-PENN'	PERMIAN		BELLOY FORMATION	PERMIAN		BELLOY FORMATION
PENNSYLVANIAN	MORROMAN?	TAYLOR FLAT	MISSISSIPPIAN?	UPPER CARBONATE	PENNSYLVANIAN	MORROMAN?	TAYLOR FLAT FORMATION	PENNSYLVANIAN	MORROMAN?	TAYLOR FLAT FORMATION
MISSISSIPPIAN	CHESTERIAN	STODDART FORMATION — KISKATINAW		STODDART FORMATION — LOWER CLASTIC	MISSISSIPPIAN	CHESTERIAN	STODDART GROUP — KISKATINAW FORMATION	MISSISSIPPIAN	CHESTERIAN	FLORAL GROUP — KISKATINAW FORMATION
		GOLATA					GOLATA FORMATION			GOLATA FORMATION
	MERAMEC	RUNDLE	DEBOLT FORMATION	MISS	DEBOLT FORMATION		MERAMEC	RUNDLE	DEBOLT FORMATION	MERAMEC RUNDLE DEBOLT FORMATION

Golata-Kiskatinaw-Taylor Flat terminology, they retain these
to describe generalized intervals. Since this study is only
concerned with the lowest portion of the clastic sequence in
the Stoddart Formation, the stratigraphic scheme of Macauley
et al. (1964) is best suited in this situation.

1.4 Regional Correlations

Halbertsma and Staplin (1960) attempted to correlate
this succession from the Peace River area to the Williston
Basin. While they did make chronostratigraphic correlations,
the lack of exact dating of the Mississippian to
Pennsylvanian transition in both the Peace River area and the
Southern Canadian Rocky Mountains (Stewart, 1978, p. 18)
makes these correlations less than definitive. Patton (1958)
has described and dated an outcrop section of similar age in
the South Nahanni River area of the Northwest Territories.

Extensive erosion at the pre-Permian unconformity has
isolated the uppper Mississippian-Pennsylvanian strata in the
Peace River area from those in the Northwest Territories and
the southeastern Canadian Cordillera. Figure 1.3 illustrates
the uncertainty of many of the correlations between these
three areas, which makes any attempt at a detailed
paleogeographic reconstruction betweeen them essentially
meaningless.

Figure 1.3   Correlation of Late Paleozoic sequence

between the Peace River area and

locations in the Southern Canadian Rocky

Mountains and the Northwest Territories.

Dashed lines represent uncertainty in the

placement of boundaries.   In particular,

notice the uncertainty in the position of

the Mississippian — Pennsylvannian

boundary.

PEACE RIVER AREA MACAULEY ET AL.(1964)			SOUTHERN CANADIAN ROCKY MOUNTAINS					NORTHWEST TERRITORIES PATTON (1958)	
			SCOTT (1964)		MCGUGAN AND RAPSON (1963)				
PERMIAN		BELLOY FORMATION	PERMIAN		ISHBEL GROUP	PERMIAN		ISHBEL GROUP	PERMIAN	
PENNSYLVANIAN	MORROWAN?	STODDART FORMATION / TAYLOR FLAT	PENNSYLVANIAN	ATOKAN	ROCKY MOUNTAIN SUPERGROUP	KANANASKIS FORMATION	PENNSYLVANIAN	L. ATÖK	SPRAY LAKES GROUP	KANANASKIS FORMATION	PENNSYLVANIAN
						TOBERMORY FORMATION		MORROWAN		TUNNEL MOUNTAIN FORMATION (RESTRICTED)	
				MORROWAN		STORELK FORMATION					
						TYRWHITT FORMATION					
						TODHUNTER FORMATION					
MISSISSIPPIAN	CHESTERIAN	KISKATINAW	MISSISSIPPIAN	CHESTERIAN	RUNDLE GROUP	ETHERINGTON FORMATION	MISSISSIPPIAN	CHESTERIAN	RUNDLE GROUP	ETHERINGTON FORMATION	MISSISSIPPIAN	CHESTERIAN	MATTSON FORMATION
		GOLATA											
	MERAMEC	RUNDLE	DEBOLT FORMATION		MERAMEC		MOUNT HEAD FORMATION		MERAMEC		MOUNT HEAD FORMATION		MERAMEC	FLETT FORMATION

1.5 Previous Interpretations

No work has been published on possible depositional environments of the Stoddart Formation or any of its members in the Peace River area. All previous work which has been cited thus far was only concerned with gross lithology, stratigraphic and biostratigraphic correlation, with occasional rather obscure references to "shallow marine" or "shallow basin" environments.

Patton (1958) was also primarily concerned with lithology, paleontology and stratigraphy of the Carboniferous section in the Northwest Territories. He does state that certain plant fossils and coal intervals in the Mattson Formation are indicative of a nearshore deltaic depositional environment (Patton, 1958) but that is the limit of his interpretation.

The situation is similar in the southeastern Canadian Cordillera. Almost all work published in the late 1950's and 1960's was concerned with gross lithology, dating of fossils and stratigraphy. Scott (1964) studied the Mississippian to Permian succession in this area (see Figure 1.3 for his nomenclature) and believed the Mississippian Etherington to the Pennsylvanian Storelk Formation represents a major regressive cycle changing from an open shelf environment, through progressively shallower water, with the Storelk interpreted as partly aeolian in nature. These formations

were uplifted and eroded before the Tobermory sandstones and Kananaskis dolomites were deposited in a transgressive cycle.

Stewart and Walker (1980), in a detailed facies study, interpreted the Tyrwhitt, Storelk and Tobermory Formations of the Pennsylvanian portion of the Rocky Mountain Supergroup (terminology of Scott, 1964) as shallow marine, coastal aeolian and shallow marine sand bodies respectively. The identification of coastal aeolian deposits in the Storelk Formation is very informative; unfortunately, the lack of exact correlations between the Peace River area and the southeastern Cordillera means that an integrated paleogeographic reconstruction involving the Stoddart Formation and the Etherington to Kananaskis Formations is not possible.

CHAPTER TWO

FACIES DESCRIPTIONS AND FACIES SEQUENCES

The basal portions of the Stoddart Formation in the Josephine Field area have been divided into ten facies on the basis of lithology, sedimentary structures and biogenic content. A very brief interpretation is included after the description of each facies. These will be elaborated on and integrated into an overall facies scheme in Chapter Five. The vertical sequence of facies is described in the second half of this chapter.

2.1 Facies Descriptions

Facies 1 - Paleosol and Coal Facies

Facies 1a - Paleosol Facies (Plate 2.1a)

Facies 1a is a light to dark green clay/silt deposit. It ranges from a blocky, massive deposit to a friable, poorly fissile, chunky one.

No bioturbation or sedimentary structures were seen in the facies. No body fossils were present, but generally roots and more indistinct carbonaceous matter could be seen on the parting planes. In addition, excellent examples of vertically penetrating, in situ roots, 6-25 cm in length

were found (Plate 2.1b).   These had often decayed and been filled with silt and were lined with tiny pyrite crystals.

This facies is interpreted to be a paleosol deposited in a dry sub-aerial environment in close proximity to a marsh as it is overlain by the coal facies.

Facies 1b - Coal Facies (Plate 2.1a)

Facies 1b was found in one place in a 48 cm thick layer. The coal was black, ranged from dull, semi-massive to very shiny and crumbly in texture and was very light in weight.

No fossils were present but probable plant remains were observed.   In addition, undulating very pyritic bands 0.5-1.0 cm were seen in the coal.

This facies is interpreted to have formed in a wet sub-aerial environment such as a marsh.

Facies 2 - Angle of Repose Cross-Bedded Sand (Plate 2.2a)

This facies consists of a cross-bedded, very fine to fine-grained, light beige sandstone.   The sand is well sorted and well rounded.   The facies has total thicknesses of 2.2-23.0 m, with generally sharp top and bottom contacts.

The dominant sedimentary structure is angle of repose cross-bedding.   The angle of the foresets ranged from a low of 5 degrees to angles as high as 25 degrees.   Sets ranged in thickness from 20 cm to greater than 45 cm while foresets were generally 1.0 cm thick. Very little to no grading was

Plate 2.1a   Paleosol and coal facies (Facies 1).
                    Coal sits sharply on chunky paleosol.
                    The core in this photograph and all that
                    follow is 3 inches in diameter.
                    6-21-83-8W6   5433 ft.

Plate 2.1b   Long, penetrating, in situ root traces
                    in the paleosol of Facies 1.
                    6-21-83-8W6   5435 ft.
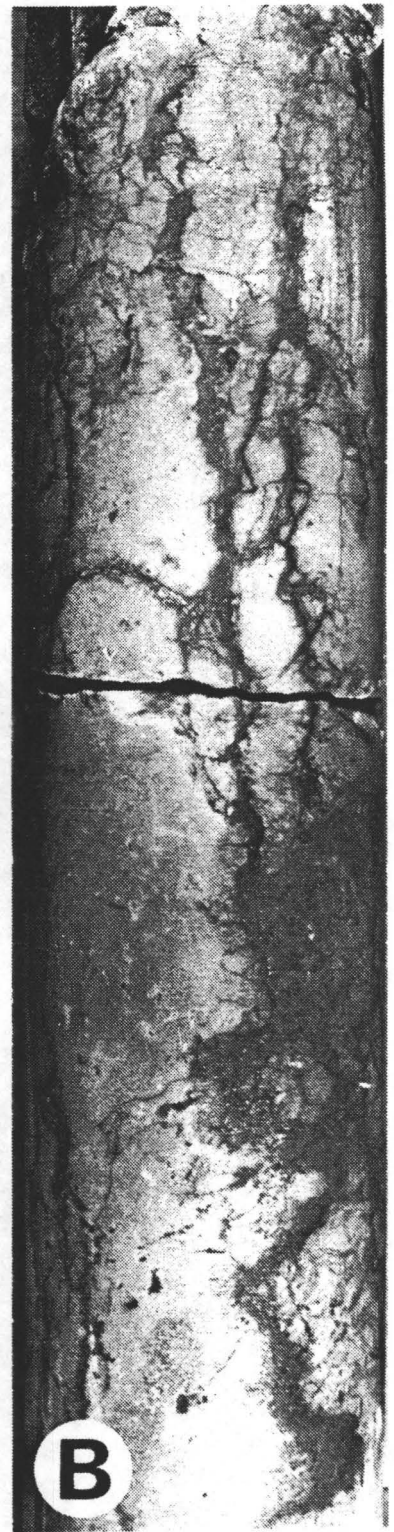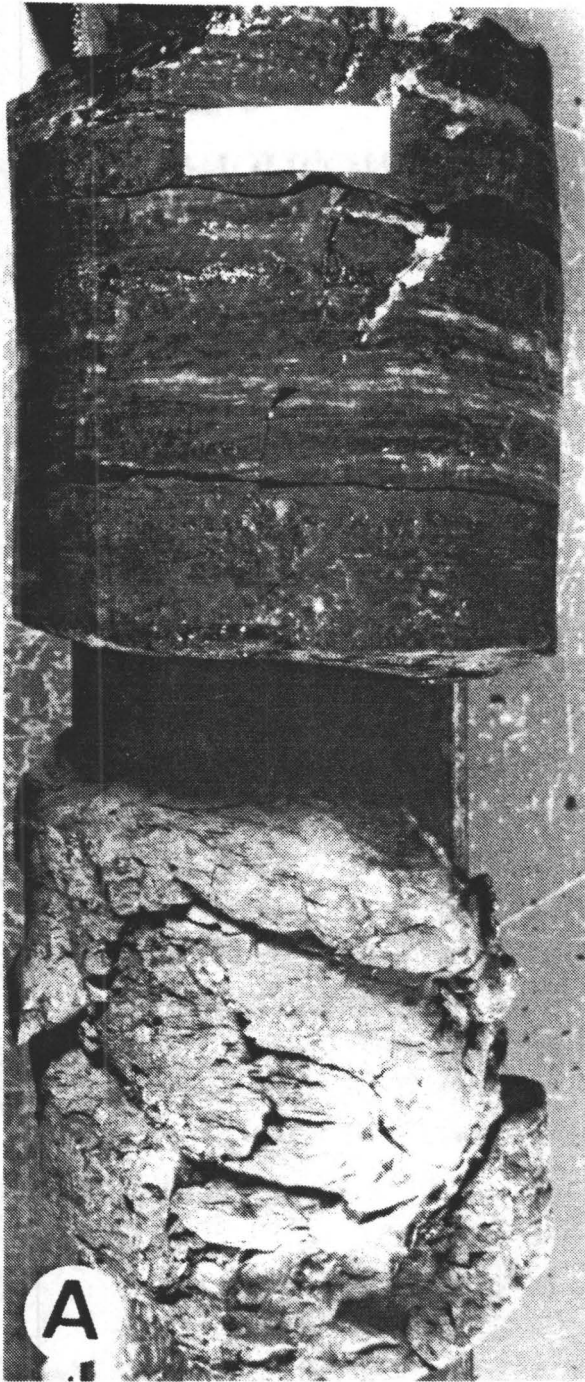
seen within each foreset. Although most of the cross-bedding appeared to be planar-tabular, this may only be an artifact of observing a 3-inch core. The cross beds generally have angular contact with the lower set boundary although some tangential contacts are seen.

On occasion, thin zones of truncated, climbing ripples with very little silt or clay in the trough of the cross-beds were seen on a foreset boundary (Plate 2.2b). Often, layers of cross-bedded sands are separated by thinner divisions (5.0-10 cm) of flat laminated sand with exactly the same composition and appearance.

The bedding which is observed in this facies is often very indistinct. This is probably a result of the excellent sorting and lack of any grading within individual cross-beds. Deformation structures were very occasionally seen in the facies. There were a large number of stylolites present in this facies. They had a tendency to form in parallel arrays at angles similar to the cross-bedding. In addition, there is common anhydrite/gypsum pore-filling. This white mineral occurs as small specks 1.0-2.0 mm in diameter or as larger (2.0 cm thick) irregular mottled patches.

This facies is generally interpreted as representing aeolian dune/interdune deposits.

Facies 3 - Graded Cross-Bedded Sandstone Facies (Plate 2.2c)

This facies is based on a single 10.9 m unit. It consists of a fine to medium-grained beige sand which is poorly to moderately sorted and is sub-rounded.

The dominant sedimentary structure is planar cross-bedding with cross beds angled at 10-30 degrees. The individual cross beds are 0.5-1.0 cm thick with sets up to 33 cm thick. Cross-beds have angular contact with the bottom set boundary. The cross-beds are easily defined on the basis of an upward grain size change from medium to fine grained.

The facies has a high percentage of pyrite crystals, has a number of stylolites formed parallel to bedding and has a number of thin beds of facies 4b (concentrated clay-clast conglomerate) which has been extensively pyritized.

This facies is very similar to facies 2 in terms of sedimentary structures and associations. The lithology of the unit is distinctive, however, because of the graded cross-beds, poorer sorting and rounding and coarser grain size.

This facies is difficult to interpret since it has many features similar to facies 2 but is distinctively different in other respects. In addition, it is lower in the section, resting almost on the top of the Debolt, than the other cross-bedded sands. This facies remains an enigma which could either be a fluvially influenced deposit or an

Plate 2.2a   Angle   of   repose   cross-bedded   sand
                    (Facies 2).   Note   high-angle, regularly
                    spaced   cross-beds.   White material is
                    anhydrite/gypsum cement.
                    10-16-83-9W6   5667 ft.

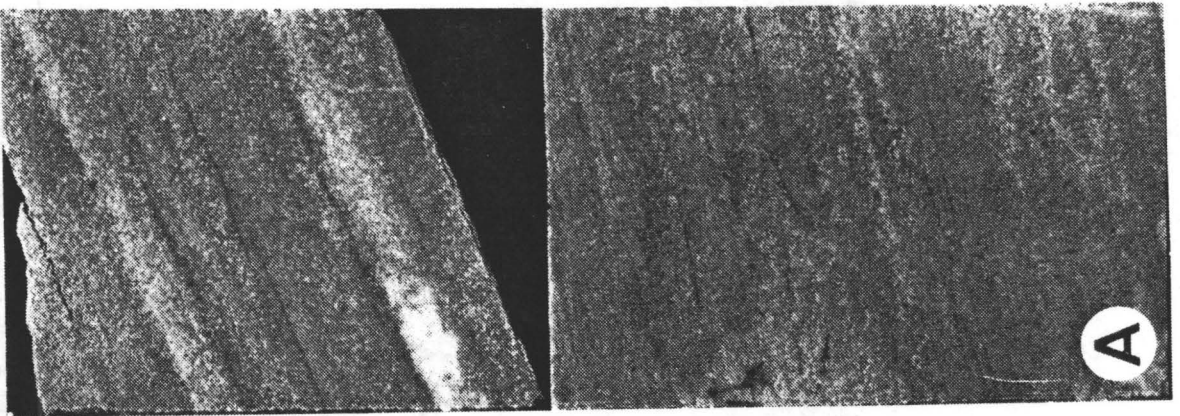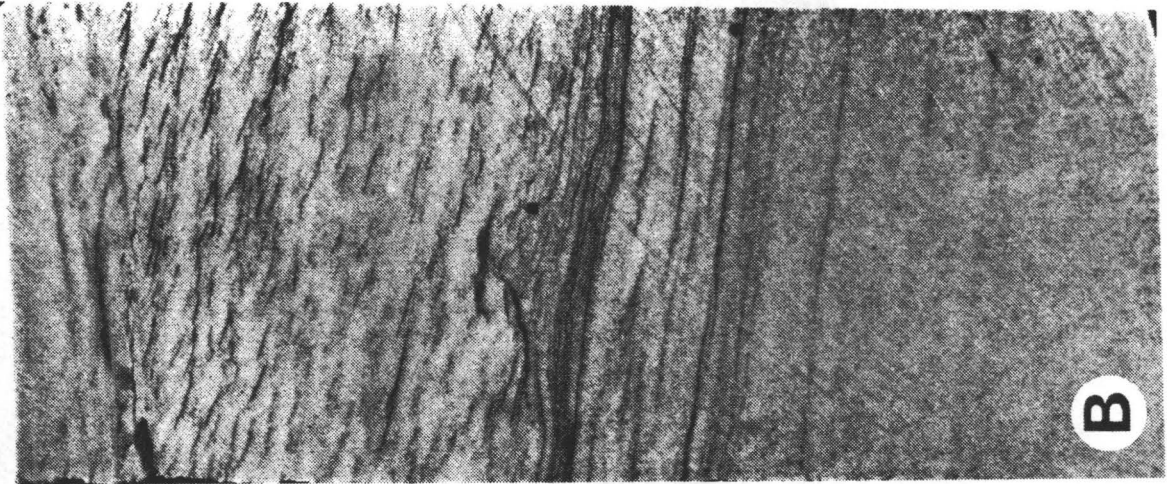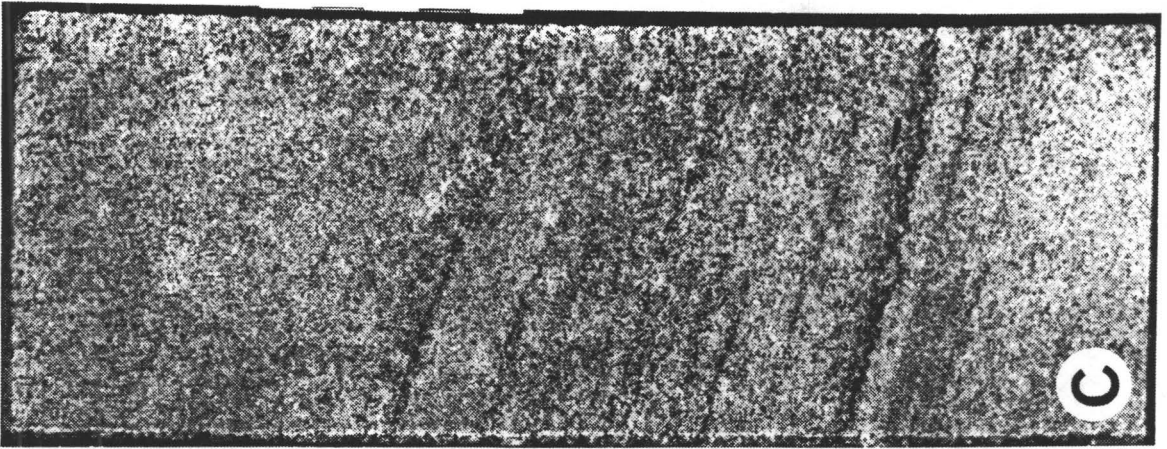Plate 2.2b   Thin, low angle   climbing   ripples found
                    within Facies 2.
                    10-15-83-9W6   5726 ft.

Plate 2.2c   Graded   cross-bedded   sandstone   facies
                    (Facies 3).   Note the coarser grain size
                    and grading found within each individual
                    cross-bed.
                    11-18-83-9W6   5778 ft.

aeolian deposit having local differences in sand supply or topography.

Facies 4 - Clay-clast Conglomerate Facies

Facies 4a - Diffuse clay-clast facies (Plate 2.3a)

This facies consists of zones of a diffuse increase in clay clast concentration within the thick clean sands of facies 2. These zones are less than one metre thick. The clasts are green to black claystone, angular to rounded, poorly sorted and range in sizse from 1-30 mm. These zones have a relatively sharp base and gradational top.

These have been interpreted as aeolian associated deposits. One possibility would be that the clay was ripped up from a dried up pond, transported only a short distance and then buried in a dune/interdune area.

Facies 4b - Concentrated clay-clast conglomerate facies (Plates 2.3b and 2.3c)

Facies 4b is composed of thin (average 4 cm) poorly sorted clay conglomerates. The clasts are sub-rounded to well rounded. They are composed of fine-grained sandstone, green siltstone and most commonly green and black mudstone, each of which can be iron stained or sideritized. The clean sands again act as the matrix and occasionally have been cemented by anhydrite. The facies is generally sharply erosive at its base with a slightly less sharp top contact

Plate 2.3a   Diffuse clay clast facies (Facies 4a).

                    Minor   numbers   of   angular clay clasts,
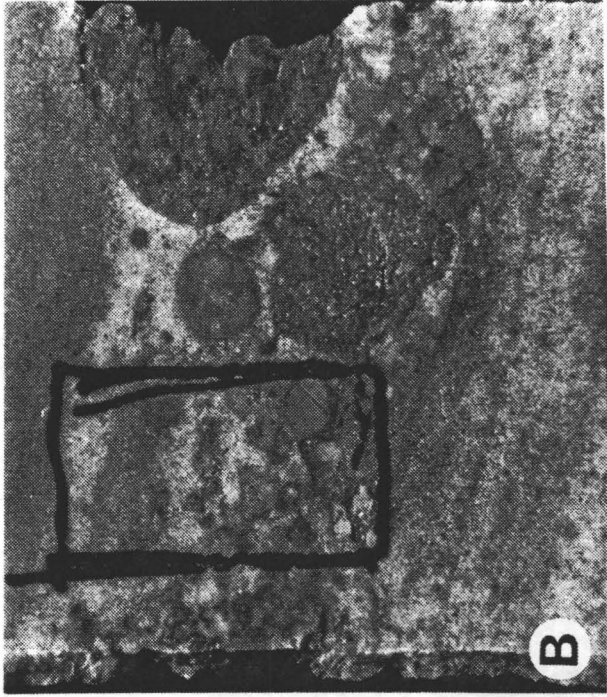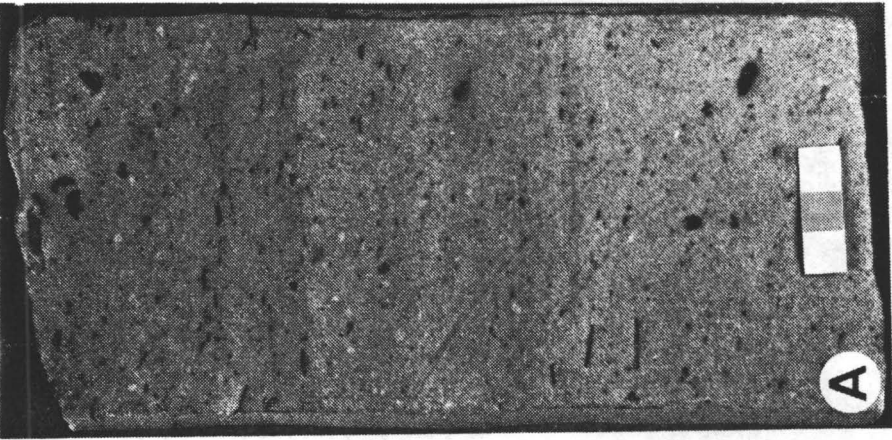
                    some of which appear to be curled.

                    10-15-84-8W6 5136 ft.

Plate 2.3b and 2.3c Two examples of concentrated clay clast

                    conglomerate facies (Facies 4b). Note

                    the erosive bases of these thin units.

                    2.3b   10-16-83-9W6 5669 ft.

                    2.3c   7-19-83-9W6 5672 ft.

and was occasionally observed to be capped by a thin mud layer.

A similar facies with slightly different characteristics was seen on two occasions. This was a slightly thicker bedded (0.6 m) conglomerate of 1-50 mm highly deformed, "wispy", black clay clasts froming approximately 25% of the unit with a clean light beige sand composing the remainder.

This facies has a common hydrodynamic interpretation in that a short period of relatively high velocity aqueous flow has deposited them. A specific environmental interpretation must await the overall sequence in which these facies occur.

Facies 5 - Rippled Facies

Facies 5a - Unidirectional Ripple Facies (Plate 2.4a)

This facies consists of very fine to fine-grained, white to light beige or light green sand, in units from 1-3 m in thickness. The sand is well sorted and rounded but has a variable amount (up to approximately 30%) of silt, which fills the troughs of truncated ripple cross-lamination.

The dominant sedimentary structure in this facies is unidirectional ripple cross-lamination. Sets are 10-20 mm in thickness, individual laminae are 1 mm thick and have angles ranging from asymptotic to 15 degrees. The ripples are generally truncated on their stoss side and occasionally are found as climbing ripples.

This facies is interpreted as occurring in the lower portion of the velocity versus size phase diagram, in an environment with a single dominant flow direction.

Facies 5b — Bidirectional Ripple Facies (Plate 2.4b)

Facies 5b is composed of very fine to fine-grained, white to light beige sandstone. The facies occurs in units up to 6 m thick. The sand is well rounded and well sorted. The facies is dominated by ripple cross-lamination, as was facies 3a, with most of the same descriptive parameters such as set thickness and angle of ripples.

There are, however, important differences between facies 5a and 5b. This facies not only has black silt/clay filling the troughs of the ripple cross-laminae but in addition has continuous, undulating laminations of black clay up to 1 mm thick. These laminae can form up to 15% of the unit. The ripples of this facies change their orientation within a unit, indicating an alternation in the flow direction not seen in facies 5a. Finally, the ripple sets are much more irregular in thickness and approach a lenticular shape in many instances.

This facies is interpreted as belonging to the same portion of the phase diagram as facies 5a but in an environment with a noticeable flow bidirectionality.

Facies 6 - Bioturbated Interlaminated Sandstone and Shale

(Plate 2.4c)

Facies 6 consists of interlaminated, sharply bounded sandstone and mudstone, with a widely variable sand to shale ratio ranging from 1:9 to 1:1. The facies occurs in units ranging from 3-7 m thick. The dark grey to black mudstone laminae range in thickness from 1-10 mm while the sandstones are only slightly thicker, ranging from 1-20 mm.

The sandstones are light beige in colour, very fine to fine-grained, well sorted and rounded; overall it appears to be a very mature sand. The sandstone laminae are often undulating and are most commonly present as discontinuous lenses, indicating a small and sporadic sand supply. Sedimentary structures are only intermittently visible but when distinct, they uniformly occur as truncated ripple cross-lamination within the lenses which could represent either current ripples or combined flow wave ripples.

The mudstone is well-laminated (average 1 mm) and fissile. Its undulating nature is a response to the surrounding sand. These laminae have been extensively bioturbated, most commonly by 1-2 mm diameter unlined, horizontal burrows (Planolites), with a smaller number of larger 5 mm diameter Planolites also present. In addition, there are occasional vertical to inclined complex, U-shaped burrows believed to be Diplocraterion. The burrows are

Plate 2.4a   Unidirectional ripple facies (Facies
                    5a).
                    7-19-83-9W6   5638 ft.

Plate 2.4b   Bidirectional ripple facies (Facies 5b).
                    Note lenticularity of sand layers and
                    continuous mud drapes.
                    10-34-82-9W6   6120 ft.

Plate 2.4c   Bioturbated,   interlaminated sandstone
                    and shale (Facies 6).   This facies is
                    generally extensively bioturbated by a
                    variety of burrows.
                    6-1-83-9W6   1823.7 m.
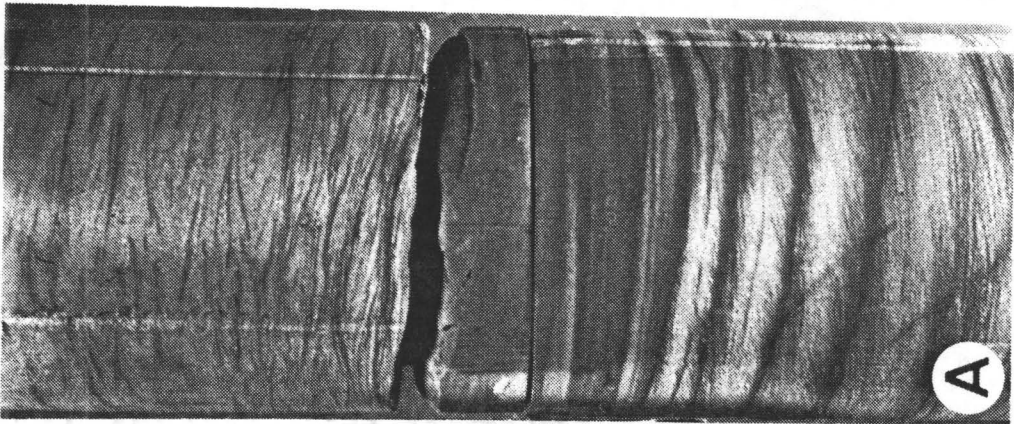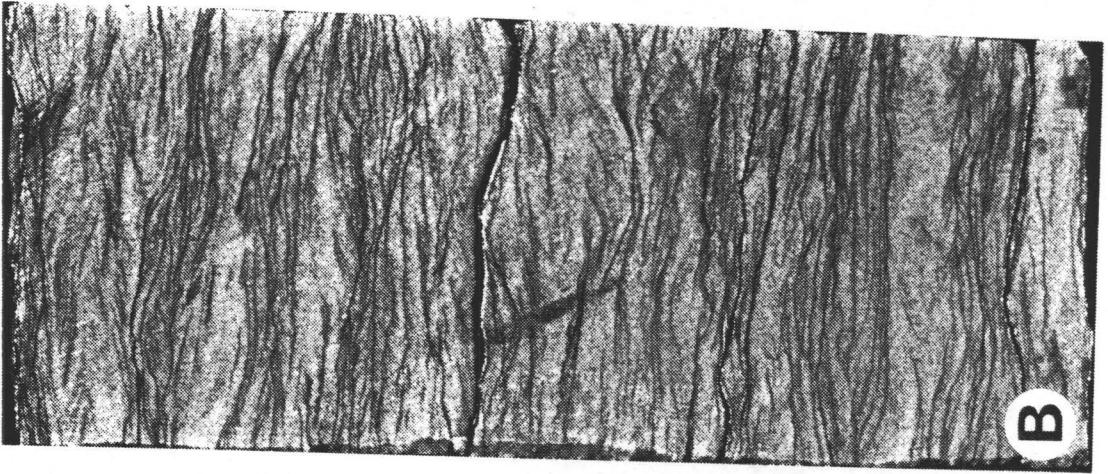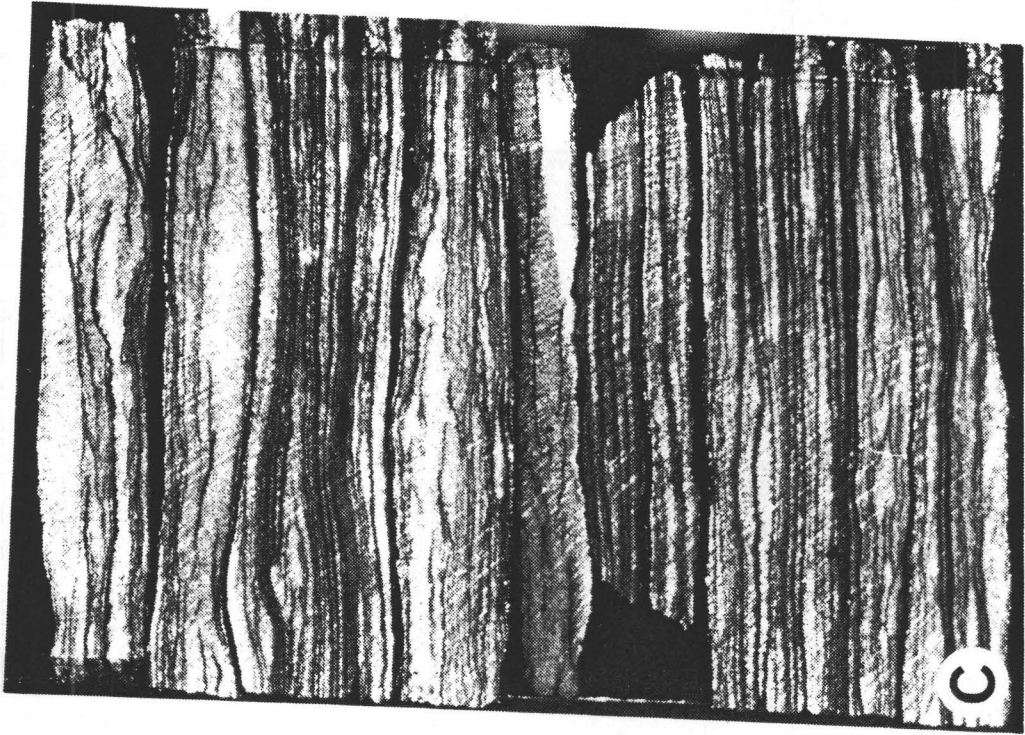
filled with sand having the same characteristics as the sandstone laminae and have commonly been replaced by pyrite.

The physical characteristics and ichnofauna present in this facies are not indicative of a single depositional environment. It is possible that they are deposited either in a mixed tidal flat or at the transition from lower shoreface to offshore; the deciding factor in each case will be the nature of the rocks associated with this facies in vertical sequence.

Facies 7 - Shell Hash Facies (Plate 2.5a)

Although the best examples of this facies were not observed in the basal portions of the Stoddart Formation, it was observed in core slightly higher in the section (approximately 46 m above the sequence on which this study concentrates) and with the same facies associations similar to those below.

The facies is composed of a thin layer (3.0-7.5 cm) of a shell hash in a dark (possibly silty) sand. The shells represent 50% of the rock and are mostly brachiopods and mulluscs (bivalves). Preservation ranges from small fragments to well preserved molds of finely grooved brachiopods. The sediment is moderately sorted and shows no sedimentary structures.

This facies is interpreted to be a reworked (possibly by tidal channels) shell layer.

Facies 8 - Varved Sand/Siltstone Facies (Plate 2.5b)

This facies was observed in only one place in a unit 5.0 m thick. It consists of a rhythmically laminated, blocky, very fine-grained white to dark grey sandstone. The laminae are distinguished on the basis of colour (light to dark), have no conspicuously grain size change and are uniformly 1-3 mm in thickness. The laminae are inclined at 15 degrees but extensive microfaulting may indicate that this inclination is not a depositional feature. No fossils were observed, but minor bioturbation and small fragments of carbonaceous material was seen on most partings.

This facies is interpreted to have been deposited in a very quiet lagoonal or lake environment.

Facies 9 - Indistinctly Bioturbated Sand Facies (Plate 2.6)

Facies 9 consists of a grey/green to light beige, fine-grained sandstone which has a relatively high mud content. The sand and mud are homogeneously mixed, and the facies is usually massive and has no sedimentary structures. Occasional thin, discontinuous and irregular mud laminae are present.

The facies has been extensively bioturbated. In some zones, the trace fauna can be identified while in other cases, the bioturbation has left a mottled, muddy sandstone with no distinct burrows. Identifiable trace fauna include: Rosselia, Teichichnus, Diplocraterion, and Planolites.

Plate 2.5a   Shell hash facies (Facies 7).   Note high
                    proportion of shells, most of which
                    appear to be reworked.
                    8-6-83-10W6   1865.8 m.

Plate 2.5b   Varved sand/siltstone facies (Facies 8).
                    Note extreme regularity of alternating
                    light and dark bands. A vertical burrow
                    is present in upper right corner.
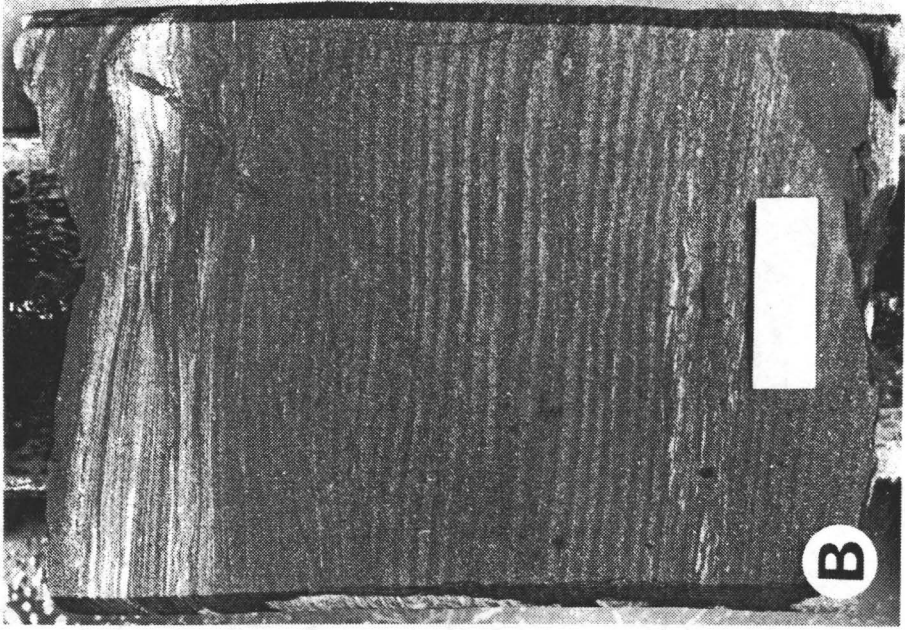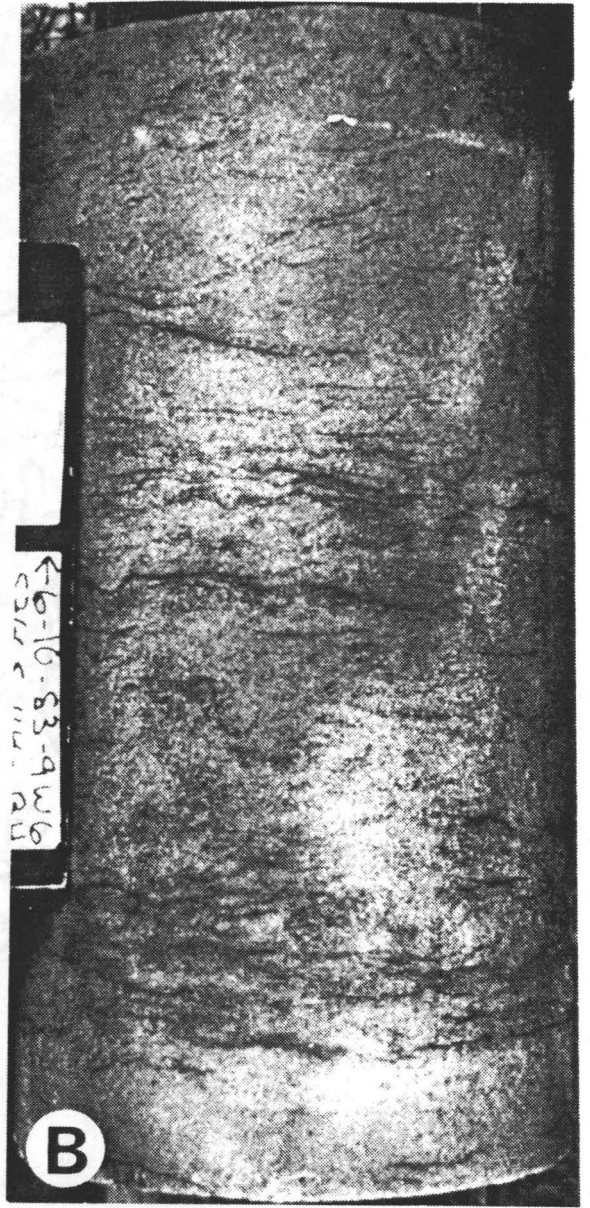   10-15-84-8W6   5166 ft.

Plate 2.6   Two examples of the indistinctly
bioturbated sand facies (Facies 9).Plate
2.6a illustrates better preservation of
burrow structures than in 2.6b, which
has a more massive appearance.

2.6a 6-21-83-8W6 5411 ft.

2.6b 6-10-83-9W6 5766 ft.

This facies is interpreted as being a result of biogenic reworking of a sand deposit in a marine setting. The sand may have been a subaerial deposit which was transgressed or the sand may have been transported into the marine setting and reworked there.

Facies 10 - Marine Mudstone Facies (Plate 2.7)

Facies 10 is a black to dark gray, slightly calcareous mudstone. It is finely laminated (<1 mm) and generally has moderate to imperfect fissility.

On occasion there is an increase in a white to beige silty to sandy component which occurs in narrow, diffuse and discontinuous layers. Very minor 1-10 mm pyrite nodules and carbonate crystals were noticed.

Bioturbation is not extensive. A minor number of Planolites and a few unidentified shallow bell shaped burrows were found. Both of these were filled by sand or silt. In addition, in one well, gold coloured Gordia traces were observed. Minor numbers of macrofossils were present, including mullusc (bivalve) and brachiopod shells, bryozoan skeletons and gold coloured "fish scales".

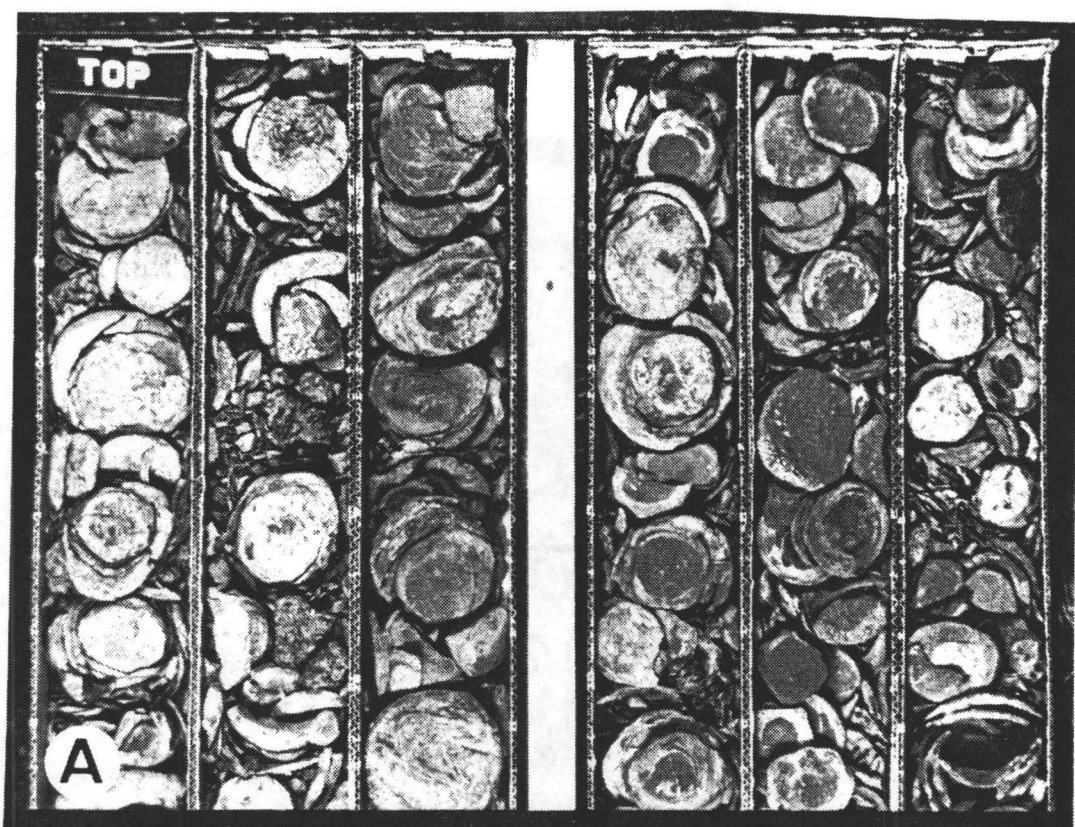This facies is interpreted to be an offshore marine deposit.

Plate 2.7

Marine mudstone facies (Facies 10). Plate 2.7a illustrates the generally fissile nature of this facies. Part of the marine fauna (bryzoan skeletons) is shown in Plate 2.7b.

2.7a   10-34-82-9W6   6074 ft.

2.7b   10-15-84-8W6   5214 ft.

A

10-15-84-8W6
5214.5ft-U22-BH

B

4.2 Facies Sequences

The very basic interpretation made after each facies description must necessarily be limited because many similar sedimentary structures and lithologies can be deposited in a number of environments.   One example would be facies 2, consisting of thick sets of angle of repose cross-bedded sands whose possible depositional environments would include aeolian, fluvial and tidal or current dominated shallow marine settings.

Once the position of such a facies is known with respect to the surrounding facies, however, a much stronger argument can be made as to its environment of deposition.   In the cores which were examined, three sequences can be defined. The first sequence appears to regressive in nature.   The second and third sequences are also regressive, and are sharply overlain by transgressive deposits.

The core from one well (10-15-84-8W6) contains the transition from the Debolt Formation into the lower most shale interval of the Stoddart Formation which represents the first and lowermost sequence present in the cores.   The transition from the Debolt Formation is conformable and in general consists of an upward increase in mud content.   The basal shales consisted of alternating units of black, calcareous marine shale (facies 10), bioturbated, interlaminated mudstone and sandstone (facies 6) and an

indistinct, bioturbated muddy dolomite which strongly resembles facies 9.

This sequence is without question marine and therefore the interlaminated, bioturbated mudstone and sandstone represent minor sand pulses which were intruded into an offshore marine sequence.

The second sequence consists of a marine shale (facies 10) sharply overlain by thick cross-bedded sands of facies 2. Within the cross-bedded sands are zones of diffuse or concentrated clay conglomerate (facies 4a or 4b). The thick cross-bedded sands are overlain by either a sharp transition back into a marine shale (facies 10) or by a rippled sand of distinctly different character (facies 5a) from the cross-bedded sands below and then by a marine mudrock of facies 10. In the core from the 6-21-82-9W6 well, the cross-bedded sand was sharply overlain by a chunky paleosol facies (facies 1a) and then by a coal (facies 1b). This in turn was covered by a 6.3 m section of indistinctly bioturbated sand (facies 9).

The association of facies in this sequence still do not uniquely identify a particular environment. The thick sequences of clean cross-bedded sand which show no bioturbation nor any body fossils makes a marine setting highly unlikely. Although the sequence contains a transition from cross-bedded sands to rippled sands in 2 cores, this is a very sharp contact with a definite change

in lithologic nature of the sands not consistent with a fluvial origin. The close association of definite sub-aerial paleosol and coal facies lying directly on the cross-bedded sands is additional evidence of a sub-aerial depositional environment. When this is combined with the lithologic characteristics and sedimentary structures noted in the facies description of the angle of repose cross-bedded sandstone, the best choice for the environment of deposition of the third sequence would be a coastal aeolian setting.

The third sequence exhibits a conformable change from dark grey or black marine shale (facies 10) to interlaminated, bioturbated, black mudstone and rippled sandstone (facies 6) to a bidirectionally rippled sand with minor shale partings (facies 5b). In sequences above the upper limit of this study, the rippled sand was underlain at times by the shell hash facies (facies 7). The bidirectional rippled sands could be overlain by an indistinctly bioturbated sand (facies 9) or by a varved sand and silt (facies 8).

The strength of the facies sequence concept can now be applied. Previously, the interlaminated, bioturbated mudstone and sandstone facies was interpreted to be minor intrusions into a marine environment based on the sequence in which it occurred. In the third sequence, the association of bioturbated mud and sand below the

bidirectionally rippled facies (occasionally underlain by a shell hash) in an overall coarsening or sanding upward sequence is indicative of an increasing proximity to the sediment supply. These deposits are part of a regressive sequence ending in an area close to the shoreline. The sequence contains facies such as a shell hash layer (facies 7) overlain by the bidirectionally rippled sands (facies 5b) and a varved sand/siltstone facies (facies 8) which, when taken within the context of this regressive deposit, are most likely part of a quiet lagoon or tidal flat environment cut by tidal channels.

The interpretation of the first sequence is that of a regressive change from a carbonate dominated platform deposit to a clastic dominated offshore marine deposit. Occasional minor inputs of sand into this environment resulted in the presence of the interlaminated bioturbated mudstone and sandstone.

The interpretation of the second sequence is also made within the context of a regressing sea. Thick coastal aeolian sediments prograde very rapidly out onto marine muds resulting in the sharp based sands seen in core. These accumulate into thick sequences of clean, high angle cross-bedded sands with occasional deposits of ephemeral streams resulting in thin clay conglomerate lags. These were eventually transgressed as well, with modification of the sands by marine wave (ie. ripples) action or by extensive

bioturbation seen in some core, before being buried by marine muds.

The interpretation of the third sequence is that during a regression, closer proximity to sand supply led to deposits which may be of tidal flat origin prograding out over the underlying offshore marine muds. When the sea transgressed over this, two situations arose which were seen in core. The first is that marine organisms completely bioturbated an overlying sand which may have been a sub-aerial coastal deposit before the deposition of marine muds. Alternatively, the marine muds may directly overlie these sand deposits.

The lack of good core and well control in the area still make interpretation of depositional environment difficult. Further evidence is needed and will be provided by discussion of the lateral variation in facies and facies sequences in Chapter Three and by the petrologic examination of Chapter Four.

At this point however, a number of important observations can be made.

1. The basal portions of the Stoddart Formation were deposited in a cyclic sequence of regression and transgression. The sand bodies, especially the thick cross-bedded sands, were deposited at the final stages of these regressive periods.

2.   The recognition of the start of a transgressive cycle on a log profile can be difficult, since it may be represented by a rapid return to marine mud or by biogenic and/or sedimentary modification of probable sub-aerial deposits.

3.   Lagoonal or tidal flat deposits are never seen above the main sands in the regressive cycles indicating the lack if a back barrier lagoon.   This is one indication that the depositional environment was coastal aeolian rather than a barrier beach complex.

CHAPTER THREE

LATERAL FACIES VARIATIONS

3.1 Gamma Ray Log Facies

The poor core control in the study area necesitates the use of petrophysical logs, specifically the gamma ray log, for the correlation of facies. Seven distinctive gamma ray profiles were very common in the basal portion of the Stoddart Formation. These will be called gamma ray facies and consist of:

1. Straight shale baseline baseline (GRF 1)
2. Broad, peaky profile (GRF 2)
3. Funnel shaped profile (GRF 3)
4. Blocky profile (GRF 4)
5. Bell shaped profile (GRF 5)
6. Blocky profile with numerous peaks (GRF 6)
7. Sharply peaky profile (GRF 7)

The characteristics associated with these facies are essentially self-evident from their names and the typical gamma ray responses (Figures 3.1 to 3.8). The straight shale baseline is only interrupted by very minor "sand" peaks. The broadly peaky profile is always present at the very base of the Stoddart Formation as well as higher in the section. It is characterized by broad peaks which have no characteristic or consistent variation. The funnel shaped profile has a consistent change from the shale baseline to a sand baseline, interrupted only by minor shale peaks and is terminated by a sharp return to the shale baseline. The blocky profile has a very sharp base, an essentially

straight sand baseline response with only minor peaks. The bell-shaped profile moves in a general trend from the sand baseline to the shale baseline interrupted by a number of small shale peaks. This log facies can either rest on the blocky profile facies or have a very sharp base resting on a shale baseline. The blocky profile with numerous peaks (Figure 3.1a) is essentially similar to the blocky profile in terms of its bottom contact but has larger and more numerous shale peaks. The sharply peaky profile (Figure 3.1b) is characterized by rapid alternation between the sand and shale baseline and has no consistent variation. Neither of the last two profiles has core control.

The importance of defining typical gamma ray facies is to determine whether they represent a specific core facies (a legend of core facies is given in Figure 3.2) or facies sequences. This has been found to be the case. The first five of these gamma ray facies are represented by core. The reliability of the correlation between core and gamma ray facies is dependent on the number of cores which can be used in the correlation. GRF 1 is essentially the same as the marine mudstone facies (facies 10) (Figure 3.3). GRF 2 represents intervals of the marine mudstone facies (facies 10), thinner intervals of bioturbated, interlaminated sandstone and shale (facies 6) and much less common units of bidirectionally rippled sand (facies 5b) (Figure 3.4). At the base of the Stoddart in the transition from the Debolt

Figure 3.1a   Blocky profile with many peaks (GRF 6).
                     No core was present in sections with
                     either GRF 6 or GRF 7 responses.

Figure 3.1b   Sharply peaky profile (GRF 7).

40
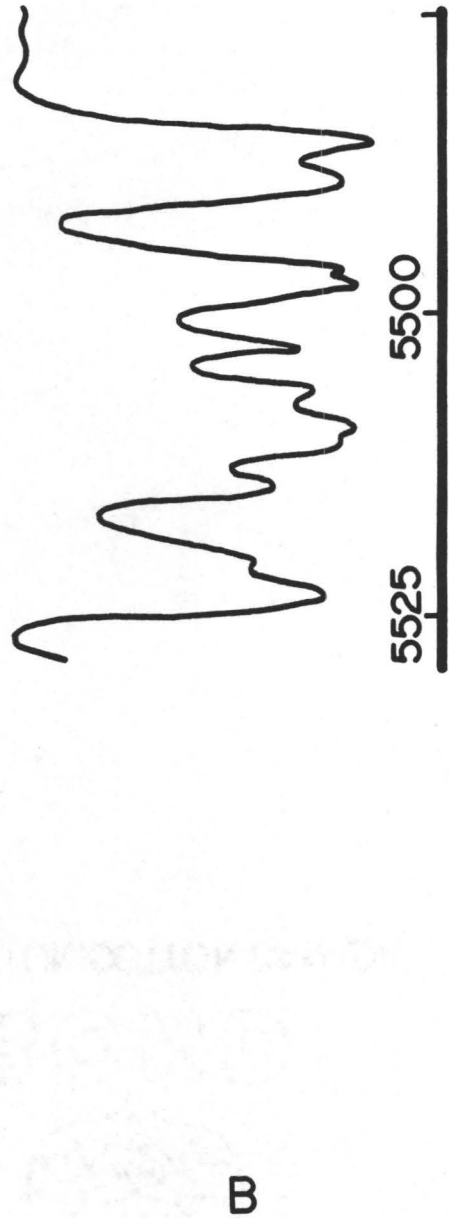
6-10-83-9W6   10-15-83-9W6

GR   GR

6050

6100

5500

5525

A   B
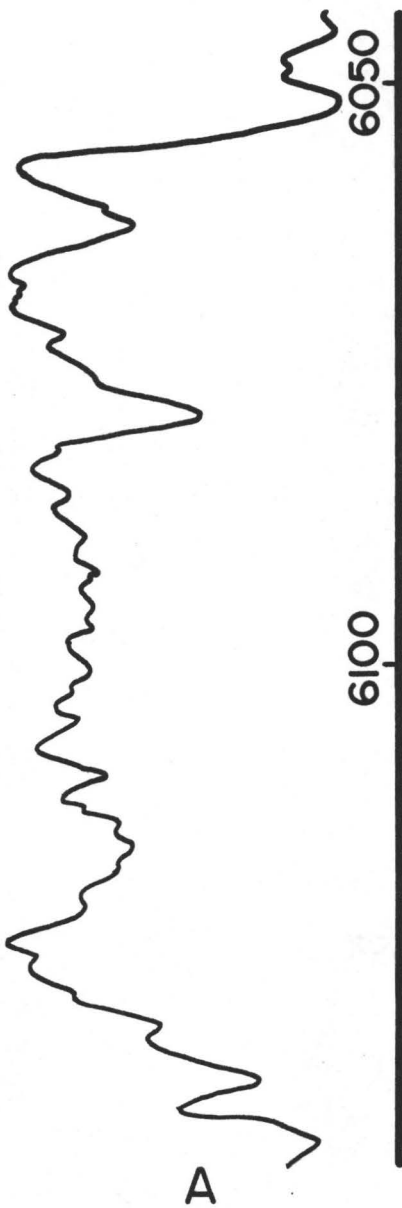
NO CORE CONTROL

Figure 3.2   Facies legend.

Facies C

Facies 1

Facies 2

Facies 3

Facies 4a

Facies 4b

Facies 5a

Facies 5b
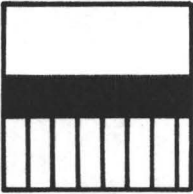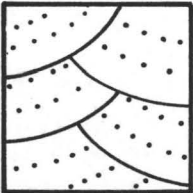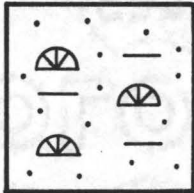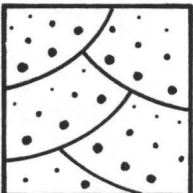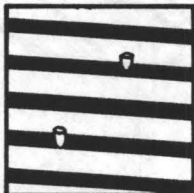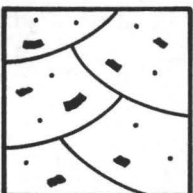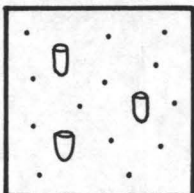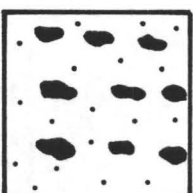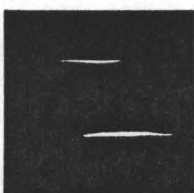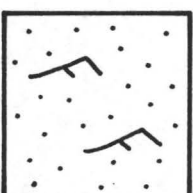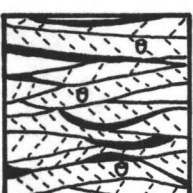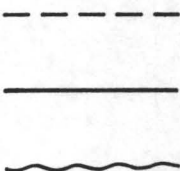
Facies 6

Facies 7

Facies 8

Facies 9

Facies 10

Bioturbation

Clay clasts

Contacts
gradational

sharp

erosive

Figure 3.3   Straight shale baseline profile (GRF 1).

II-18-83-9W6

GR   FACIES

5700

20   IO

5750

Oft

cly slt vf f m c peb
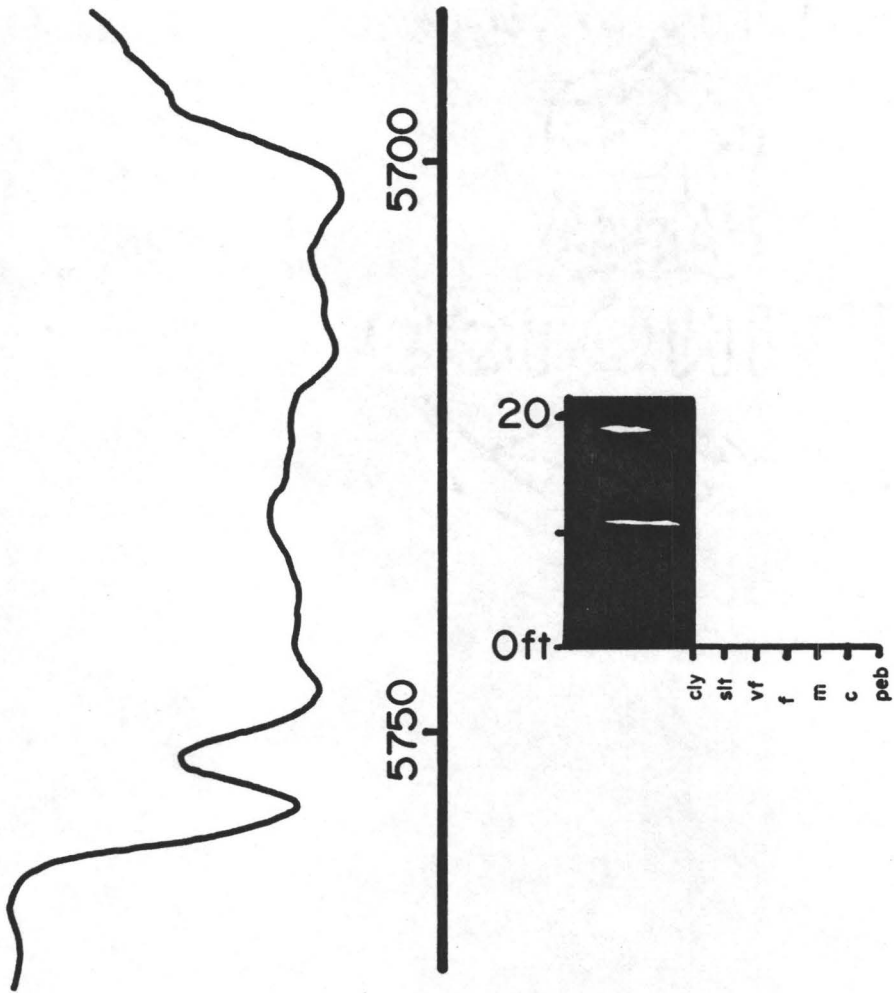
Figure 3.4   Broad peaky profile (GRF 2).

II-3-82-9W6

GR

FACIES

1975

2000

10

5b

10

5

6

10

0m

cly slt vf f m c peb
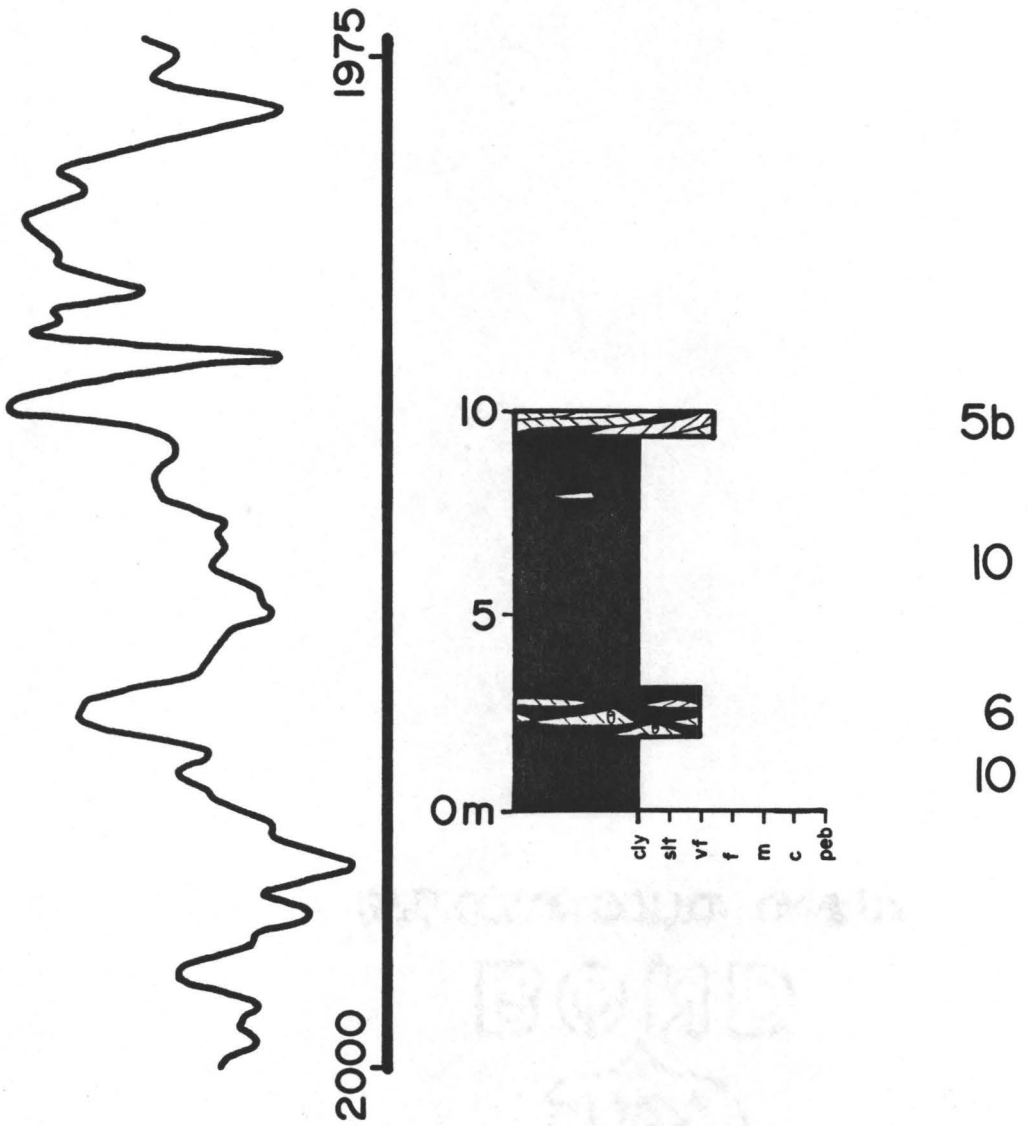
carbonates there are also intervals of a muddy dolomite within this gamma ray facies. The first two gamma ray facies represent marine environments.

GRF 3 (Figure 3.5) has been recognized in three cores. It is composed of a conformable change from marine mudstone (facies 10) to bioturbated, interlaminated sandstone and shale (facies 6) to bidirectionally rippled sand (facies 5b). The sharp return to the shale baseline represents an equally rapid change to marine conditions.

GRF 4 (Figure 3.6) is equivalent to the angle of repose cross-bedded sandstone facies (facies 2) with the minor peaks representing diffuse or concentrated clay clast conglomerates (facies 4). A large peak seen in the middle of one of these blocky sand facies represents an interval of the paleosol and coal facies (facies 1) (Figure 3.7).

GRF 5 (Figure 3.8) was seen in core twice and in both of these cores, it represented a change from cross-bedded sand to unidirectionally rippled sand (facies 5a). In one well, thin units of cross-bedded sand, and indistinctly bioturbated sand were also seen. This transition to rippled sands has previously been interpreted as reworking of sub-aerial sands, rather than the fining upward sequence associated with the point bar in a meandering river.

The vertical sequences of gamma ray facies present in the basal portion of the Stoddart Formation are relatively few in number. Every sequence starts with the broadly peaky

Figure 3.5   Funnel shaped profile (GRF 3).

6-1-83-9W6
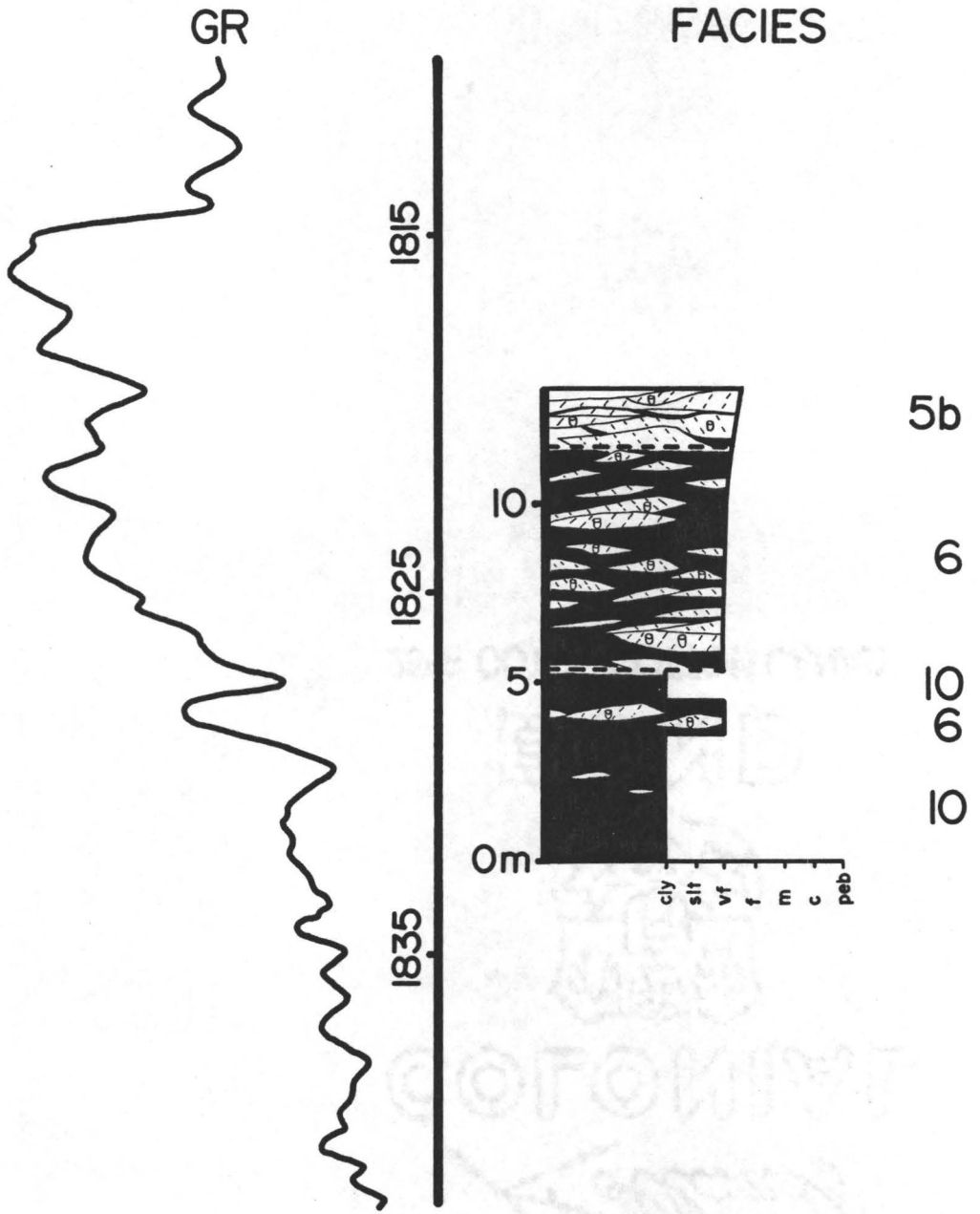
Figure 3.6   Blocky profile (GRF 4).   Minor peaks
caused by clay clast conglomerate.

10-16-83-9W6

GR

FACIES
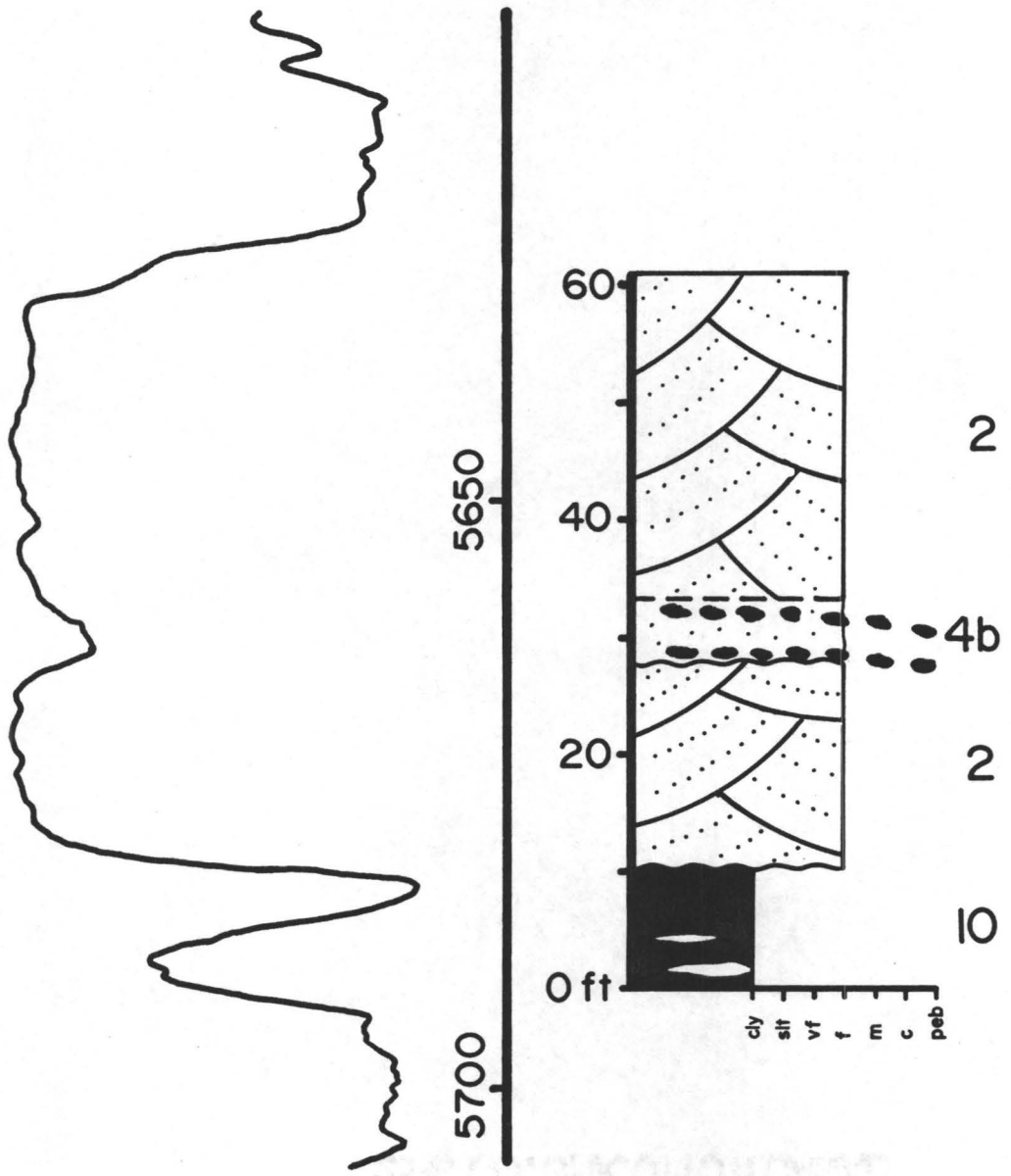
Figure 3.7   Blocky profile (GRF 4).   Large peak in
                  this response is caused by the presence
                  of a unit of   paleosol   and coal
                  (Facies 1).

6-2l-83-9W6

GR   FACIES
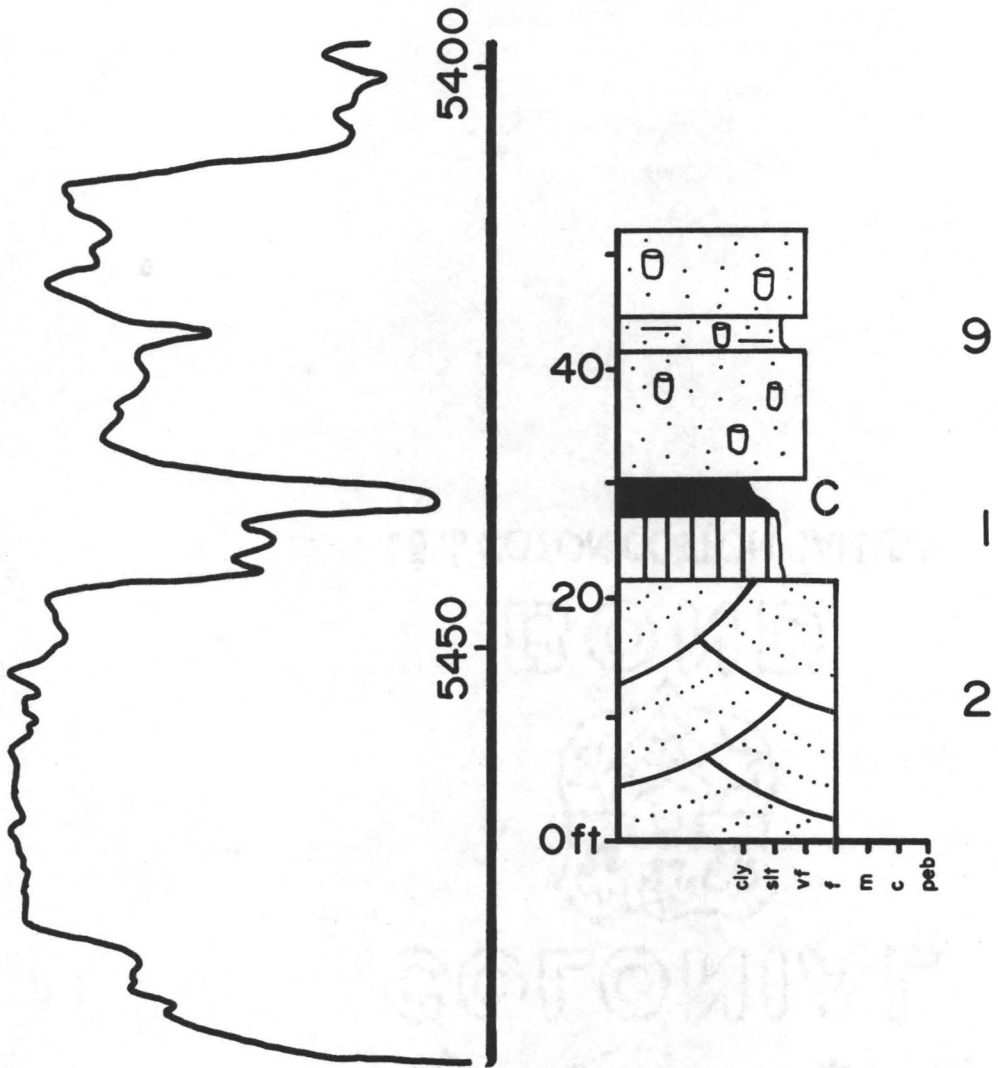
Figure 3.8   Bell shaped profile (GRF 5). This is
                    essentially a blocky profile at the
                    base.   Sharp based rippled sands
                    containing a fine fraction, which are
                    believed to be a result of marine
                    reworking, are present at the top of the
                    response.

7-I9-83-9W6

GR · · · · · · · · · · · · · · · FACIES

5a

2

4a

4b

2

4b

2

IO

cly slt vf f m c peb
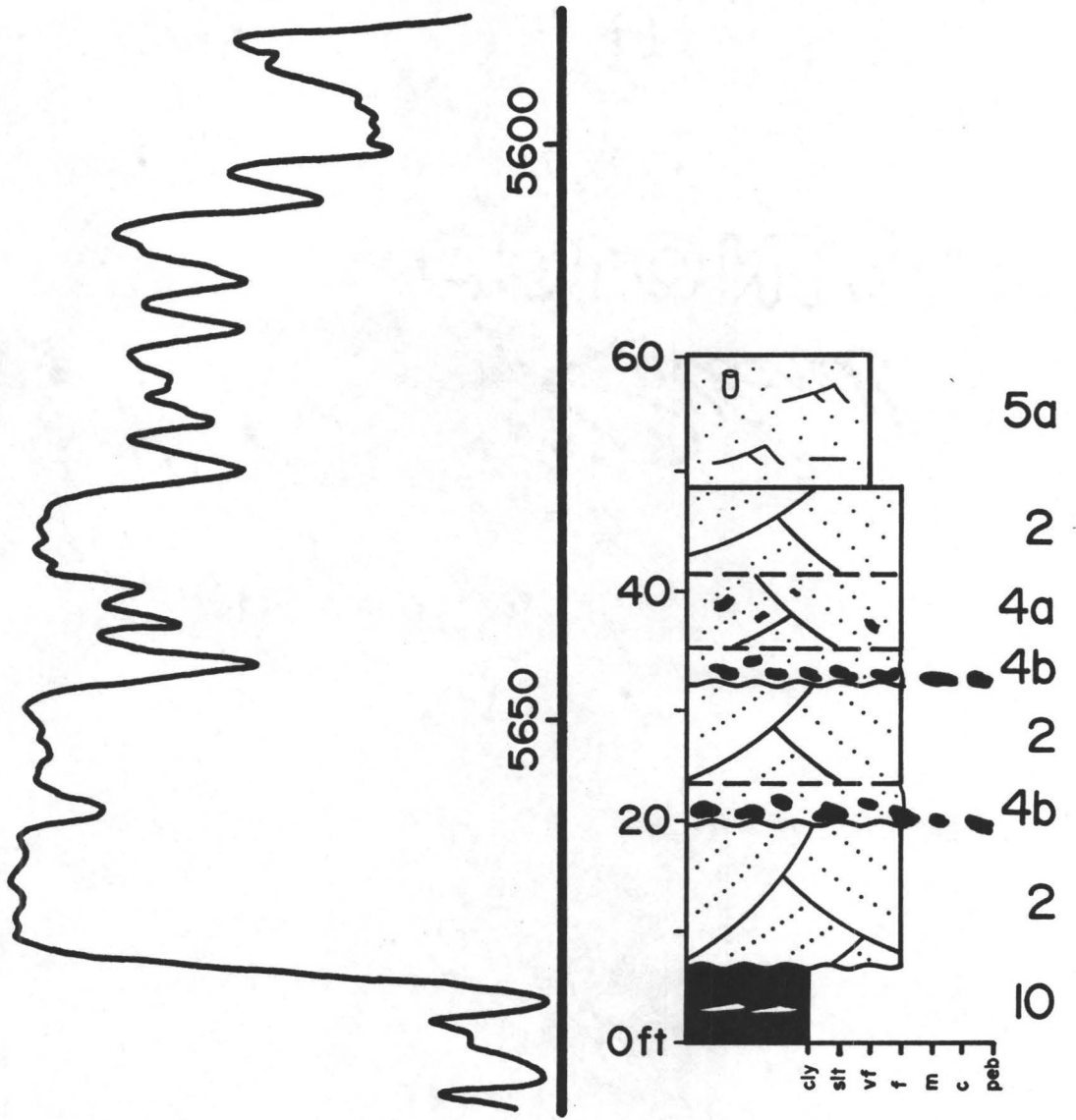
facies (GRF 2) which is sometimes overlain by a variable thickness of shale baseline facies (GRF 1).

The first sequence has the blocky profile facies (GRF 4) overlying the GRF 2/GRF 1 sequence below and then capped by a rapid transition back to GRF 1. The second sequence is similar but has the bell shaped profile (GRF 5) overlying the blocky facies (GRF 4) before returning to GRF 1. Both of these sequences then have a conformable transition to the funnel shaped profile (GRF 3).

The third sequence is similar to both the first and second. The difference is that the thickness of GRF 4 or GRF 4 plus GRF 5 is so great that the upper portion of the sequence consisting of the shale baseline (GRF 2) and funnel-shaped profile (GRF 3) is not recognized.

The fourth sequence does not have a blocky profile (GRF 3). Instead, there is a large thickness of shale baseline (GRF 1) overlain by the conformable transition to the funnel-shaped profile (GRF 3).

3.2 Cross-Sections

Four cross-sections were constructed within the study area (Figure 3.9). Only gamma-ray logs were used in these cross-sections. Within the predominantly sand and shale sequence of the basal Stoddart Formation, no other

Figure 3.9   Map illustrating well and core control.
                    Locations   of   cross-sections   are   as
                    shown.

T84

T83

T82

RIOW6   R9   R8

A   B   B'   C   C'   D   D'   A'
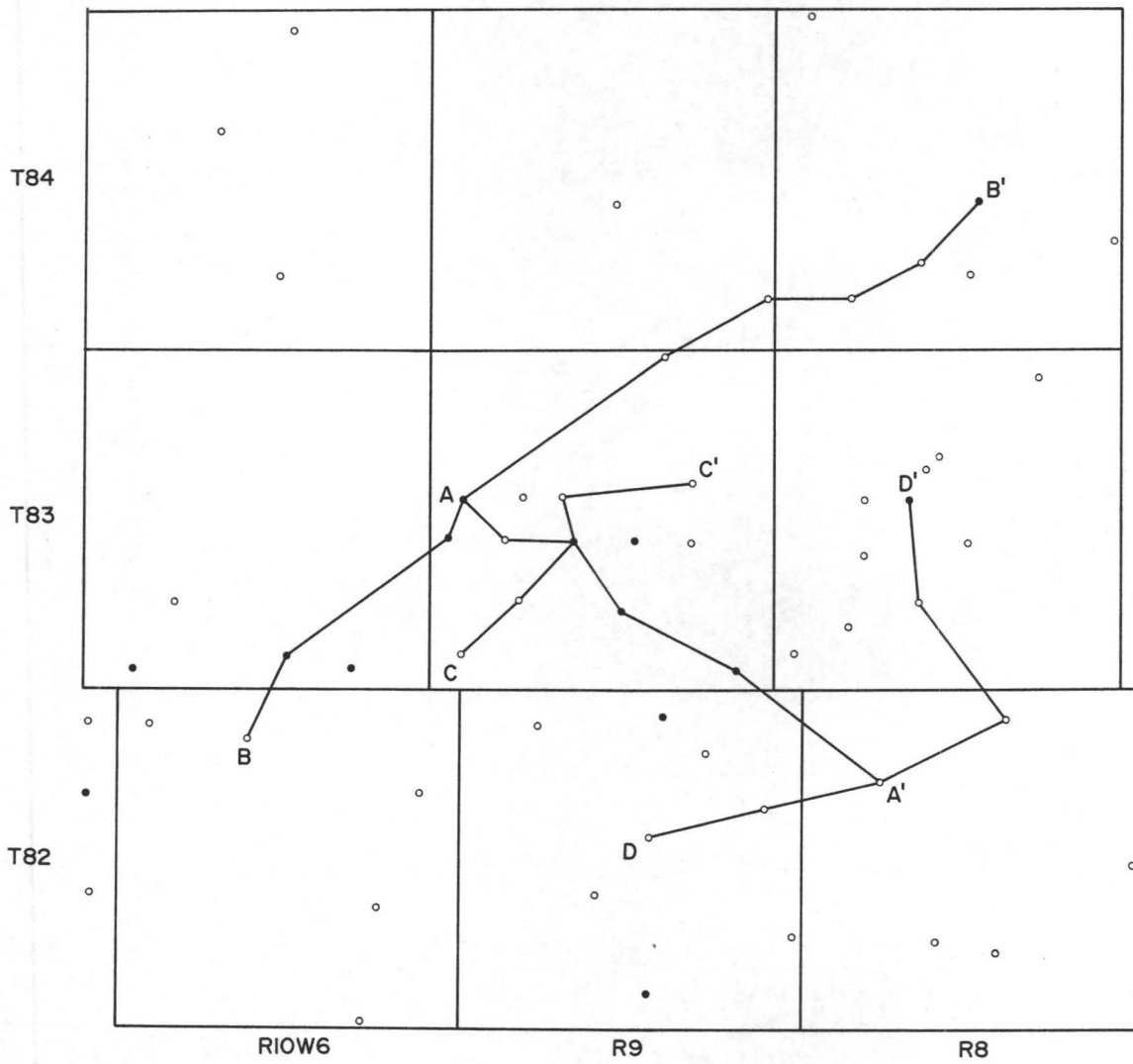
○   Wells

●   Core examined

6.0 km

3.0 mi.

Scale

petrophysical log added significantly to the accuracy of correlation.

The datum which was used was a shale peak recognizable on all logs approximately seven to ten metres below the Debolt top. Ideally, a datum should represent a consistent and continuous flat surface present during deposition of a particular sedimentary unit (Sea level is a perfect datum for present day deposition). The datum chosen possesses the required consistency and continuity but while it probably represented a relatively level basin-wide surface when it was deposited, it does not appear to have been level at the time of deposition of the basal Stoddart sands.

The only other possible datum would be the base of the main sands (Surface A on the cross-sections) themselves. Three problems arise with this choice; the first is that this surface is probably erosive; second, the lateral variation and discontinuity of the sands themselves would make correlation of this datum very difficult; and last, by using the base of these sands as a datum, it would mask any original depositional topography. There are no other markers seen on the logs which could be confidently traced across more than a small portion of the study area.

An examination of the cross-sections reveals that surface A often cuts out the lower marker sand b on the sections. The reason could be that this marker was not deposited or that it has been eroded away. This marker,

however, occurs in the transitional sequence from the Debolt carbonates into the Stoddart Formation clastics, a sequence which is consistent over the whole study area. It is not very probable that in two localized areas in the middle of the study area deposition of this transitional sequence simply stopped. A more reasonable proposal is that the marker has been eroded out. This could be explained in at least three ways: first, the marker was eroded by a river cutting into it; second, the section was eroded by wind cutting down and forming a deflation hollow; or third, normal faulting left some areas higher than others, and the highs were then eroded off before deposition of the main sands.

Evidence supporting either of the latter two mechanisms is that the log responses in wells immediately adjacent to each other, are relatively constant above surface A regardless of whether the lower marker sand has been eroded away or not (compare 10-16-83-9W6 to 6-10-83-9W6 in Figure 3.10, 10-9-84-8W6 to 10-15-84-8W6 in Figure 3.11 and 10-8-83-9W6 to 10-16-83-9W6 in Figure 3.12). This would not be expected if fluvial processes were acting to erode the lost section and deposit fluvial sediments while next to it aeolian processes were depositing sand on top of this section.

Evidence derived from core is minimal and ambiguous. Only one core was cut through the sand where the marker had

been eroded off, and this was composed mainly of the enigmatic facies 3 which resembled the cross-bedded sand facies (facies 2) in many respects but whose origin is very uncertain.

Any of the mentioned mechanisms could account for the observed sequence but there is not enough evidence to be absolutely certain of the cause. It is possible that all three mechanisms contributed to the erosion of the section.

Cross-Section A-A' (Figure 3.10)

This section illustrates the erosional loss of the lower marker sand B by surface A in both the 11-17-83-9W6 and 6-10-83-9W6 wells. It also illustrates the loss of the basal sand between Surface A and correlation line b (CL-b) between the 6-10-83-9W6 well and 6-1-83-9W6.

The major correlation problem in this section is between the 6-1-83-9W6 well and the 6-29-82-8W6 well. In the latter well there is a re-emergence of the blocky gamma ray profile seen in the wells to the west. The predominant gamma ray peak in the middle of the blocky profile is believed to correlate with a paleosol and coal facies observed in core. The extreme variation between these wells makes correlation of anything but the lower marker sands impossible.

The uppermost correlation line (CL-c) is relatively constant across the section (except at 6-29-82-8W6) and

Figure 3.10   Cross-section A-A'.   Description   and
                     discussion in text.

Northwest
A

Southeast
A'

| 7-19-83-9W6 | 11-17-83-9W6 | 10-16-83-9W6 | 6-10-83-9W6 | 6-1-83-9W6 | 6-29-82-8W6 |
| GR | GR | GR | GR | GR | GR |

5400

?

c

b

c

c

c

c

c

?

b

b

?

?

Surface A

Lower marker
sand B

Lower marker
sand A

Datum

?

?

?

?

?

5500

5600

5700

5800

5500

5600

5700

5800

6000

6100

6200

1850

1825

1875

1900
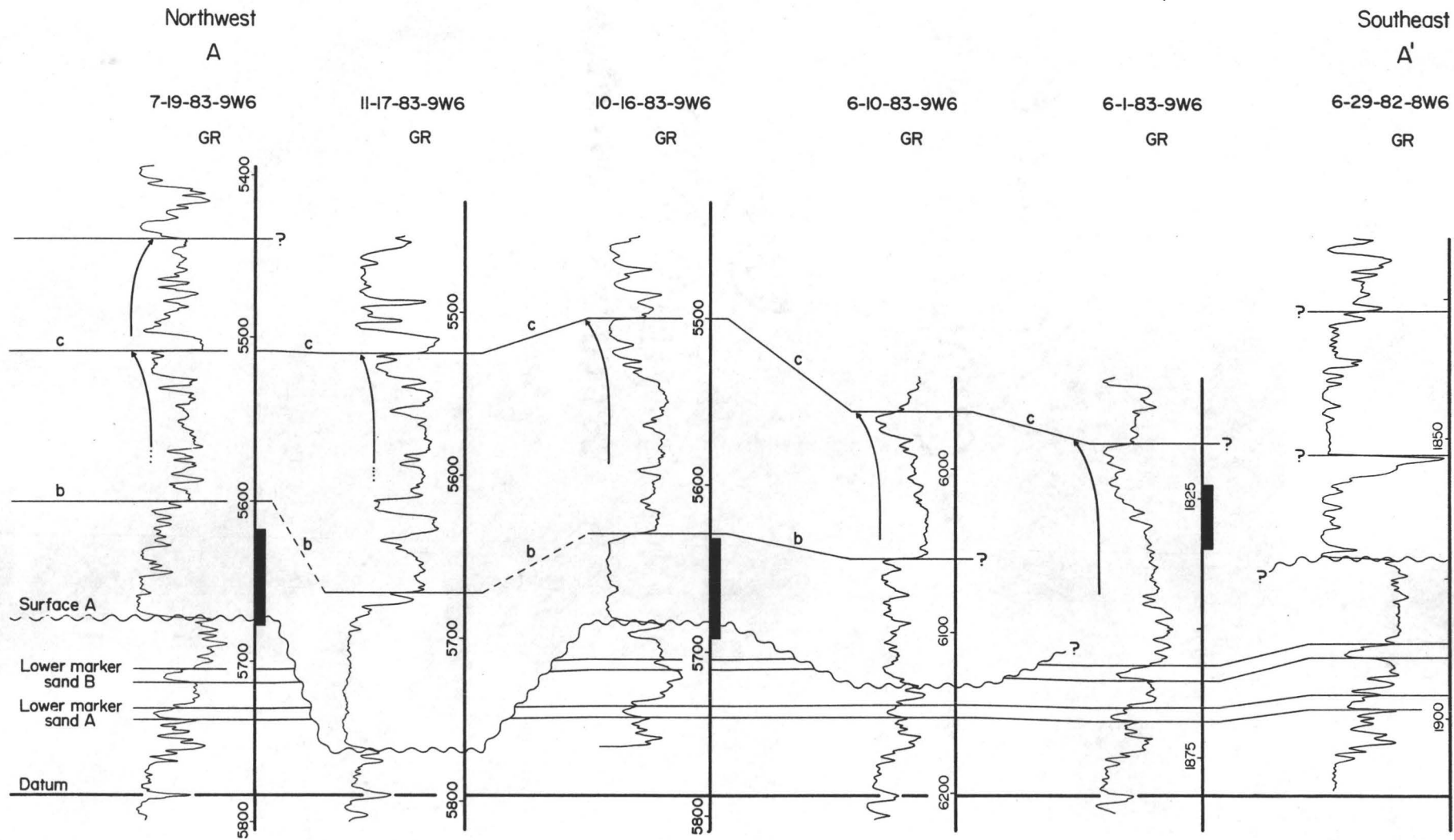
represents the sharp top of a well-defined coarsening upward cycle (representative of the funnel-shaped profile, GRF 3).

Cross-section B-B'   (Figure 3.11)

This section crosses most of the study area.   Surface A again cuts out the lower marker sand B in several wells.

CL-c is relatively easy to correlate and represents the change to a dominantly shale lithology (GRF 1) at the top of a fining upward gamma ray response (GRF 5). CL-b represents the base of this fining upward sequence which in core is a transition from fine-grained cross-bedded sands to very fine-grained rippled sands. The interval between Surface A and CL-b representing the blocky profile (GRF 4) shows a consistent decrease in thickness from both ends of the section to the middle. These correlations are well-defined except at the 13-35-83-9W6 well where CL-c was rather arbitrarily positioned immediately above the last occurrence of large sand peaks.

In the southwestern wells a coarsening upward cycle followed by a fining upward cycle can be correlated along the tops of these cycles (CL-d, CL-e).   The top of the fining upward cycle can not be correlated past 7-19-83-9W6.

In the wells farther to the northeast only the top of a coarsening upward cycle (CL-c) can be correlated above CL-c. This is only tentatively correlated to the coarsening upward cycle in the southwestern wells due to uncertainty in making

Figure 3.11   Cross-section B-B'.   Description   and

discussion in text.

Southwest
B

Northeast
B'

3-33-82-10W6
GR

10-3-83-10W6
GR

11-18-83-9W6
GR

7-19-83-9W6
GR

13-35-83-9W6
GR

16-1-84-9W6
GR

14-5-84-8W6
GR

10-9-84-8W6
GR

10-15-84-8W6
GR
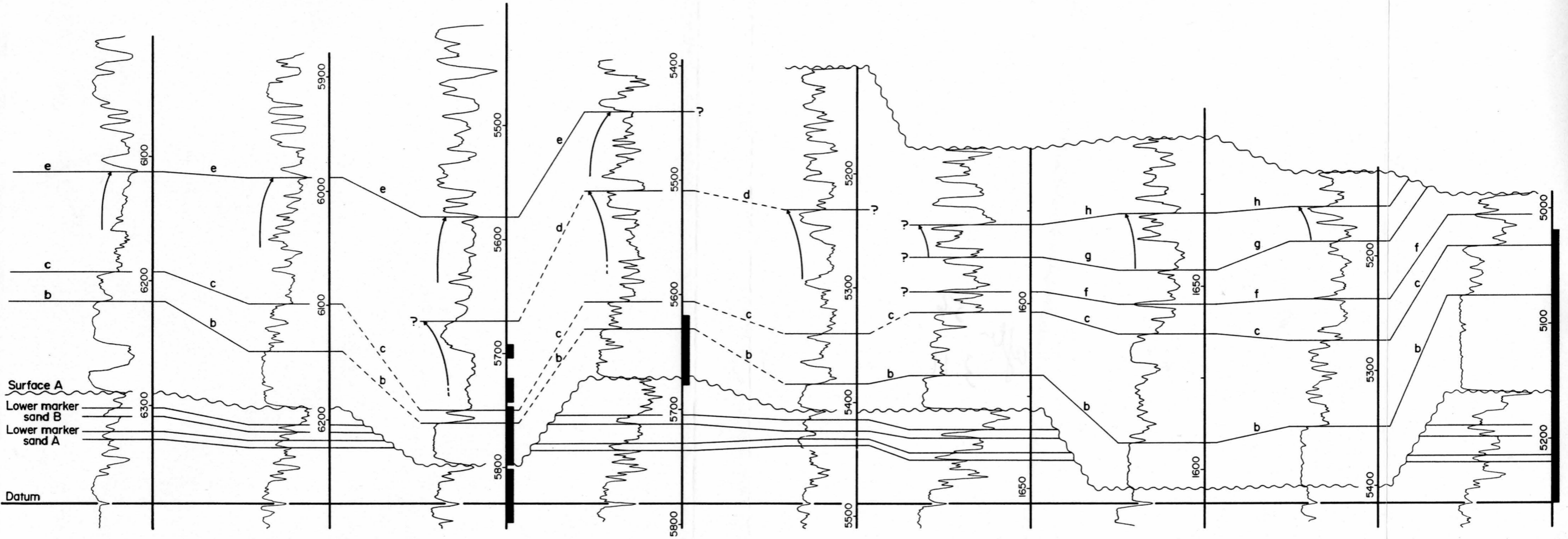
the correlation through the 13-35-83-9W6 well. The correlation of the top of the coarsening upward cycle is helped by several distinctive sand peaks which are correlated as CL-f and CL-g. The main implication of this correlation is that there appears to be an infilling of sediment in the 14-5-84-8W6 and 10-9-84-8W6 wells compared to the 16-1-84-9W6 well. This may, however, only be part of a general thinning of the basal section towards the middle wells which was also noted in the decreasing thickness of the blocky sands.

The base of the Belloy unconformity is shown at the top of the section and is cutting out the upper markers.

Cross-Section C-C' (Figure 3.12)

Most correlation lines on this section are well defined. Surface A again erodes the lowest sequence in one well (11-18-83-9W6) removing the lower marker sand B.

One interesting point on this cross-section is the complete loss of the blocky sand between Surface A and CL-b between wells 10-16-83-9W6 and 6-21-83-9W6 and its reappearance beyond 6-21-83-9W6 as a thin coarsening upward profile with a blocky response at the top. The correlation of the top of a coarsening upward sequence (CL-c) above CL-b is possible across the entire section. The base of this sequence, however, is variable in some wells.

Figure 3.12   Cross-section C-C'.   Description   and
discussion in text.

Southwest C — Northeast C'

Cross section showing GR logs for wells 10-6-83-9W6, 10-8-83-9W6, 10-16-83-9W6, 6-21-83-9W6, and 10-23-83-9W6, with correlation markers c, b, Surface A, Lower marker sand B, Lower marker sand A, and Datum.
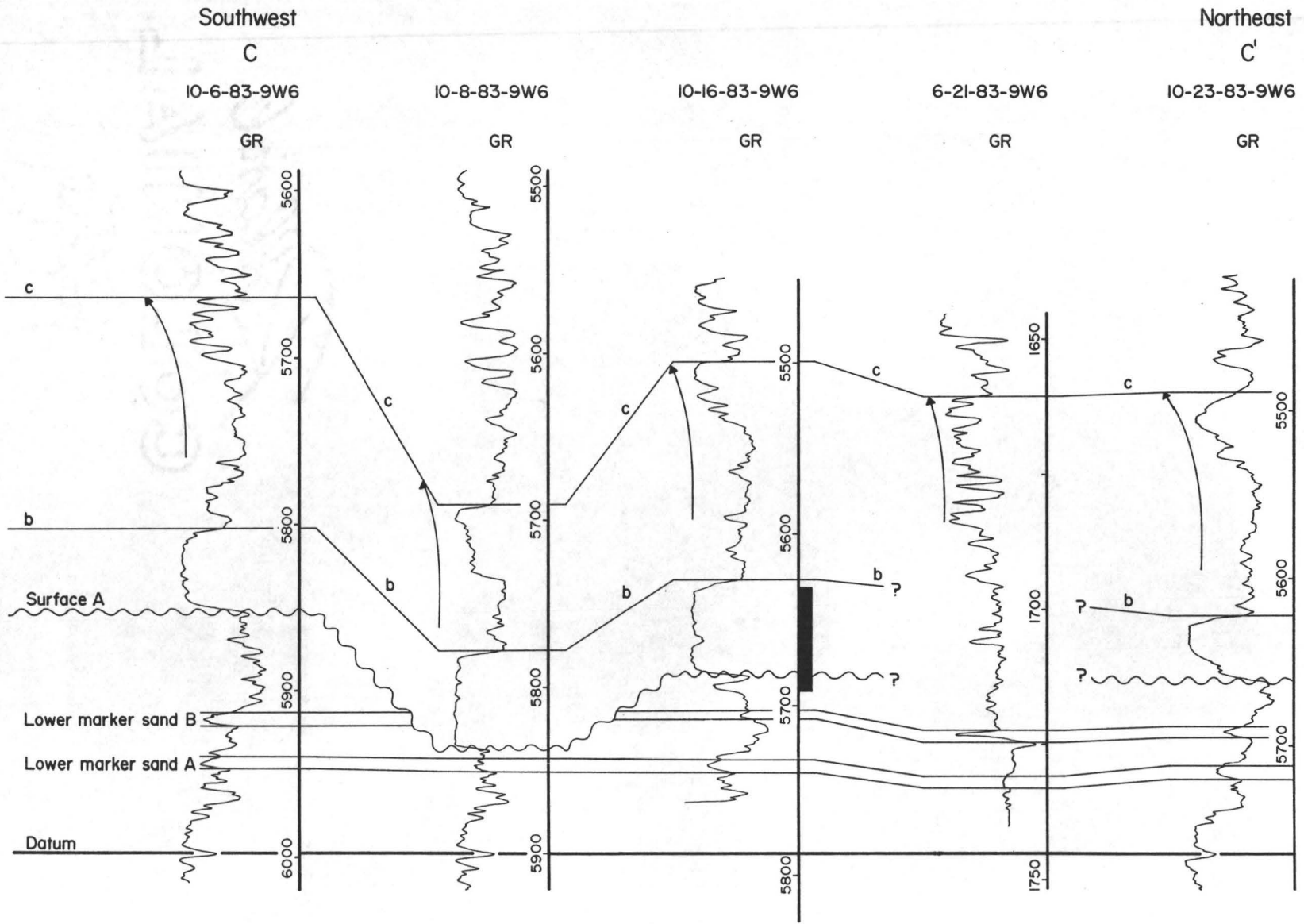
Cross-Section D-D'   (Figure 3.13)

This section poses several problems in correlation. As in cross-section A-A', there is a dramatic change in the gamma ray response, in this case between 14-24-82-9W6 and 6-29-82-8W6, which makes any correlation except of the lower marker sands impossible. This is, however, the only section in which both the lower marker sands are continuous across the entire length of the section.

Surface A was correlated at the sharp based transition from a straight shale baseline (GRF 1) to a dominantly blocky profile. CL-b was determined by observation of core to represent the top of a paleosol and coal facies (facies 1). This facies can be correlated across the northwestern portion of the section.   The other significant problem is the correlation of the top of the predominantly sandy unit above CL-b.   This correlation line (CL-c) was placed at the transition from a dominantly blocky profile to one with significant shale peaks, but is rather poorly defined. The reason for the huge increase in thickness between CL-b and CL-c in the 10-34-82-8W6 well is not known and with no core available to determine the nature of the sand, no definite answer is possible.

The two wells to the southwest were correlated at the top of two successive coarsening upward cycles (CL-d and CL-e) which could not be seen in the wells farther to the northeast.

Figure 3.13   Cross-section D-D'.   Description   and

discussion in text.

Southwest
D

Northeast
D'

6-22-82-9W6
GR

14-24-82-9W6
GR

6-29-82-8W6
GR

10-34-82-8W6
GR

10-9-83-8W6
GR

6-21-83-8W6
GR

3.3   Isopach Map

The isopach map (Figure 3.14) contains two sets of contours.   The first is an isopach from the Debolt datum to Surface A. The most important fact to observe on this isopach is that there are two rapid decreases in isopach thickness (to under 10 m) in T83-R9-W6 and T84-R8-W6. These are the areas in which significant erosion of the lower sequence occurred. If faulting did play   a role in the erosion of the lower sequence then two WNW to ESE trending normal faults would be inferred to exist along the northern margins of these isopach decreases.

The only problem associated with the creation of this map is the inability to define Surface A when a coarsening upward cycle instead of a blocky, sharp based sand rests on the lower marine shale sequence.   In this case, two shales lie one on top of the other and the location of Surface A is impossible to determine. This problem is localized to the most southern edge of the study area.

The second set of contours represents an isopach of the basal sand sequence, starting from Surface A to the top of the sand.   This isopach at times incorporates sands of slightly different character and also includes minor shale intervals. The justification for doing this is that sands of significant thickness with a blocky gamma ray profile have been tentatively interpreted to be sub-aerial deposits.   The

Figure 3.14   Isopach map.   Two separate sets of
                   contours are present. Solid lines   are
                   for the datum to Surface A isopach.
                   Dashed lines are for the basal sand
                   sequence isopach. Discussion in text.

T84

T83

T82

RIOW6   R9   R8
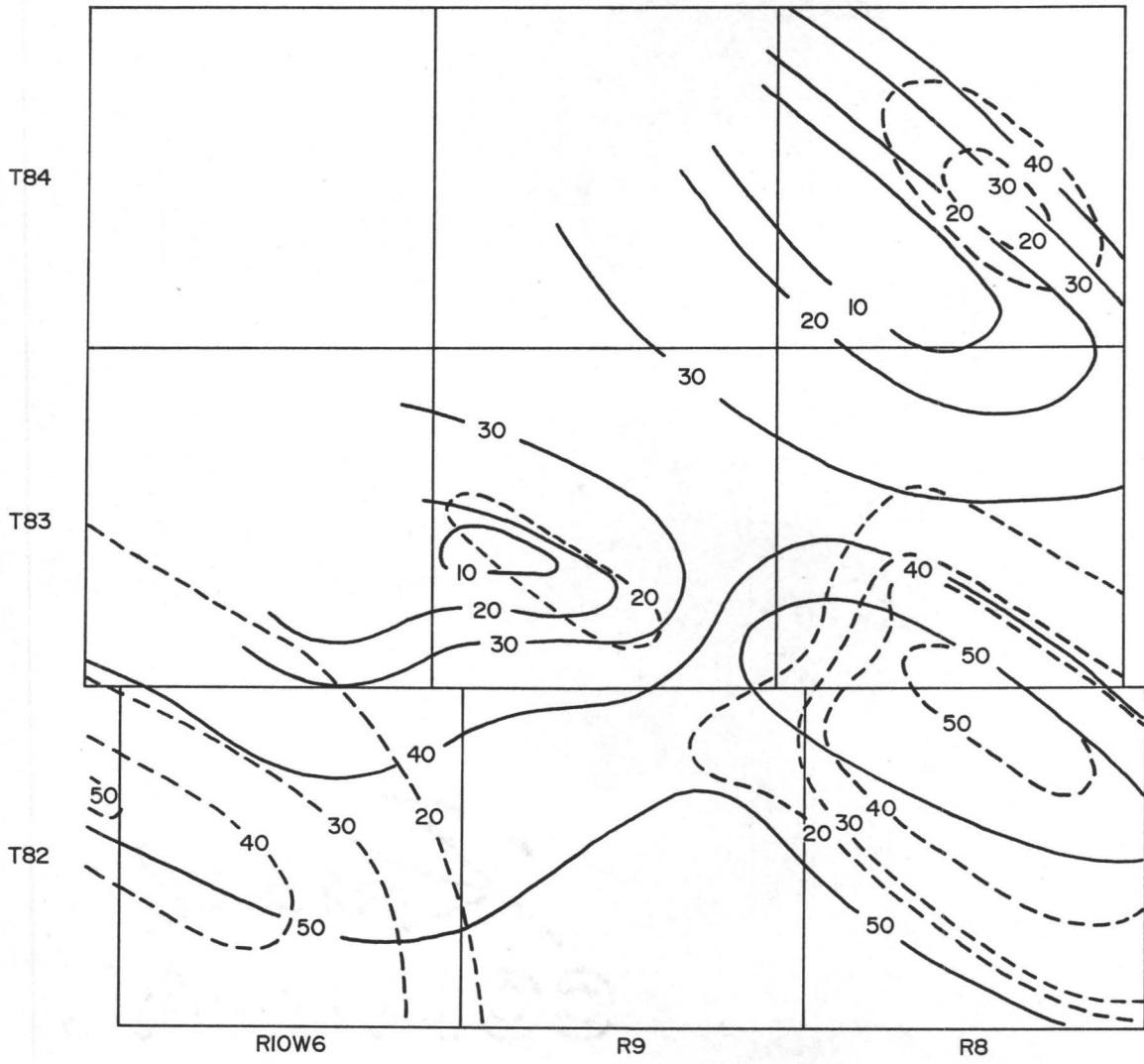
——— Datum to Surface A Isopach

– – – Basal Sand Sequence Isopach

Contours in metres

6 km
3 mi

Scale

isopach is only meant to indicate the relative thickness of various sands which are believed to have been deposited in a dominantly sub-aerial environment. It does not indicate the thickness variations of a single, continuous sand body.

The important point to recognize is that there is little correlation between the anomalies of the two isopachs. Areas of thick sand are found on areas of thick shales, thin shales or on the transition between the two. This indicates that the process which led to variations in the lower sequence below Surface A did not influence the deposition of the main basal sands above Surface A.

CHAPTER FOUR

PETROLOGY

To determine the composition, cementation history and possible provenence of the sands, numerous thin sections were cut from the different sand facies. Six of these sections, representing the cross-bedded sand facies (facies 2), the bidirectional rippled sand facies (facies 5b), the indistinctly bioturbated sand facies (facies 9), bioturbated interlaminated sandstone and mudstone (facies 6) and a carbonate cemented cross-bedded sand were studied on a petrographic microscope, under plane and cross polarized light. The modal percentages of the constituents were determined by a point count of 400 grains. To calculate the mean size and sorting of the specimens, the geometric mean size of 100 quartz grains was determined (method of Middleton, 1962) for five samples representing the first three facies above. The basic quartz type used by Basu et al. (1975) to determine the provenance of the source rocks was also calculated for these five samples. The remainder of the slides were examined in less detail to ensure that no significant textural or compositional characteristics escaped notice.

Seven samples were examined under cathodolumenescent microscope to add textural details and to determine the

cementation history. Four samples were examined under a scanning electron microscope to reveal the surface textures of quartz grains, the relationship of cements within the sample and to identify detrital and authigenic clays.

4.1 Modal Percentages

Table 4.1 summarizes the results of the modal analysis of the six sections. Quartz is the major component of all the slides. The only other consistently present constituent is clay and to a lesser degree, chlorite. Only trace amounts of feldspar were found since its untwinned character made it difficult to identify under the petrographic microscope. An examination using the cathodoluminescent microscope, where all feldspars are distinctively coloured might yield a higher modal percentage. Minor constituents found in a single section each include organic material, glauconite and sedimentary rock fragments. The main cements are quartz, dolomite and anhydrite/gypsum. Porosity is dominantly intercrystalline and varies according to facies and cement type.

The composition of each sample is plotted on a quartz-feldspar-rock fragment ternary diagram (Figure 4.1) (after Folk, 1968). Most samples plot as quartz arenites, one sample plots as a sublitharenite, while two samples which have high clay content would be termed quartz wacke or an

Table 4.1 Results of modal percentage calculations.

Sample	Location	Facies
1a	10-16-83-9W6 5641 ft	2 quartz cemented
1b	same	2 anhydrite/gypsum cemented
2a	10-15-84-8W6 5119 ft	2
2b	10-15-84-8W6 5076 ft	2 carbonate cemented
3	10-34-82-9W6 6120 ft	5b
4	6-1-83-9W6 1824.9 m	6
5	6-21-83-9W6 5149 ft	9

Sample	Quartz	Clay	Chlorite	Organics	Glauconite	SRF	Qtz O/G	Anhy/Gyp	Carbonate	Porosity	Other
1a	67.0	–	<1	–	–	–	18.5	<1	–	13.0	–
1b	64.0	1.0	<1	–	–	–	2.5	31.5	–	–	<1
2a	62.5	4.5	<1	–	–	–	14.8	<1	–	15.8	<1
2b	46.8	12.5	<1	–	–	–	3.5	–	33.8	2.0	1.0
3	76.5	<1	<1	–	–	5.8	9.0	–	2.5	2.5	3.0
4	44.2	16.5	–	6.2	–	–	8.8	1.0	17.2	1.5	4.5
5	67.5	12.8	–	–	3.8	–	7.8	–	–	4.5	2.8

Figure 4.1   Classification   of   sandstone   samples
                    using normalized percentages of quartz,
                    feldspar   and   rock   fragments.   (After
                    Folk, 1968)
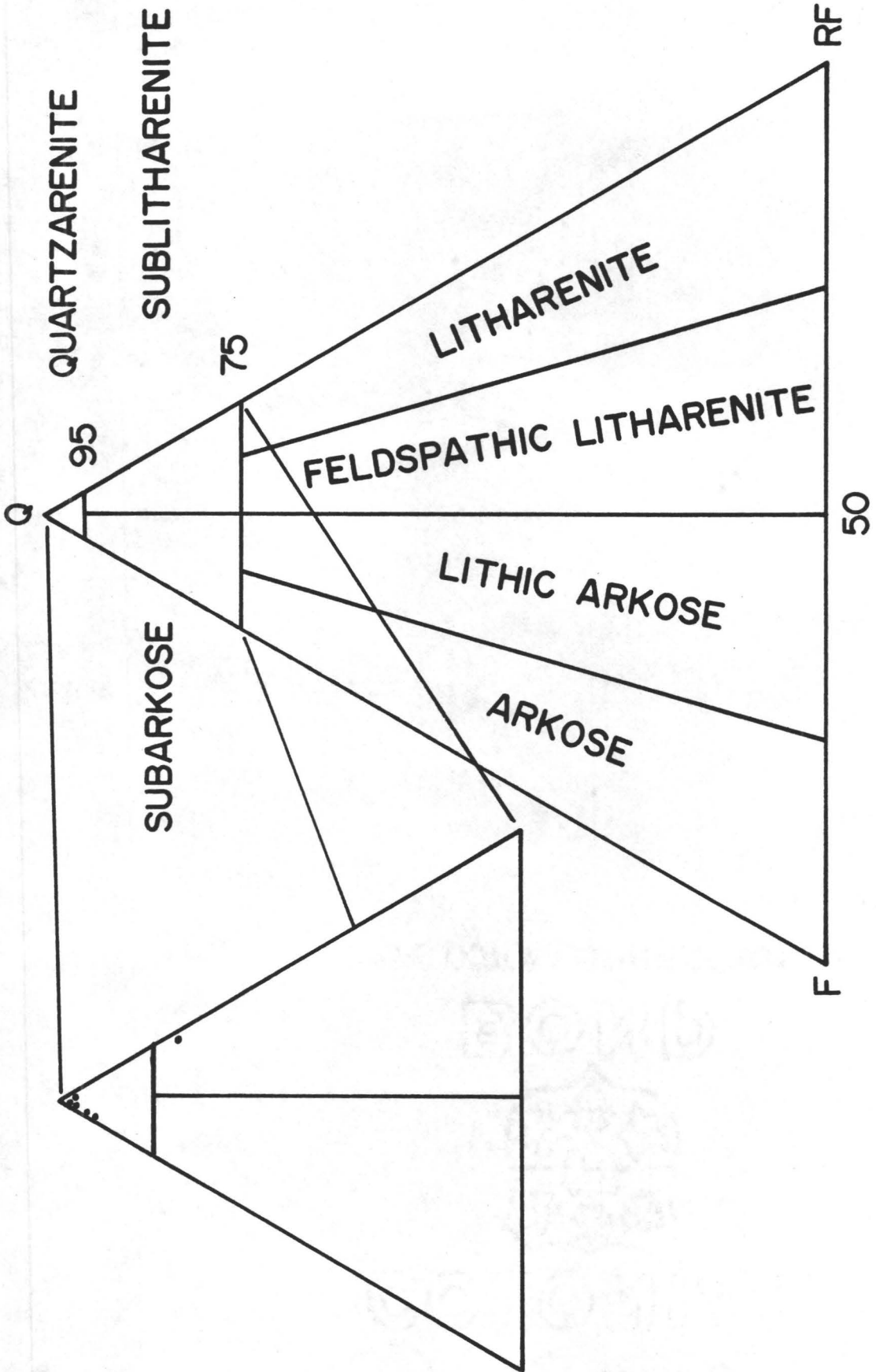
immature quartz arenite depending on the classification used
(Blatt et al., 1980, p. 373).

4.2 Constituents and their Textures

Quartz

The mean size, sorting and skewness was calculated using
the descriptive measures of Folk and Ward (1957) based on
the distribution of the geometric mean size of 100 quartz
grains.   Angle of repose cross-bedded sands (facies 2) were
found to be fine-grained, well sorted and had very little
skew.   One sample of this facies was and positively skewed.
The samples representing the indistinctly bioturbated and
bidirectionally rippled sandstone facies (facies 5b) were
very fine-grained, well sorted and had very little skew
(Figure 4.2).   Visual observation indicate that the grains
are generally sub-rounded to well rounded. Little preferred
orientation of quartz grains could be seen in the samples,
which is an observational problem related to the low
percentage of highly elliptical grains in the sample.

Quartz grains can be divided into one of four basic
types (after Basu et al., 1975):

1.   non-undulatory

2.   undulatory; requiring greater than 5 degrees to become
     fully extinct

Figure 4.2   Histograms and cumulative percentage

                          plots of five sandstone samples.

	Location	Mean Gr. Size(phi)	Sorting(phi)	Skewness
A	10-16-83-9W6 5684 ft facies 2	2.43 (fine sand)	.453 (well sorted)	.183 (nearly symmet)
B	10-15-84-8W6 5119 ft facies 2	2.57 (fine sand)	.377 (well sorted	.093 (nearly symmet)
C	7-19-84-8W6 5681 ft facies 2	2.37 (fine sand)	.457 (well sorted)	.768 (pos. skew)
D	6-21-83-8W6 5419 ft facies 9	3.63 (very fine sand)	.467 (well sorted)	.149 (nearly symmet)
E	10-34-82-9W6 6120 ft facies 5b	3.58 (very fine sand)	.480 (well sorted)	.257 (nearly symmet)

Numerical values for mean grain size, sorting and skewness

determined using method of Folk and Ward (1957).   Division

into classes using values of Dalrymple (1977).
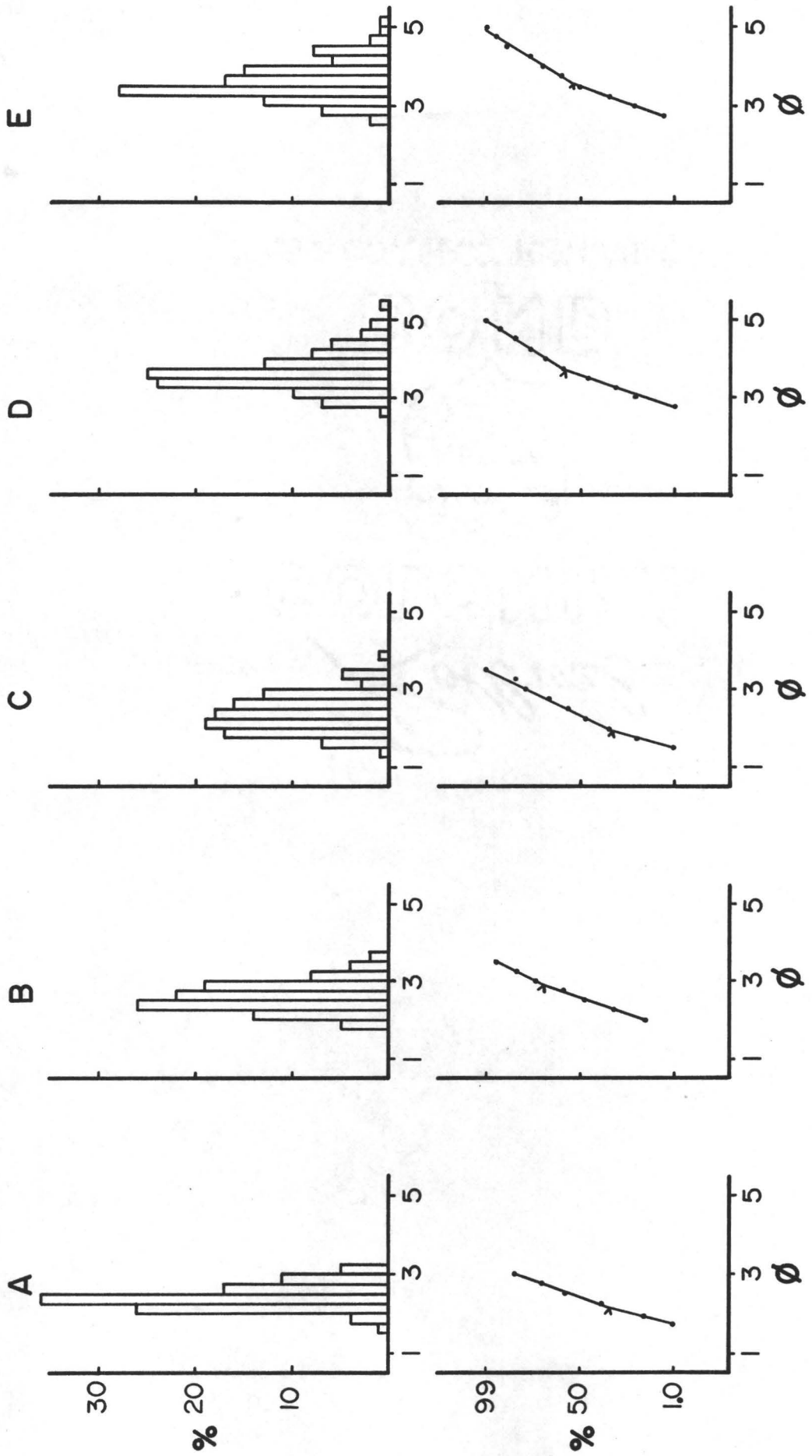
3.   polycrystalline; 2 to 3 crystals per grain

4.   polycrystalline; >3 crystals per grain

The mixture of these grain types has been used to identify the type of source rock of the sediment (Basu et al., 1975). The composition of the 100 grains in each of the five samples studied was tabulated (Table 4.2) and plotted on a double triangle diagram using the four quartz types (Figure 4.3) as the apices. The position of these points indicates a plutonic origin for the quartz, although they are very close to the boundary with the middle to high rank metamorphic region. Examination of the quartz grains under the cathodolumenescent microscope supports this conclusion. The majority of the quartz grains lumenesce a light blue to violet colour (Plate 4.1b) which is indicative of a plutonic terrain (Zingernagel, 1978, p. 12).

The sand grains often have syntaxial quartz overgrowths defined by thin dust lines (Plate 4.2) an these overgrowths tended to obscure the nature of the contacts between quartz grains. Observations using the C.L. microscope indicate that the fine-grained sediment most commonly has tangential to concavo-convex contacts (Plate 4.1b) while the very fine-grained sediment has contacts ranging from concavo-convex to slightly sutured.

Table 4.2   Percentages of the four basic quartz

                           types.

                           Sample   Location

                           1   10-16-83-9W6   5684 ft

                           2   10-15-84-8W6   5119 ft

                           3   7-19-83-9W6   5681 ft

                           4   6-21-83-8W6   5419 ft

                           5   10-34-82-9W6   6120 ft

Sample	Monocrystalline		Polycrystalline	
	non-undulose	undulose	2-3 crystals	>3 crystals
1	81	18	1	-
2	87	12	1	-
3	83	17	-	-
4	84	16	-	-
5	84	16	-	-

Figure 4.3   Plot relating basic quartz types to provenance of source rocks. (after Basu et al., 1975)

Polycrystalline quartz
(2–3 crystal units per grain; ≥75%
of total polycrystalline quartz)

PLUTONIC

MIDDLE & UPPER
RANK METAMORPHIC

Non-
undulatory
quartz

Undulatory
quartz

LOW RANK
METAMORPHIC
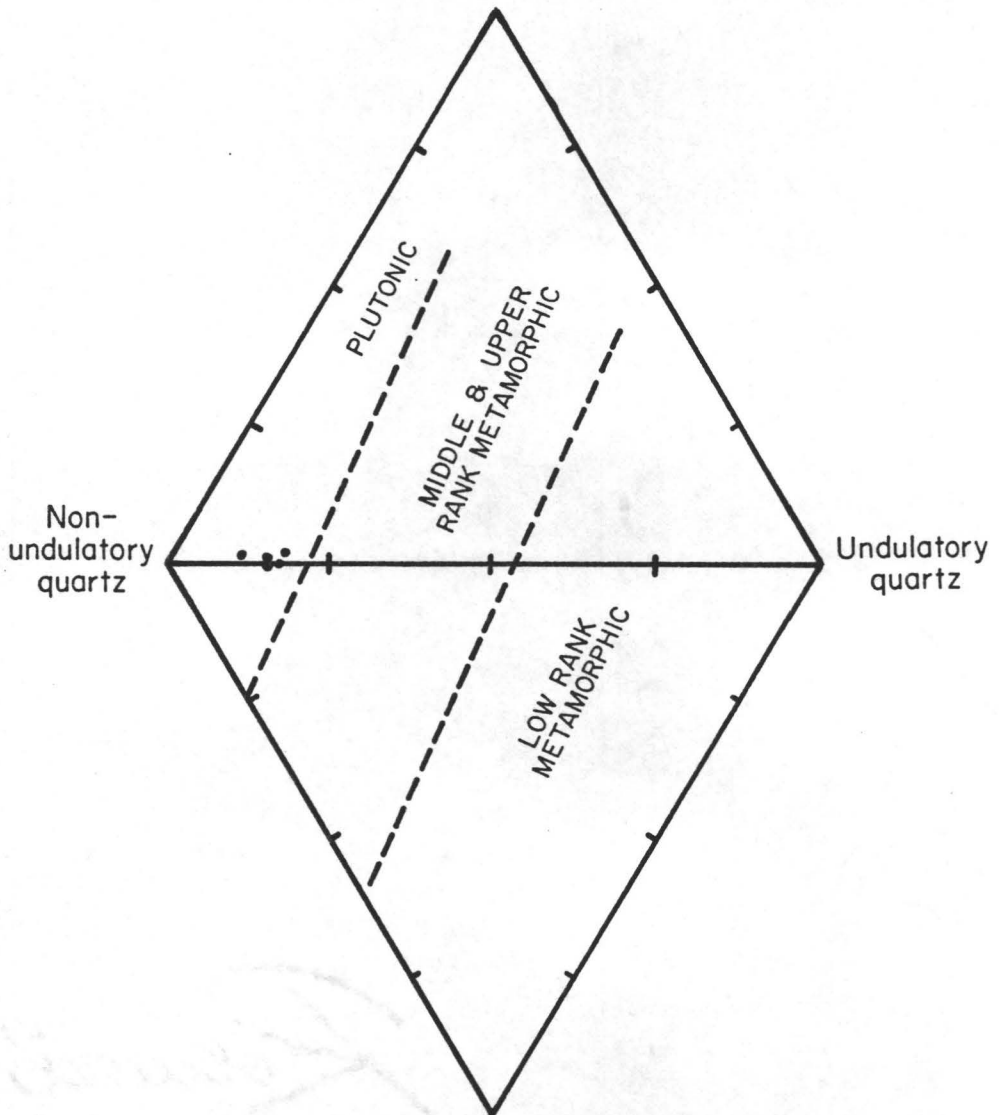
Polycrystalline quartz
(>3 crystal units per grain; >25%
of total polycrystalline quartz)

Plate 4.1   Plane   polarized   photomicrograph (4.1a)

and   cathodolumenescent   photomicrograph

(4.1b) of an quartzarenite sample. Note

the light blue to violet lumenescence of

the quartz grains in 4.1b.

(10-16-83-9W6   5641 ft; 28 X mag.)
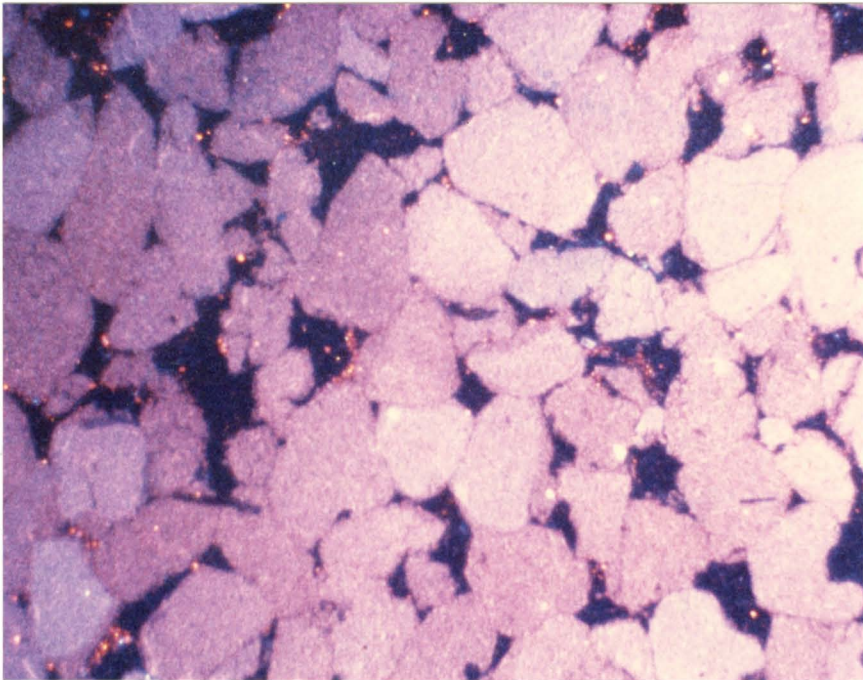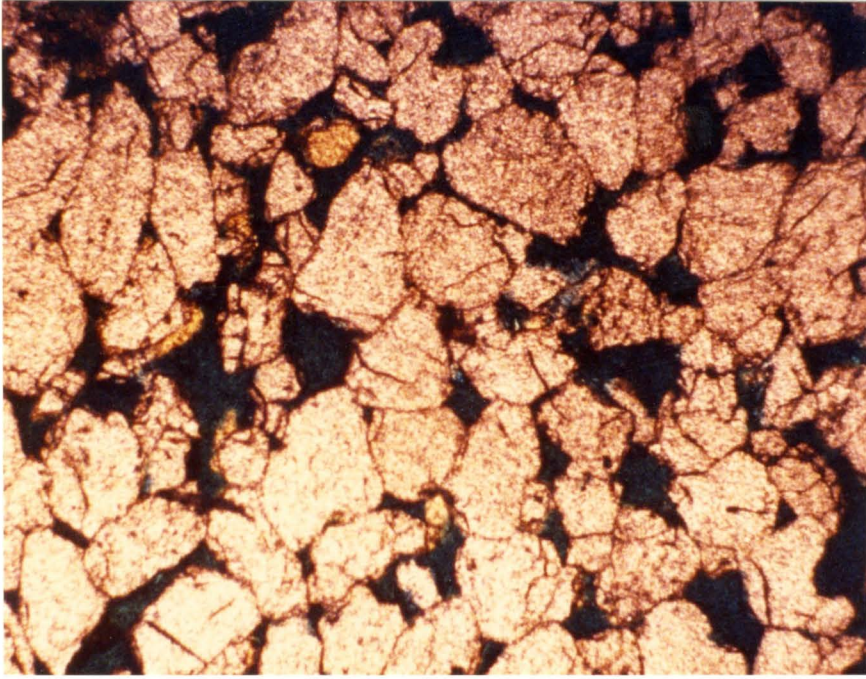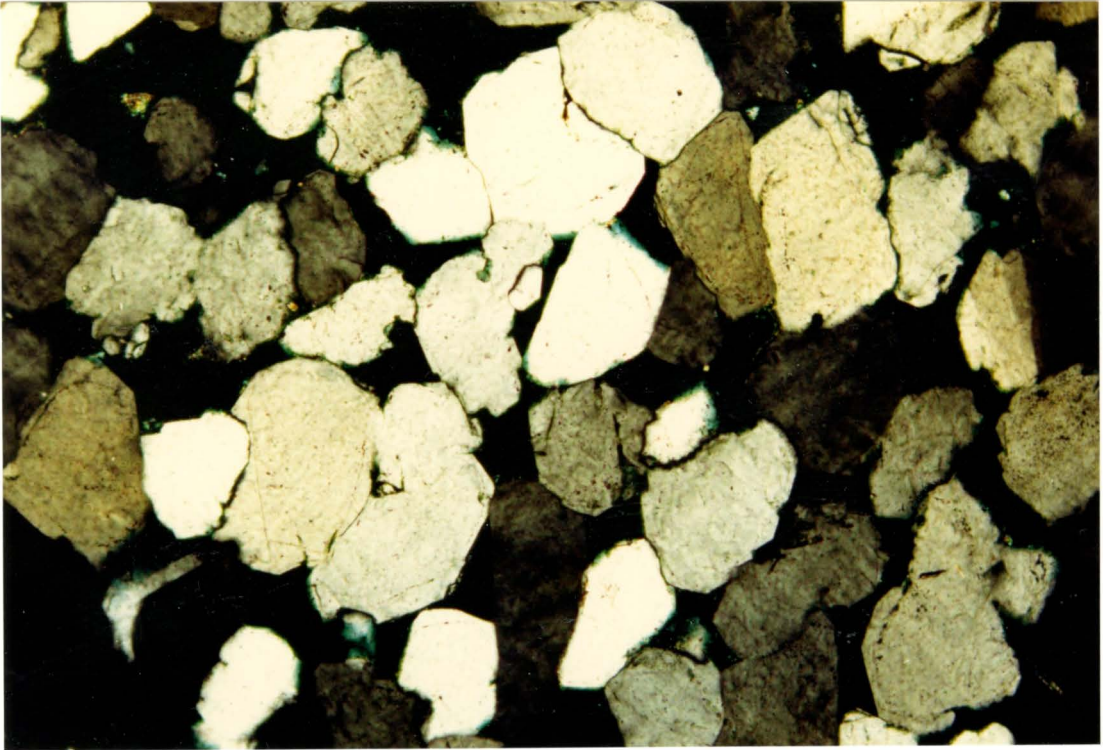
Plate 4.2   Photomicrograph of quartzarenite under
                   cross polarized light (4.2a) and plane
                   polarized light (4.2b). Note syntaxial
                   quartz overgrowths which are sometimes
                   defined by thin dust lines.
                   (10-16-83-9W6 5684 ft; 63 X mag.)

Clay and Chlorite

The percentage of clay and chlorite varies tremendously within the samples. The cross-bedded sands, interpreted to be aeolian, have very little clay or chlorite while the samples from other facies, having subaqueous interpretations, have increased clay and chlorite (Plate 4.3). It is very difficult to separate these minerals into detrital or authigenic components. Evidence of clay preventing quartz overgrowth nucleation as well as preventing corrosion by calcite and anhydrite/gypsum cements (Plate 4.4) is found in a number of samples.

Other Constituents

The samples from facies interpreted to be sub-aqueous also show the most variety in minor constituents. Various samples contained abundant organic matter, glauconite or sedimentary rock fragments. The presence of these constituents is due to both the poorer winnowing of these environments compared to the aeolian setting, as well as the fact that some of these constituents would only be produced in a sub-aqueous environment.

4.3 Cements

Carbonate

Excluding the dolomite derived from primary carbonate which is found at the base of the Stoddart Formation in the

Plate 4.3   Sample   of   indistinctly   bioturbated
                   sandstone. Note the interstitial clay
                   which fills most of the pore space.
                   (6-21-83-8W6 5419 ft; 63 X mag. PPL)

Plate 4.4   Anhydrite at   contact 1 is corroding the
                   quartz grain while at contact 2, a thin
                   layer   of   clay? is preventing such
                   corrosion.
                   (6-10-83-9W6 5743 ft; 250 X mag. PPL)
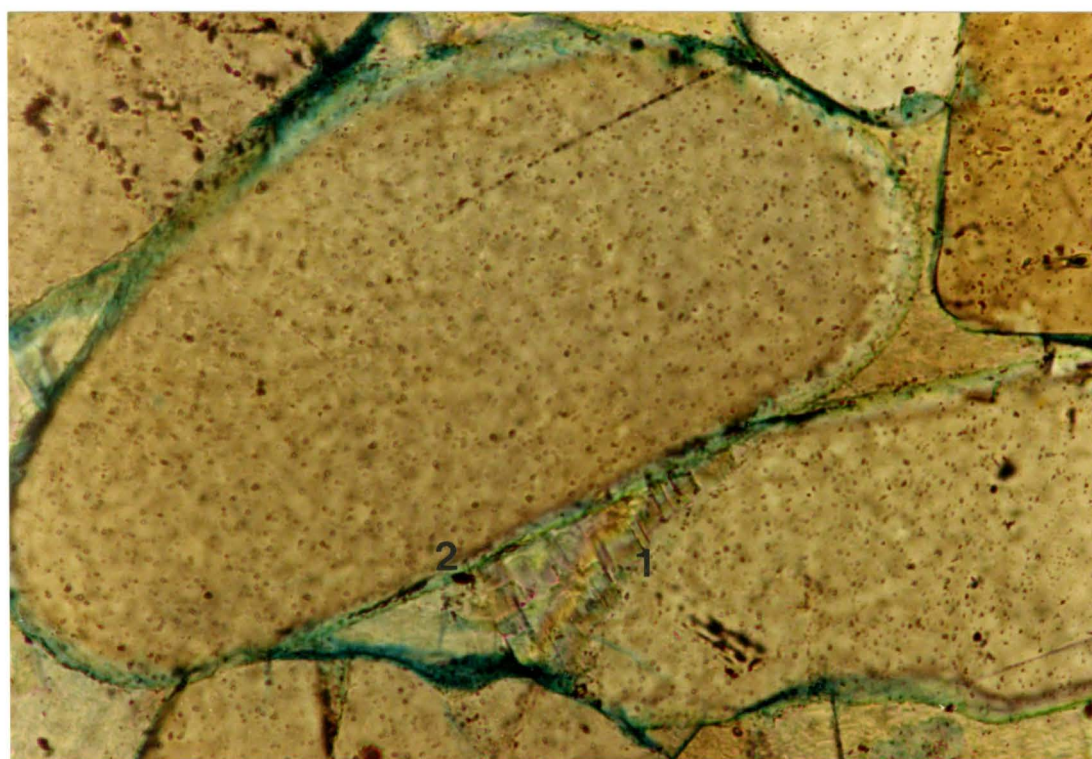
transition from the Debolt Formation, dolomite is also found as a cement in the samples taken from the sand facies. The dolomite is restricted to the upper portions of the sequence studied. In the thick sand unit of the 10-15-84-8W6 well, a systematic decrease of carbonate cement with depth is recorded while quartz cementation increases. The carbonate has a distinctly bimodal occurrence (Plate 4.5). Samples taken from higher in the well have better definition of the rhombohedral dolomite morphology and have a rim of calcite cement around the dolomite rhombohedrons (compare Plate 4.6 and Plate 4.7).

In the carbonate cemented sample which was point counted, approximately 34% carbonate cement was present. Blatt et al. (1980, p. 345) state that carbonate cement rarely exceeds 30%, which is the optimal original porosity of a sandstone, unless the carbonate etches and replaces the detrital grains. Plate 4.5 illustrates that this is the case in these samples. This plate also illustrates that detrital quartz grains appear to be floating in carbonate cement which Tucker (1981, p. 57) believes is due to displacement of grains during carbonate precipitation.

Quartz

Quartz is the most important cement in the samples. It occurs as euhedral syntaxial growths on detrital quartz grains. These overgrowths can often be defined by a

Plate 4.5   Carbonate cemented sandstone.   Note the distinctly   bimodal   occurrence   of carbonate.

(10-15-84-8W6 5040 ft; 63 X mag., CPL)

Plate 4.6   Good rhombohedral shape is present in some   dolomite   crystals.   A thin calcite coating is present on most of the dolomite.

(10-15-84-8W6 5040 ft; 28 X mag.,

CL light)

Plate 4.7   Dolomite   cemented   sandstone   found stratigraphically lower than the one in Plate 4.6.   Note lack of both good dolomite rhombs and calcite coating.

(10-15-84-8W6 5070 ft; 28 X mag.,

CL light)
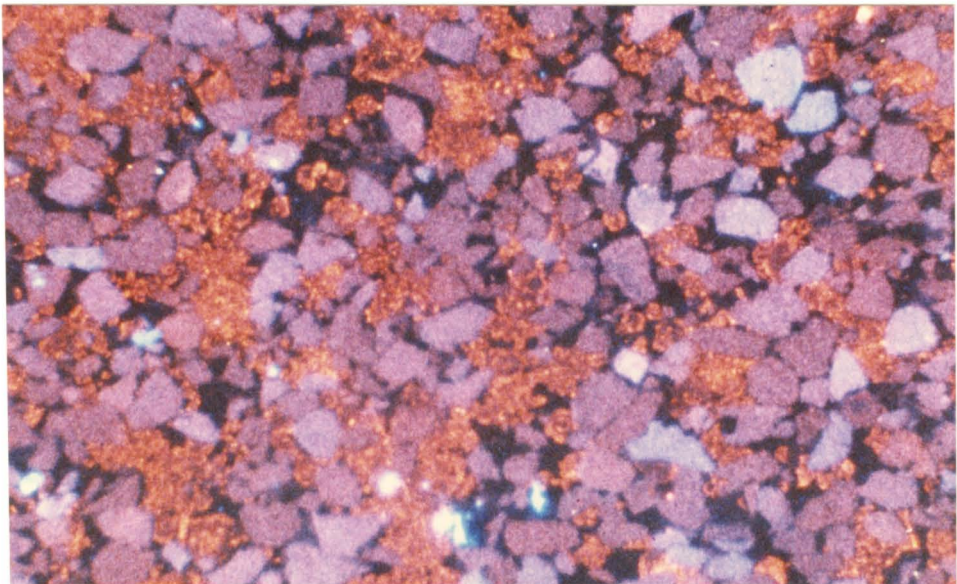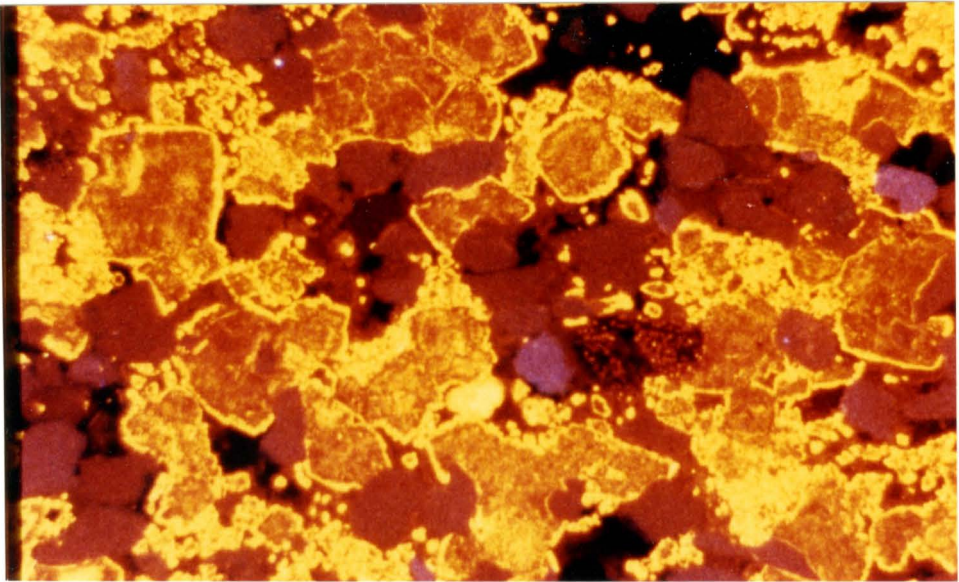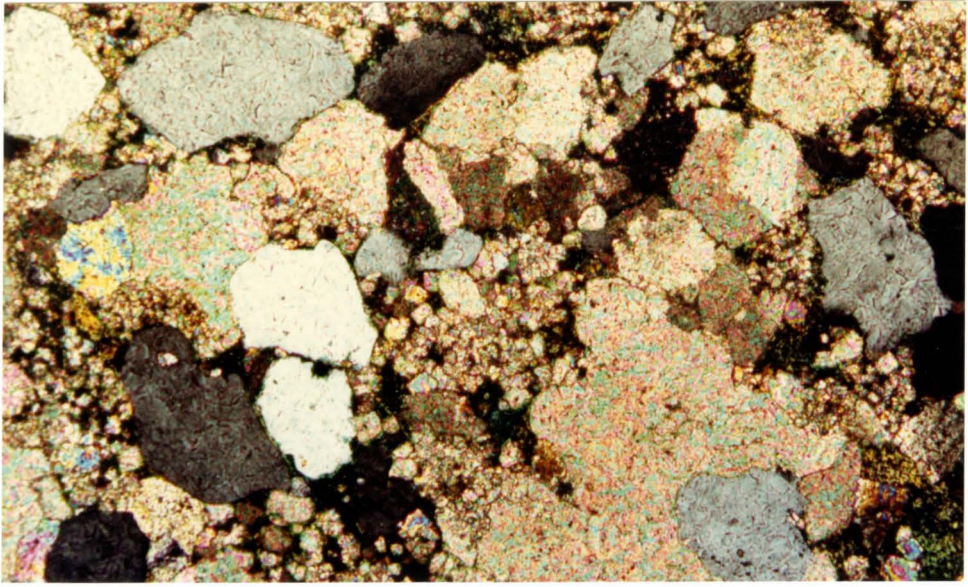
thin dust coating on the original grain (Plate 4.2b) but are difficult to distinguish when the coating is not present, except under a C.L. microscope.

The growth of quartz overgrowths is prevented or restricted in three situations in the samples. These are: 1) when there is a large percentage of interstitial clay in the sample; 2) if the sample has been previously cemented by calcite; and 3) when the sand is very fine and there is much less initial pore space in which the quartz overgrowths can form.

Numerous sources of diagenetic silica to form quartz cement have been reported. Many of these, such as diagenetic dissolution of silicate minerals, devitrification of volcanic detritus, dissolution of the siliceous tests of some microorganisms or silica released during the diagenetic change of mixed layer smectite-illite to pure illite (Blatt et al., 1980, p. 344), can not be applied to these samples. However, pressure solution of quartz, expressed as stylolites (Plate 4.8) or penetration of grain-grain contacts, can act as a source for diagenetic silica and are extensively found in these samples. Sibley and Blatt (1976) demonstrated that pressure solution could only account for one-third of the volume of secondary silica present in a quartz cemented sandstone. The only other source for the remaining cement would be from precipitation of silica from subsurface waters (Blatt et al., 1980, p. 344). Sibley and

Blatt (1976) concluded that vertical rather than horizontal circulation of groundwater was required to precipitate the neccessary amount of silica.

Anhydrite

Anhydrite cement is present predominantly in high angled, cross-bedded sands in discontinuous patches and small specks. The presence of anhydrite cement has a very corrosive effect on the quartz grains and quartz overgrowths (Plate 4.9). Levandowski et al. (1973) noted similar etching of quartz grains by anhydrite but did not advance a process to explain it. Table 4.1 (first two rows) illustrates the fact that the modal percentage of anhydrite/gypsum is equal to the porosity, most of the quartz overgrowth plus some of the detrital quartz percentage in the anhydrite free zone.

The presence of anhydrite/gypsum cement in a sand interpreted to be aeolian might reasonably thought to be from precipitation in small evaporating brine pools. The petrographic evidence indicates that this is not the case. Comparison of Plate 4.10 and 4.11 indicate that there is no significant difference in the nature of grain contacts betweeen an anhydrite/gypsum cemented zone and a quartz cemented zone from a single thin section. In addition, Plate 4.10 has examples of anhydrite etching both detrital

Plate 4.8   A stylolite traversing a quartzarentite
                     sample.

                     (10-3-83-10W6 6156 ft; 63 X mag., PPL)

Plate 4.9   Corrosion   of   quartz grains (Q) by
                     anhydrite (A) and gypsum (G).

                     (10-16-83-9W6 5641 ft; 160 X mag., CPL)
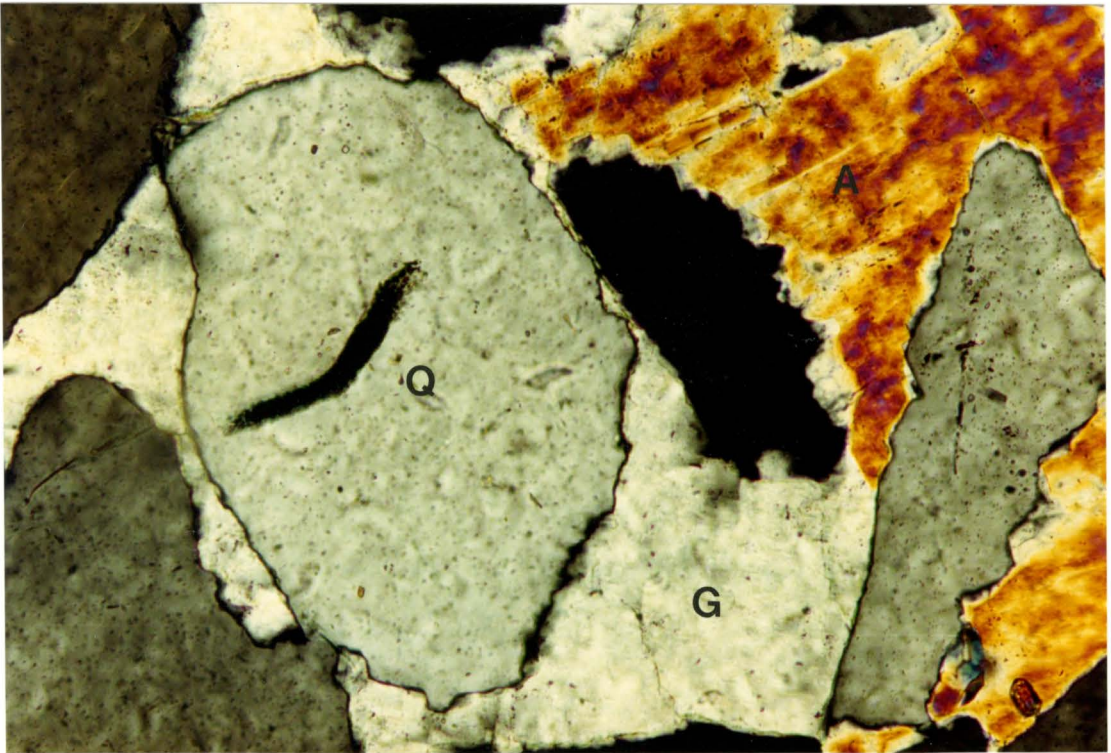
Plate 4.10   Anhydrite/gypsum cemented sandstone.
              Note tangential to concavo-convex
              contacts. Arrow indicates a thin
              meniscus of quartz overgrowth which has
              survived corrosion.
              (10-16-83-9W6 5641 ft; 35 X mag.,
              CL light)

Plate 4.11   Quartz cemented sandstone from same thin
              section as 4.10.   Contacts are also
              tangential to concavo-convex.
              (10-16-83-9W6 5641 ft; 35 X mag.,
              CL light)
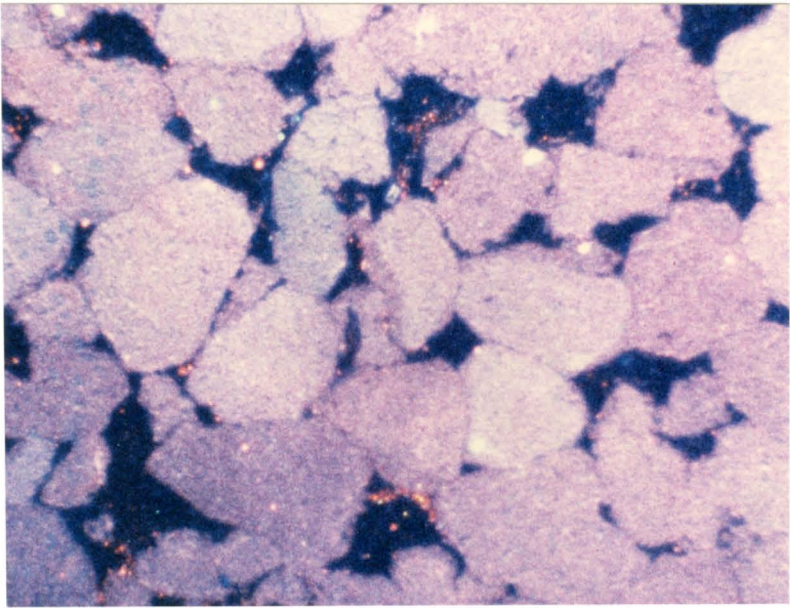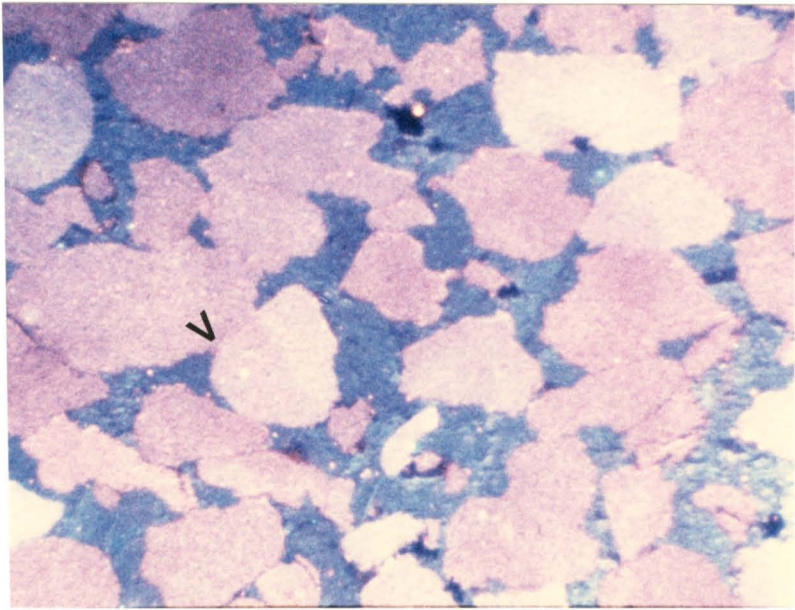
grains and overgrowth but leaving a small meniscus between two adjacent quartz grains.

4.4 Porosity

Three major porosity types were observed:

1. intergranular
2. thin porosity rims on detrital grains
3. fracture porosity created by the separation of mud lamellae

Plates 4.12, 4.13 and 4.14 illustrate these porosity types. Intergranular porosity is by far the most common.

An appreciable amount of porosity is only found in the fine-grained sands which are cemented by quartz and are free of clay. Both carbonate and anhydrite/gypsum cements completely seal the sand. Very fine-grained sands have very little porosity due to a lower primary porosity in addition to the increased interstitial clay found in these sands.

4.5 Scanning Electron Microscope Results

Four samples were examined using a scanning electron microscope to study quartz surface textures, the relationship of different cements and to identify clays and other fine-grained components in the samples.

Plate 4.12   Intergranular porosity.

                    (10-16-83-9W6 5641 ft; 63 X mag., PPL)

Plate 4.13   Thin porosity rim around quartz grain.

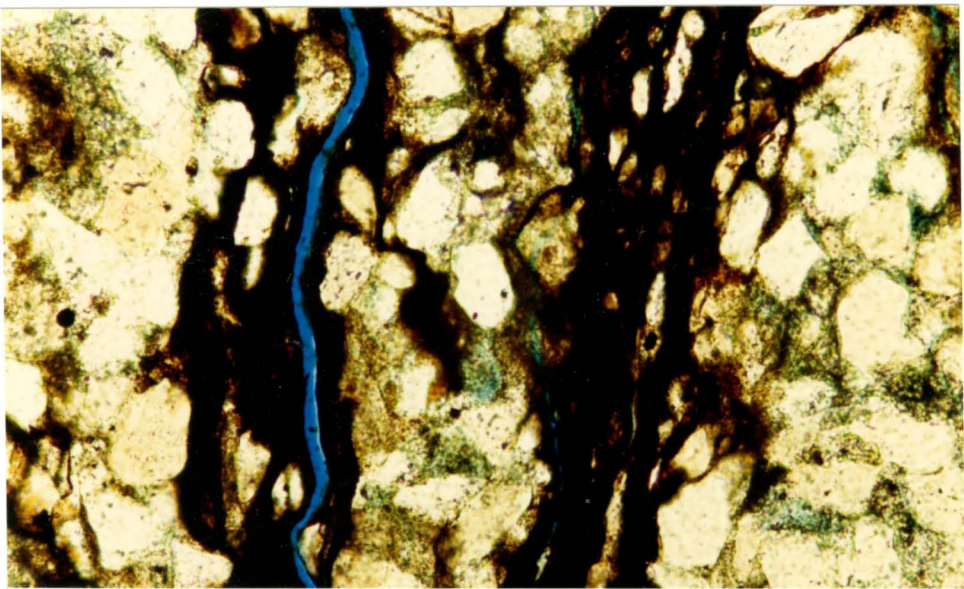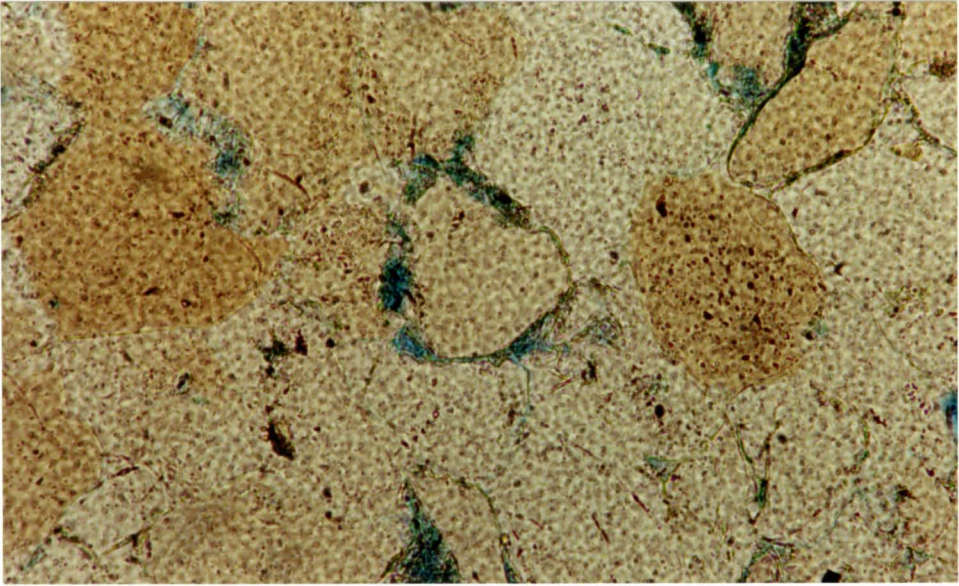   (10-34-82-9W6 6120 ft; 160 X mag., PPL)

Plate 4.14   Fracture porosity in mud lamella.

                    (6-1-83-9W6 1824.9 m; 160 X mag., PPL)

Quartz Surface Textures

Krinsley and Doornkamp (1973, p. 8) believe that grain morphology is diagnostic of the environmental history of the area from which the grains have come. An environmental interpretation is only valid when a number of complimenting characteristics are present with strong intensity. In the samples examined, the most common textures observed were precipitated and mechanically formed upturned plates and irregular solution-precipitation surfaces (Plate 4.15). The roundness of grains is obscured by quartz overgrowths (Plate 4.16b). Minor numbers of V-shaped pits are seen in some samples (Plate 4.15d).

There is not enough evidence in the samples to identify an environment from surface textures alone. In addition, a diagenetic overprint may easily have obscured primary textures. Nevertheless, except for the mechanical V-shaped pits which indicate this sand may have spent time in a beach environment, none of the surface textures would contradict an aeolian interpretation of these sands.

Cement History

No new information on the cementation history could be extracted from the SEM examination although it did confirm previous observations. Plate 4.16a illustrates the lack of quartz overgrowths in samples with high clay content (compare to Plate 4.16b).

Plate 4.15   Quartz surface textures as observed
                    under SEM.   Textures dominated by
                    precipitated and mechanically formed
                    upturned plates and irregular solution-
                    precipitation surfaces.   Minor numbers
                    of V-shaped pits (4.15d) observed in
                    some samples.

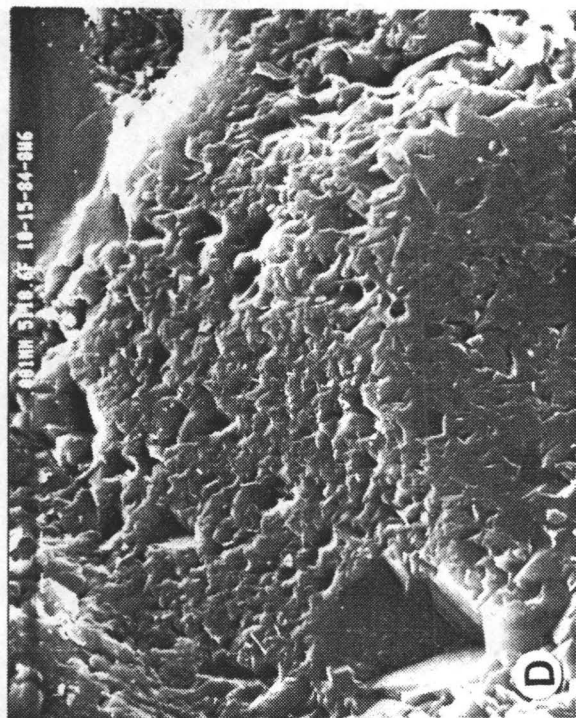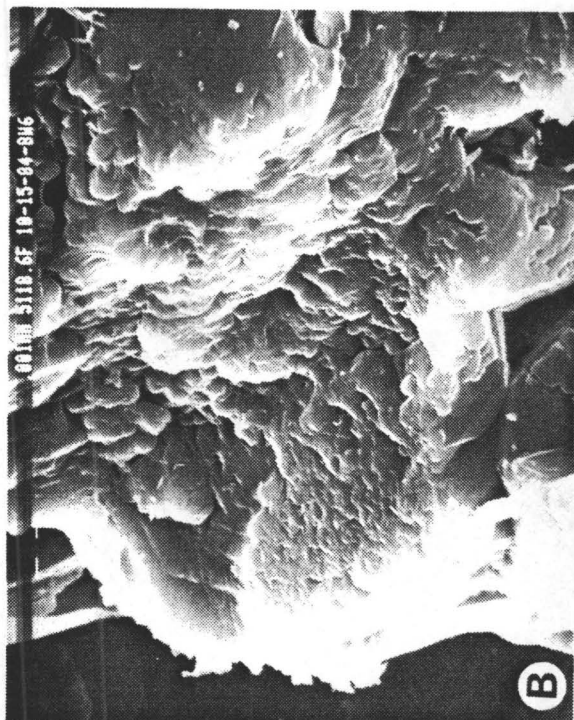   (10-15-84-8W6 5118.6 ft

                         a - 1600 X mag.

                         b - 2500 X mag.

                         c - 400 X mag.

                         d - 2500 X mag.)
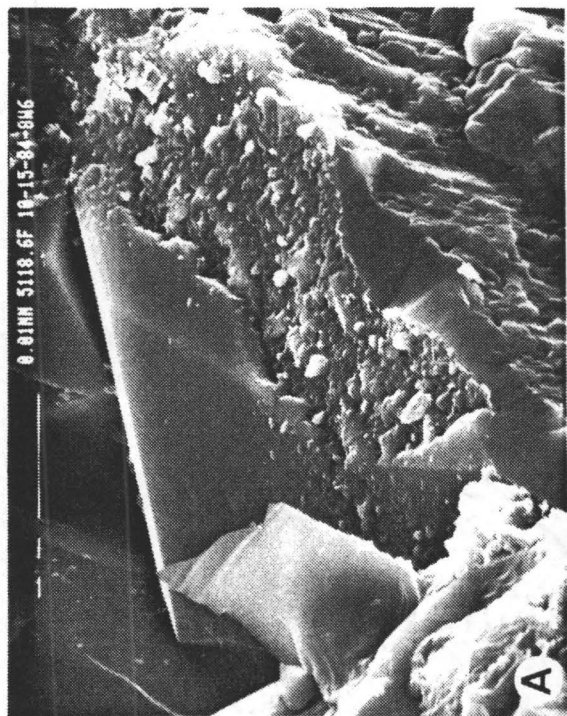
Excellent quartz overgrowths are present in most samples (Plate 4.16c) while clay material or the quartz grain in Plate 4.16d appears to be inhibiting the growth of quartz overgrowths on its surface.

The corrosive effect of anhydrite/gypsum cement (Plate 4.17b with Energy Dispersive X-ray analysis (EDX) - Plate 4.17d) can be seen in Plate 4.17c. The material in Plate 4.17c was analysed as quartz but has a very angular surface where anhydrite/gypsum cement contacted and etched the quartz grain.

Clay Mineralogy

Three fine-grained constituents were identified by the SEM and EDX analysis. These were kaolinite booklets growing on grains and filling pore throats (Plates 4.18a and c). Plate 4.18b shows illite growing on the surface of quartz grains; illite was also seen filling pore throats. An iron rich chlorite was seen in one sample as well (Plate 4.18d).

4.6 Petrologic Interpretation and Conclusions

The sand of the cross-bedded sandstone facies (facies 2) is well sorted, well-rounded, fine-grained and mineralogically mature. All these characteristics are typical of wind transported sands. In addition, the lack of a coarse tail in these samples (Figure 4.2a and b) has been

Plate 4.16a   High proportion of interstitial clay
               prevents   the   formation   of   quartz
               overgrowths. Compare to 4.16b.
               (6-1-83-9W6   1824.86 m; 175 X mag.)

Plate 4.16b   Syntaxial   quartz overgrowths developing
               on quartz grain.
               (10-16-83-9W6   5641.7 ft; 85 X mag.)

Plate 4.16c   An   excellent   example   of   a   quartz
               overgrowth.
               (10-3-83-10W6 6156.1 ft; 1300 X mag.)

Plate 4.16d   Apparent   inhibition   of   quartz
               overgrowths by clay on surface of grain.
               (10-3-83-10W6   6156.1 ft; 900 X mag.)
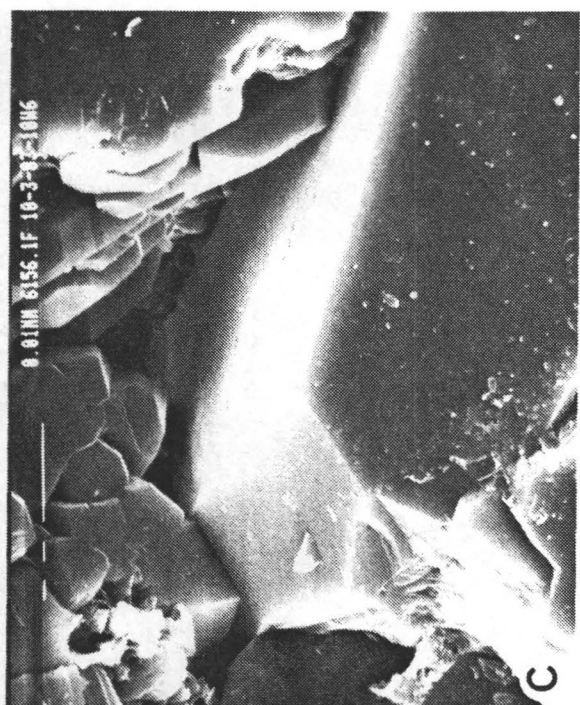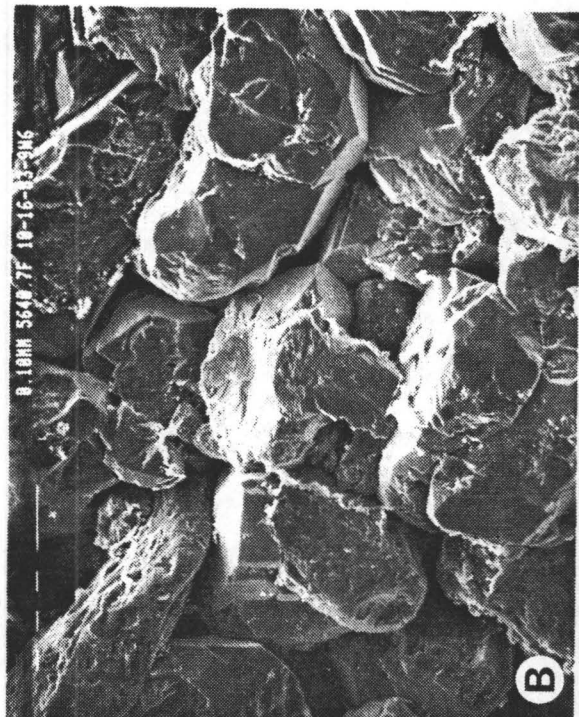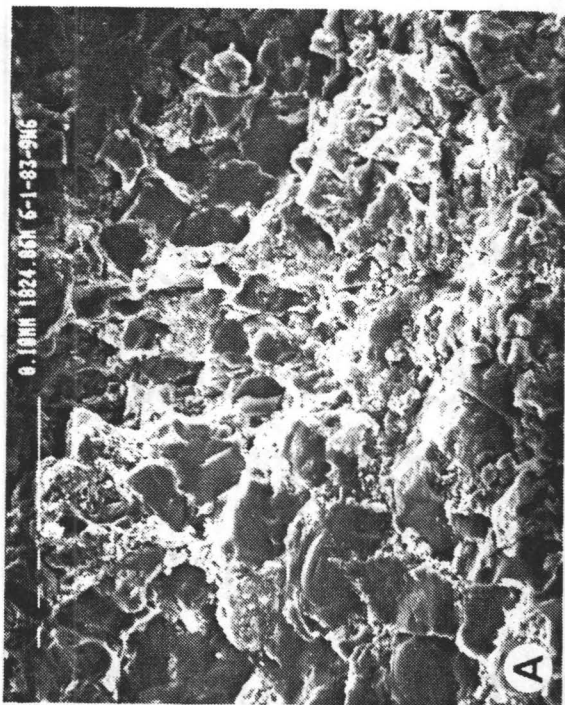
Plate 4.17a   Very angular surface on quartz grain.
                     Anhydrite/gypsum cement present around
                     edge of grain.
                     (10-16-83-9W6 5640.7 ft; 175 X mag.)

Plate 4.17b   Enlargement of anhydrite/gypsum cement.
                     EDX analysis (4.17d) was taken at point
                     indicated by the arrow.
                     (10-16-83-9W6 5640.7 ft; 450 X mag.)

Plate 4.17c   Enlargement of surface of quartz. (EDX
                     analysis at arrow indicates only silica
                     present). The very angular nature of the
                     surface is believed to be a reflection
                     of   the   corrosion   caused   by
                     anhydrite/gypsum cement.
                     (10-16-83-9W6 5640.7 ft; 450 X mag.)

Plate 4.17d   EDX analysis of cement in 4.17b.   Equal
                     amounts of   Ca and   S indicate the
                     material is anhydrite or gypsum.
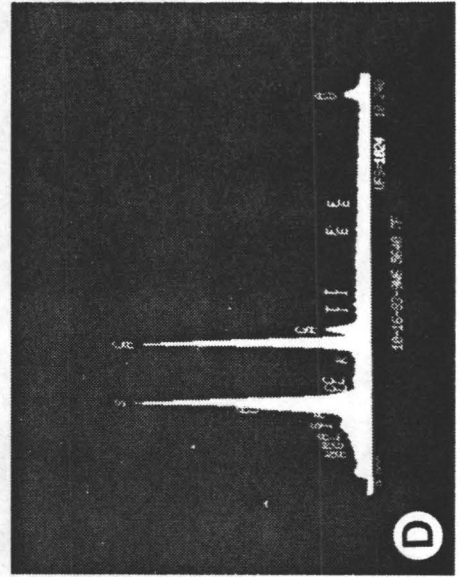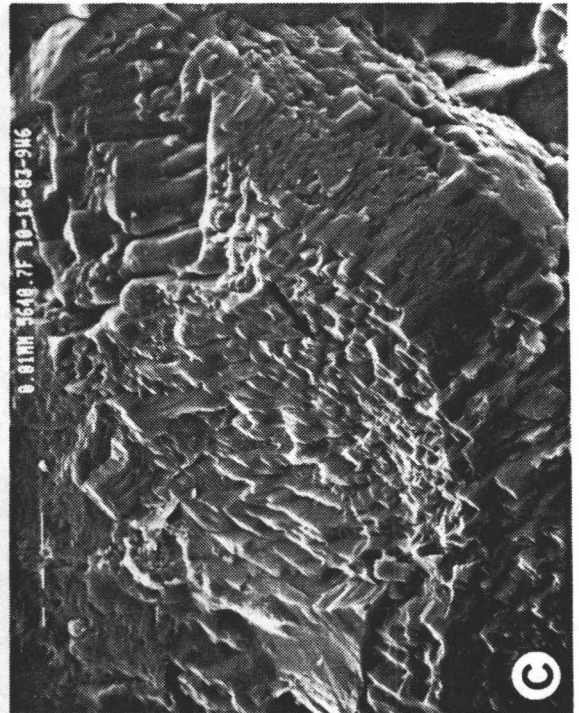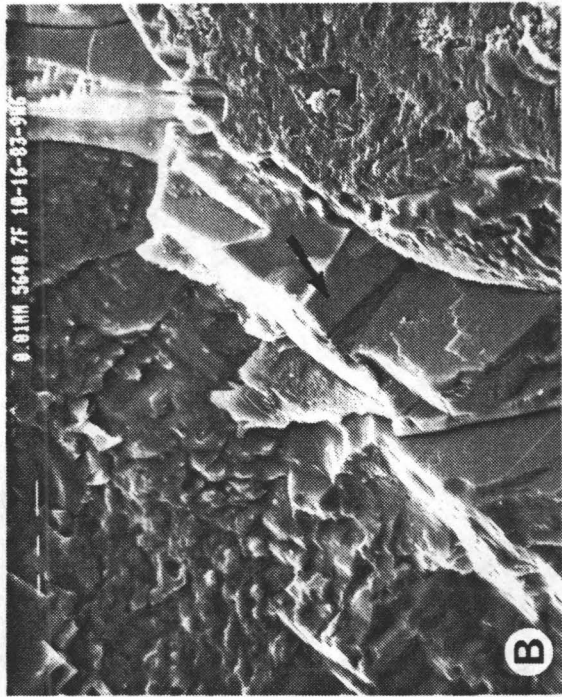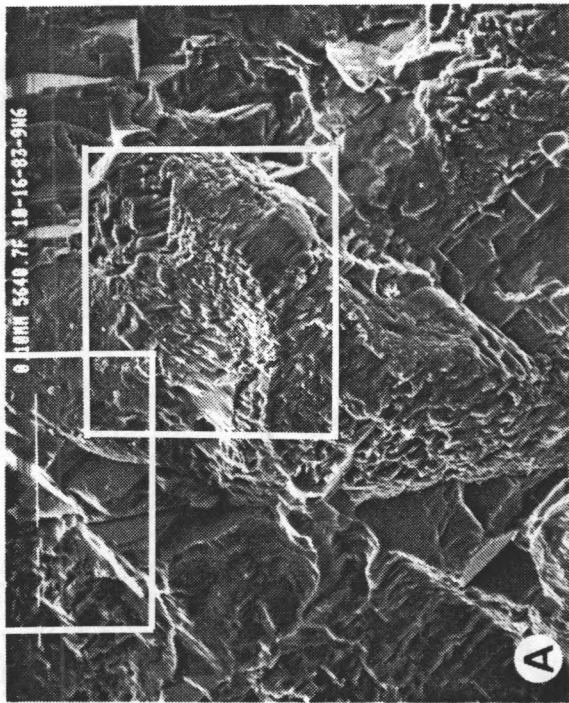
Plate 4.18   Various anthigenic pore filling materials.

4.18a and 4.18c - kaolinite

4.18b - illite

4.18d - iron rich chlorite

(4.18a - 10-3-83-10W6   6156 ft; 900 X mag.

 4.18b - 10-3-83-10W6   6156 ft; 3000 X mag.

 4.18c - 10-16-83-10W6   5640.7 ft; 1250 X mag.

 4.18d - 10-16-83-10W6   5640.7 ft; 900 X mag.)
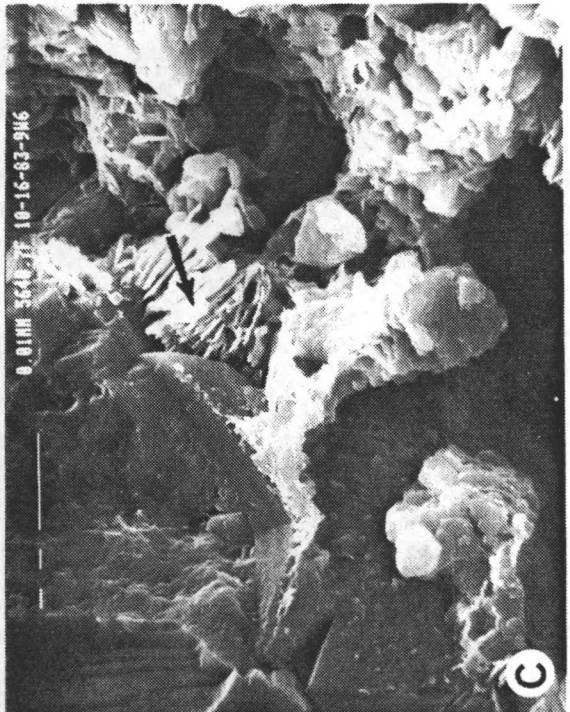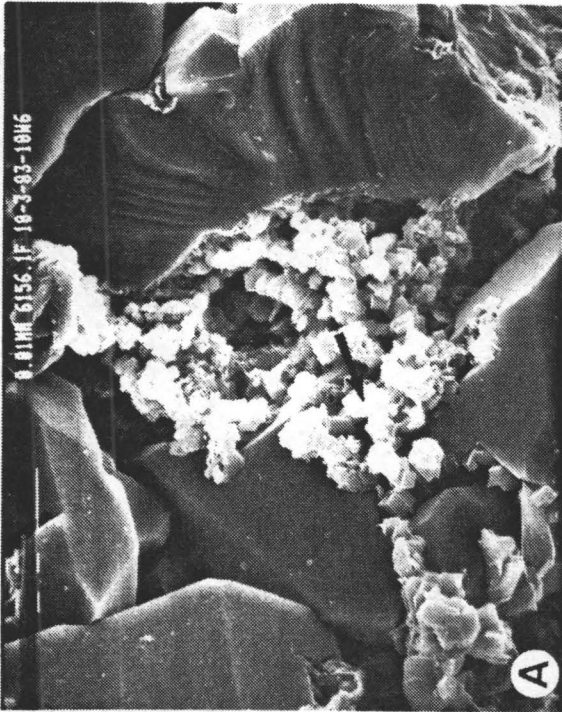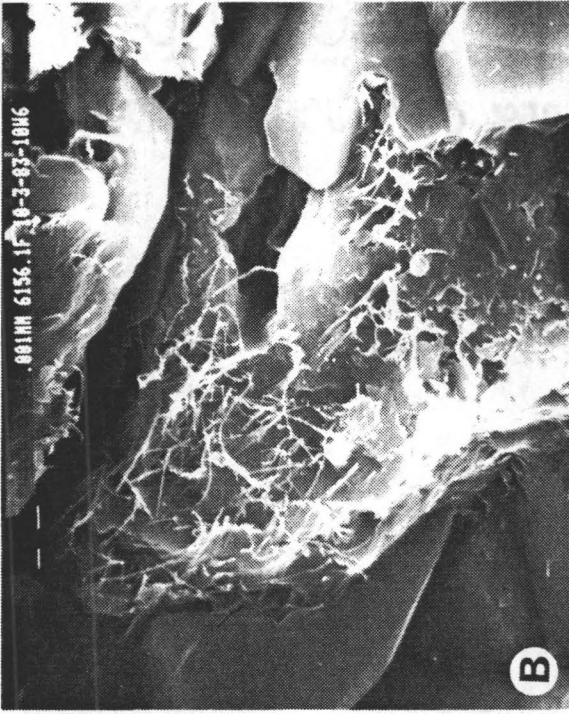
used (Friedman, 1961) to distinguish dune sands from beach and river sands. The SEM examination illustrates that the surface textures of the quartz grains are also consistent with this interpretation. The sands generally have low to moderate sphericity and therefore a preferred orientation is difficult to discern in the sand.

The sands which were interpreted to have been deposited in sub-aqueous environments are very fine-grained and well-sorted. The presence of increased clay and chlorite are the main distinguishing features of these sands, while the sand component itself is very similar in character (although fine-grained) to the sub-aerial samples. This indicates that either all the samples were derived from the same source or that the sub-aqueous sands had originally blown into the water from the shoreline.

The analysis of the type of quartz in these samples (according to Basu et al., 1975) indicated a plutonic origin for the sand. This result is supported by the luminescent colour of the quartz seen on the C.L. microscope. Therefore, the source for most of the sand in all the samples is believed interpreted to be a plutonic terrain.

The next problem in the interpretation of the samples involves the origin of the clay. In many instances clay can be seen inhibiting carbonate, quartz (Plate 4.17d), and anhydrite cement growth (Plate 4.4). In addition, the highest percentage of clays are found in facies interpreted

to be sub-aqueous in origin. Therefore, most of the clay is interpreted to be detrital in origin. However, both SEM and petrologic observations indicate that there was minor growth of authigenic clay and chlorite which lines quartz overgrowths and fills pore space (Plate 4.19). The clay was probably derived from the small amount of feldspar present in the samples.

The textural relationship of the cements helps to determine the relative timing of their precipitation. The timing of the carbonate is the hardest to prove. Carbonates are usually an early cement, and these samples exhibit a downward decrease in the amount of carbonate cement from a proposed transgressive transition into marine conditions. These facts indicate that the carbonate cement is the earliest present and probably precipitated from marine derived pore water circulating down into the sand.

The quartz cement is the second to form and has most likely precipitated from circulating silica rich pore fluids as well as silica derived from nearby pressure solution of the detrital grains. The timing of this cement can be deduced from the fact that no quartz overgrowths were dissolved by the calcite while anhydrite/gypsum dissolved both detrital grains and quartz overgrowths.

The corrosion of the quartz cement by anhydrite/gypsum indicates that the sulphate cements are later than the quartz cement. The anhydrite/gypsum must have precipitated

from circulating pore fluids but the explanation for its discontinuous occurrence is not known. As was mentioned above, minor amounts of authigenic clay then formed on the surface of grains and in pore throats.

Porosity is dominantly intergranular. Compaction and cementation has reduced primary porosity to a maximum of 16%. Intergranular porosity is only retained in quartz-cemented sands; both carbonate and anhydrite/gypsum cements essentially seal the rock. Porosity rims which were observed around some detrital grains are interpreted to have formed due to late stage removal of a protective detrital clay coating.

CHAPTER FIVE

INTERPRETATION AND CONCLUSIONS

5.1 Basal Stoddart Cross-bedded Sands

The focus of this interpretation will be on the depositional environment of the angle of repose cross-bedded sand facies. Thick sequences of cross-bedded sandstone are found in three major environments: marine, which includes tidal channels, offshore areas dominated by alongshore currents or an open shelf dominated by tidal currents; fluvial, including meandering or braided rivers; and aeolian environments.

There are several reasons why a marine interpretation of any kind would not adequately explain these sand bodies. Modern examples of thick tidal sand waves or sand ridges have been documented (Houbolt, 1968; McCave, 1971), which are composed of cross-beds having maximum angles of only 5-6 degrees on the steeper lee faces with megaripples moving down the lee sides to form compound cross-stratification. Intruding ocean currents are reworking shelf sand off Southeast Africa into dunes up to 17 metres high with 25 degree lee faces (Flemming, 1978; Flemming, 1980). However, the absence of clay in the Stoddart sands, the total absence of both bioturbation and marine fauna, and the facies associations of the cross-bedded sandstone facies, would

make a marine depositional environment of any kind very unlikely in this situation.

A dominantly fluvial system would be the next possible depositional environment of the cross-bedded sands. There is an absence, however, of many of the associated facies common in a fluvial environment such as overbank fines with root traces, and a regular fining upward sequence from cross-bedded sands to rippled sands is not present. The lack of vertical accretion deposits composed of overbank fines would not eliminate a braided river deposit in which overbank fines are less commonly deposited and only rarely preserved (Walker and Cant, 1984). The scale of the sand units described in this study (up to 26 metres observed in core) is larger than most outcrop point bar reconstructions as well as modern examples of meandering and braided deposits (examples in Walker and Cant, 1984). Subsurface studies, however, have included reconstructions of both meandering (examples in Walker and Cant, 1984) and braided fluvial systems (example in Cant, 1982) which have sand thicknesses much greater than those observed in the basal Stoddart. The fining upward response observed on the gamma-ray log in some of the Stoddart wells is a uniformly thin (7-13 metres) interval whose thickness is independent of the thickness of clean sand below. This may indicate that the process leading to the fining upward gamma-ray response is due to transgression over various thicknesses of cross-

bedded sands rather than the fining upward present in a fluvial environment. The strongest evidence against a fluvial interpretation may lie in the stratification styles present in the cross-bedded sands which will be discussed below.

The only remaining possibility for thick cross-bedded sands is an aeolian depositional environment. The interpretation of many "classic" aeolian sandstones of the western United States is based on very large scale cross-bedding (examples tabulated in Walker and Middleton, 1979) and the absence of marine fossils (Stewart and Walker, 1980). Walker and Harms (1972) also discuss a multitude of secondary characteristics such as wind generated ripples, raindrop impressions, slump scars and reptile tracks which they use to interpret the Lyons sandstone as aeolian. In addition, compositional (Glennie, 1970, p.11), textural (Ahlbrandt, 1979) and surface texture criteria (Krinsley and Doornkamp, 1973) have been used to characterize aeolian sediments. Bigarella (1972) feels that many of these latter criteria are inconclusive; however, they are valid as supporting evidence for an environmental interpretation based on other criteria. Increasingly, authors are looking to basic stratification types to characterize aeolian environments (Hunter, 1977; Kocurek and Dott, 1981) since many of these types, such as wind ripple-generated climbing

translatent strata, have characteristics unique to the
aeolian environment.

In many recent studies, the areal distribution of
stratification types has been used to determine the dune
type (Kocurek and Dott, 1981). It would not be possible to
make a similar reconstruction of the dune type in the basal
Stoddart based on the vertical distribution of
stratification styles in the cross-bedded sands since the
distinctness of cross-bedding varies tremendously and the
statification type is often indeterminant. Most of the
cross-bedded sand is planar-tabular in nature, has thin
(1.0cm) indvidual, inclined cross-beds which dip at angles
up to 25 degrees but often at angles less than this. Giant
trough cross-beds, which have been used to interpret
numerous ancient sandstones as aeolian (Stewart and Walker,
1980; Szigeti and Fox, 1981; Walker and Harms, 1972) can not
be distinguished in a three inch drill core. This large
scale of cross-bedding has not been found to be a uniquely
distinctive aeolian characteristic (Hunter, 1981). Much of
the cross-stratification in aeolian dunes. There are
indications (discussed below) that the cross-beds of the
basal Stoddart Formation are of this smaller scale. The
planar-tabular sets, together with wedge-planar sets are
types which are commonly found in formations interpreted to
be aeolian (Walker and Harms, 1972; Brookfield, 1977;
Andrews, 1981). The types of stratification which are

recognized as cross-bedded sand would be classified by Hunter (1977) as either grainfall laminae, formed by grainfall deposition in zones of flow separation, or sand flow cross-strata, formed by avalanching of noncohesive sand on dune slipfaces. The very tabular nature of the cross-beds, their intermediate dip angle and thickness as well as their sharp, non-erosional contacts indicate that most of the cross-bedded sand described from the basal Stoddart is grainfall lamination (Hunter, 1977). Although sand-flow cross-stratification was found to be the most abundant in most aeolian sandstones studied by Hunter (1981), the Lyons sandstone in one locality was found to be predominantly (80%) composed of grainfall laminae. Grainfall laminae are more common in the lower parts of small dunes rather then the lower parts of large dunes (Hunter, 1981). The thin cross-beds in the basal Stoddart, therefore may be indicative of preservation of the lower portions of small scale dunes.

The reason for most cross-beds occurring at angles less than angle of repose can be easily accounted for. The most likely part of a dune to be preserved will be the lower portion where the dips of individual cross-beds decrease well below angle of repose. In addition, a number of dune types such as seif dunes have relatively few angle of repose faces due to their method of accretion (Walker and Harms, 1972). Finally the process of post-depositional compaction

could lead to a decrease in the dips of cross-beds from 34 degrees (angle of repose) to approximately 27 degrees (Walker and Harms, 1972).

The most useful stratification type for the separation of aeolian from sub-aqueous deposits are aeolian climbing-ripple structures which have been defined by Hunter (1977) as ripple-foreset cross-laminae and climbing translatent strata. These stratification types have characteristics which are uniquely aeolian and allow for definite interpretations of ancient strata (Kocurek and Dott, 1981).

Climbing translatent strata are formed by the migration of ripples under conditions of net sedimentation, with each strata representing the movement of a single ripple under these conditions (Kocurek and Dott, 1981). Aeolian ripples form in a number of places on a dune including 1) the stoss side of dunes, 2) on the lateral edge of crescentic dunes, and 3) on the base or actual slipface of the lee side of dunes. The first occurence would rarely be preserved since the stoss side of dunes are almost never preserved (Kocurek and Dott, 1981).

The features of climbing translatent strata which characterize them as aeolian are thin, uniform, inversely graded laminae with few visible foresets and a large wavelength to height ratio. Water ripples have normally graded strata with coarser grains deposited in the troughs and abundant well developed foresets (see Figure 3 in

Kocurek and Dott, 1981). The ripples which are within sequences of cross-bedded sands of the basal Stoddart Formation have similar characteristics (see Plate 2.2b) and are believed to be subcritically climbing translatent stratification, often accompanied by ripple-foreset cross-lamination.

The final distinctive facies found within the cross-bedded sands are diffuse and concentrated clay clast conlomerate (Facies 4a and 4b). The presence of diffuse zones of angular and on occasion slightly upturned clay clasts is interpreted to be dessicated clay layers which have been transported only a short distance. Clay can be very common in wadi deposits (Glennie, 1970) and mud cracks have been used as evidence of the dessication of such features. The low percentage of clay flakes in the diffuse clay facies indicates that they do not represent the original dessicated and cracked mud layer. If this mud was dried and then transported only a short distance before being buried and preserved by wind-blown sand, it would create a deposit very similar to what is observed in the diffuse clay facies.

The concentrated clay clast conglomerate is believed to represent actual wadi deposits. Wadis deposits, in general, are formed by a sporadic and abrupt type of fluvial transport and show features of small braided stream deposits interbedded with aeolian sediments (Glennie, 1970; Kocurek,

1981). In the cross-bedded sand of the basal Stoddart, medium sized clay clasts were transported and deposited in thin, poorly sorted layers. These layers cut erosively into the aeolian strata below and often are filled in by wind-blown sand after the flow has ceased. Many wadis have been reported as interdune deposits in marginal facies, frequently adjacent to alluvial fans (Glennie, 1970; Kocurek, 1981). The scale of adjacent positive features, however, does not need to be as large as in these examples. The amount of relief which was shown to exist on surface A (up to 26 metres) could provide the necessary topography to explain the presence of wadi conglomerates.

The specific depositional area in which aeolian dune sands could occur are very numerous. These would include an inland desert as well as numerous coastal environments such as coastal dune complexes, a beach-barrier complex topped by aeolian dunes or a delta environment subjected to substantial wave energy.

Determining the correct environment from these alternatives is essentially a process of elimination. The evidence of the cross-bedded sands which was discussed in the facies sequences, as well as the lack of marginal desert facies such as significant alluvial deposits indicates that the sands were deposited in a coastal environment. The main evidence for eliminating the barrier island and delta environments is the lack of facies indicative of these

environments in close association with the cross-bedded sands. Blatt et al. (1980, p. 674) state that to prove a true barrier origin, it is necessary to show that the barrier was separated from the land by a lagoon. This separation is not indicated by the facies sequences observed in core and therefore the barrier island environment must be eliminated. A similar argument against a deltaic environment is used; no facies typical of this environment were observed associated with the cross-bedded sands making a deltaic interpretation unlikely. This leaves a coastal dune complex as the only major remaining environment.

The contour shape of isopach maps of porous section (sand) can be used to infer possible depositional environments (Miall, 1984). The variation in the thickness of the total sand sequence isopach of the basal Stoddart Formation indicates that the sands are lenticular to oval in shape. Although well control is poor around the margins of study area, this shape does resemble the regular variation in sand thickness present in areas dominated by lenticular aeolian sand bodies. These have been interpreted to represent the alternation between draa and interdraa deposits (Steele, 1983 in Collinson, 1986).

5.2 Base of Basal Stoddart Cross-bedded Sand

The cross-bedded sand of the basal Stoddart Formation rests abruptly on a sequence of marine shales and sands. This basal sequence is the first sequence which was described in Chapter Two. It represents a conformable change from shelf carbonate deposition in the Debolt Formation to clastic deposition of marine shales and minor interlaminated bioturbated mudstone and sandstone. The minor sand represents short lived pulses of coarser clastic material from the shoreface. There are no other indications of shoreface derived sands which may have been reworked in an offshore environment such as hummocky cross-stratification (described by Walker, 1984). In addition, no shoreface sand facies were seen in this lower marine sequence.

Both the cross-sections and the isopach from the datum to the base of the cross-bedded sand indicate that there has been up to 26m of erosion of the underlying marine sequence. This could be explained by at least three mechanisms; first the marker was eroded by a fluvial system; second the erosion surface represents a deflation surface formed by wind erosion; or third, normal faulting left some areas higher than others, and the highs were partially peneplaned by wind erosion before deposition of the main sands.

Evidence in support of one particular mechanism is not conclusive. The regularity of the log sequence above the

erosion surface was used in Chapter Three as evidence against the possibility of fluvial erosion but this can not be completely eliminated. Deflation could easily cause the variation in the underlying marine sequence. The scale and localized nature of the erosion is well within the scale of observed deflation hollows. An example from Al Fugaha, Libya is an almost circular hole 2-3 km in diameter and 60-70m deep (Glennie, 1970, p. 26). The largest example of a deflation hollow covers an area of 18 000 sq.km. Wind is a very effective agent of sediment removal and only slight variation in lithology or degree of cementation could lead to differential deflation (Glennie, 1970, p. 23).

Possibly the variation on the erosion surface is due to deflation on topographic highs elevated by normal faults. This might explain the asymmetry of the erosion surface, as seen on the isopach map, where the marine sequence gradually gets thinner on the southern side of the eroded area while there is a very abrupt change in thickness on the northern side. The implication of the observed thickness variation is that faults on the northern edges of the eroded areas left topographic highs which gradually decreased to the south. Differential deflation of this surface in proportion to the topographic height of the uplifted surface could lead to the observed differences in the thickness of the underlying marine shale sequence.

While no conclusion can be made concerning whether deflation occurred on topographic highs or eroded down into the sub-aerially exposed marine sequence, this erosion has several implications. First the uncertainty associated with the topographic level of the erosion surface during depostion of the cross-bedded sands supports the use of a datum in the Debolt Formation. Second, the presence of wadi deposits, which are usually associated with marginal alluvial facies within a desert, can be explained as outwash off the topographic highs created by either deflation mechanism.

5.3 Top of Basal Stoddart Cross-bedded Sand

The cross-bedded sands are overlain by variable amounts of marine shale. The rapid transgression back to marine conditions is not accompanied by identifiable shoreface facies.   There are indications, including bioturbation, layers of muddy sand and ripples of subaqueous origin, that some reworking of cross-bedded sands near the top of the sand accumulations occurred.   In other wells the return to marine conditions is very sharp with no indications of marine reworking.

This brings up the question of preservation of the majority of the cross-bedded sands and the variable amount of reworking observed at the top of the cross-bedded sands.

The preservation of aeolian sands is based on three factors: the original thickness of the sands; the amount of early cementation; and the nature of the transgressing sea. Glennie (1970, p.9) illustrates an example of early carbonate-cemented sands which form along the coastline protecting underlying uncemented sand from marine reworking during a transgression. In addition a sea will only regularly rework sediment down to wave base, so that a rapidly transgressing, relatively quiet sea will rework only a minimum of sand and the reworked sediment would protect the underlying sand. Examples from the Lower Permian Yellow Sands of northeastern England indicate that only the upper 1-2 metres of the sand show signs of aqueous reworking (Smith and Pattison, 1970 in Collinson, 1986). Therefore there are processes which would allow preservation of most of the aeolian sands present in the basal Stoddart Formation, as well as providing a possible explanation for the minimal reworking of the sands and lack of shoreface sub-aqueous facies.

The rapid sea level fluctuations envisioned to explain the sharp contacts between marine and continental deposits could be caused by one of at least two processes, or possibly a combination of both. The first would be relatively large vertical movements in the Peace River arch area along normal faults which were active on a regional scale through Mississippian and Pennsylvanian time

(Sikabonyi and Rodgers, 1959). The second process would be sea level changes caused by the onset and/or fluctuations in the Pennsylvanian and Permian glaciation of Gondwanaland (Stewart and Walker, 1980). The dating of the start of this glaciation has large margins of uncertainty and may have extended back to the Late Mississippian.

5.4 Other Coarse Clastic Deposits in the Basal Stoddart

A second type of coarse clastic deposit is present in the basal Stoddart and consists of the third sequence described in Chapter Two. It must be stressed that this sequence is distinctly separate from the cross-bedded sand sequence and they do not appear to grade directly into each other either vertically or laterally. On the gamma ray log this sequence is present as a coarsening upward profile and consists of a conformable transition from marine shale to interlaminated bioturbated mudstone and sandstone to bidirectionally rippled sandstone and in one core was observed to change to a bioturbated sand at the top of the sequence.

The coarsening upward sequence is observed on petrophysical logs over most of the study area. It is a distinct unit unrelated to the cross-bedded sand facies and is separated from the cross-bedded sands by a variable thickness of marine shale. Where the cross-bedded sands are

not present, this sequence is the first coarse clastic deposit in the basal Stoddart. Where the cross-bedded sands are very thick, this sequence can not be positively identified above them.

The facies which are present in this sequence are very similar to those of a tidal flat deposit in which flaser, lenticular and wavy bedding are very common (Elliot, 1986). The vertical coarsening upward sequence, however, is the opposite to what is expected in a prograding tidal flat environment (Klein, 1985). Similar facies to those found in this sequence may also be found in other areas such as the deltaic environment. In addition the coarsening (sanding) upward sequence is very common in a prograding delta front. An example of a prograding tide-dominated delta with similar facies to those found in the Stoddart Formation is given by Elliot (1986, p. 133).

The emphasis of this chapter is on the interpretation of the cross-bedded sand facies, with considerably less space devoted to the discussion of the other coarse clastic deposits. The interpretation of these deposits is limited to: 1) the recognition that they represent a wide-spread regressive sequence changing from offshore deposits to ones which were deposited in much closer proximity to the shoreline and; 2) the short discussion found above of the environments where this sequence might occur.

5.5 Conclusions

1. The basal sands of the Stoddart Formation which possess a blocky gamma-ray profile are dominantly of aeolian origin. This conclusion is primarily based on the internal stratification styles within the cross-bedded sands. The basal sands form a coastal dune complex. The lack of associated facies expected in barrier-beach and wave-dominated deltaic environments eliminate these possibilities as the depositional site.

It is recommended that any future facies studies of this unit use extensive examination of the stratification styles within the cross-bedded sand to delineate any fluvial or marine influences which may be present in these sands.

2. The petrographic examination of the cross-bedded sand indicates that it has all the compositional and textural parameters which have been used to characterize aeolian sediments by previous authors. It is recognized that these parameters show wide variability within aeolian environments and are used in this study only as supporting evidence in the interpretation of the cross-bedded sands. In addition the surface textures of the quartz grains support the interpretation of an aeolian environment.

3. The surface on which the cross-bedded sand is deposited is believed to represent a sub-aerial erosion surface. A wind-eroded deflation surface is felt to better explain the meagre available evidence. The presence of

possible normal faults along the edges of the most intense erosion is proposed but the scarcity of data does not permit a final conclusion.

4. The swift changes from offshore marine to continental environments with no indications of shoreface facies between them indicate sudden relative sea level fluctuations and rapid shoreline progradation and regression. The cause of the relative sea level change is most likely related to vertical movement along faults in the Peace River arch area and is possibly augmented by glacially induced sea level fluctuations.

REFERENCES

AHLBRANDT, T.S., 1979, Textural parameters of eolian deposits: in McKee, E.D., ed., A Study of Global Sand Seas. United States Geological Survey Professional Paper 1052, p. 21-51.

ANDREWS, S., 1981, Sedimentology of Great Sand Dunes, Colarado: Society of Economic Paleontologists and Mineralogists, Special Publication 31, p. 279-291.

BASU, A., YOUNG, S.W., SUTTNER, L.J., JAMES, W.C. and MACK, G.H., 1975, Re-evaluation of the use of undulatory extinction and polycrystallinity in detrital quartz for provenance interpretation: Jour. Sed. Petrology, v.45, p. 873-882.

BIGARELLA, J.J., 1972, Eolian environments: their characteristics, recognition and importance: in Rigby, J.K., and Hamblin, W.K., eds., Recognition of Ancient Sedimentary Environments, Society of Economic Paleontologists and Mineralogists, Special Publication 16, p. 12-16.

BLATT, H., MIDDLETON, G.V., and MURRAY, R.C., 1980, Origin of Sedimentary Rocks, Prentice-Hall, Englewood Cliffs, 782p.

BROOKFIELD, M.E., 1977, The origin of bounding surfaces in ancient aeolian sandstones: Sedimentology, v.24, p. 303-332.

CANT, D.J., 1982, Fluvial facies models and their application: in Scholle, P.A and Spearing, D., eds., Sandstone Depositional Environments, Am. Assoc. Petroleum Geologists, Memoir 31, p. 115-137.

COLLINSON, J.D., 1986, Deserts: in Reading, H.G., ed., Sedimentary Environments and Facies, Blackwell, p. 95-154.

DALRYMPLE. R.W., 1977, Sediment dynamics of macrotidal sand bars, Bay of Fundy, Unpubl Ph.D thesis, McMaster University, 635p.

ELLIOT, T., 1986, Siliciclastic shorelines: in Reading, H.G., ed., Sedimentary Environments and Facies, Blackwell, p. 155-188.

FLEMMING, B.W., 1978, Underwater sand dunes along the southeast African continental margin - observation and implications: Marine Geology, v.26, p. 177-198.

_____, 1980, Sand transport and bedform patterns on the Continental Shelf between Durban and Port Elizabeth (southeast Africa continental margin): Sedimentary Geology, v.26, p. 179-205.

FOLK, R.L., 1968, Petrology of Sedimentary Rocks. Hemphill Publishing Co., Austin, Texas, 182p.

_____ and WARD, W.C., 1957, Brazos River bar: A study in the significance of grain size parameters: Jour. Sed. Petrology, v.27, p. 3-27.

FRIEDMAN, G.M., 1961 Distinction between dune, beach and river sands from their textural characteristics: Jour. Sed. Petrology, v.31, p. 514-529.

GLENNIE, K.W., 1970, Desert Sedimentary Environments, Amsterdam, Elsevier, 222p.

HALBERTSMA, H.L., 1959, Nomenclature of Upper Carboniferous and Permian strata in the subsurface of the Peace River area: Alta. Soc. Petroleum Geologists Jour., v.7, p. 109-118.

_____, 1961, Floral Group, a new rock unit for Chester and probable Chester strata in the Peace River area: Alta. Soc. Petroleum Geologists Jour., v.9, p. 270-272.

_____ and STAPLIN, F.L., 1960, The Mississippian-Pennsylvanian boundary from the Peace River area to the Williston basin: Alta. Soc. Petroleum Geologists Jour., v.8, p. 363-373.

HOUBOULT, J.J.H.C., 1968, Recent sediments in the southern bight of the North Sea: Geologie en Mijnbouw, v.47, p. 245-273.

HUNTER, R.E., 1977, Basic stratification styles in small eolian dunes: Sedimentology, v.24, p. 361-387.

HUNTER, R.E., 1981, Stratification styles in eolian sandstones: some Pennsylvanian to Jurassic examples from the western interior U.S.A; Society of Economic Paleontologists and Mineralogists, Special Publication 31, p. 315-329.

KLEIN, G.DeV., 1985, Intertidal flats and intertidal sand bodies: in Davis, R.A.; ed., Coastal Sedimentary Environments, Springer-Verlag, p. 187-224.

KOCUREK, G., 1981, Erg reconstruction: the Entrada Sandstone (Jurassic) of northern Utah and Colarado: Paleogeography, Paleoclimatology, Paleoecology, v.36, p. 125-153.

_____, and DOTT, R.H., 1981, Distinctions and uses of stratification types in the interpretation of aeolian sand: Jour. Sed. Petrology, v.51, p. 579-595.

KRINSLEY, D.H. and DOORNKAMP, J.C., 1973, Atlas of Quartz Sand Surface Textures, University Press, Cambridge, 91p.

LAVOIE, D.H., 1958, The Peace River arch during Mississippian and Permo-Pennsylvanian time: Alta. Soc. Petroleum Geologists Bull., v.6, p. 69-74.

LEVANDOWSKI, D.W., KALEY, M.E., SILVERMAN, S.R. and SMALLEY, R.G., 1973, Cementation in the Lyons sandstone and its role in oil accumulation, Denver Basin, Colarado: Amer. Assoc. Petroleum Geologists Bull., v.57, p. 2217-2244.

MACAULEY, G., 1958, Late Paleozoic of the Peace River area, Alberta: in Goodman, A.J., ed., Jurassic and Carboniferous of Western Canada-a symposium, Am. Assoc. Petroleum Geologists, John Andrew Allan Memorial Volume, p. 289-308.

_____, PENNER, D.G., PROCTER, R.M. and TISDALL, W.H., 1964, Carboniferous: in McCrossan, R.G. and R.P. Glaister, eds., Geol. History of Western Canada, Alta. Soc. Petroleum Geologists, p. 89-102.

MCCAVE, I.N., 1971, Sand Waves in the North Sea off the Coast of Holland: Marine Geology, v.10, p. 199-225.

MCGUGAN, A., and RAPSON, J.E., 1963, Permo-Carboniferous stratigraphy between Banff and Jasper, Albera: Bull. Canadian Petroleum Geologists, v.10, p. 352-368.

MIALL, A.D., 1984, Deltas: in Walker, R.G., ed., Facies Models, Geological Association of Canada, Geoscience Canada Reprint Series, v.1, p. 105-118.

MIDDLETON, G.V., 1962, Size and sphericity of quartz grains in two turbidite formations: Jour. Sed. Petrology, v.32, p. 725-742.

MONGER, J.W.H., SOUTHER, J.G. and GABRIELESE, H., 1972, Evolution of the Canadian Cordillera: a plate-tectonic model: Amer. Jour. Sci., v.272, p. 577-602.

PATTON, W.J.H., 1958, Mississippian in the South Nahanni River area, Northwest Territories: in Goodman, A.J., ed., Jurassic and Carboniferous of Western Canada-a symposium: John Andrew Allan Memorial Volume, p. 309-326.

RUTGERS, A.T.C., 1958, Stoddart Formation of northeast British Columbia: in Goodman, A.J., ed., Jurassic and Carboniferous of Western Canada-a symposium, Am. Assoc. Petroleum Geologists, John Andrew Allan Memorial Volume, p. 327-330.

SCOTT, D.L., 1964, Stratigraphy of the Lower Rocky Mountain Supergroup in the Southern Canadian Rocky Mountains: Unpubl. Ph.D. Thesis, Univ. of British Columbia, 133p.

SIBLEY, D.F. and BLATT, H., 1976, Intergranular pressure solution and cementation of the Tuscarora Orthoquartzite: Jour. Sed. Petrology, v.46, p. 881-896.

SIKABONYI, L.A. and RODGERS, W.J., 1959, Paleozoic tectonics and sedimentation in the northern half of the west Canadian basin: Alta. Soc. Petroleum Geologists Jour., v.7, p. 193-216.

STEWART, W.D., 1978, Pennsylvanian shallow marine and aeolian sediments, Tyrwhitt, Storelk and Tobermory Formations of southeastern British Columbia: Unpubl. MSc. Thesis, McMaster Univ., 277p.

STEWART, W.D., and WALKER, R.G., 1980, Eolian coastal dune deposits and surrounding marine sandstones, Rocky Mountain Supergroup (Lower Pennsylvanian), southeastern British Columbia: Canadian Journal of Earth Sciences, v.17, p. 1125-1140.

SZIGETI, G.J., and FOX, J.E., Unkpapa Sandstone (Jurassic), Black Hills, South Dakota: an eolian facies of the Morrison Formation: Society of Economic Paleontologists and Mineralogists, Special Publication 31, p. 331-349.

TUCKER, M.E., 1981, Sedimentary Petrology-An Introduction, Blackwell Scientific Publications, Oxford, 252p.

WALKER, R.G., 1984, Shelf and shallow marine sands: in Walker, R.G., ed., Facies Models, Geological Association of Canada, Geoscience Canada Reprint Series, v.1, p. 141-170.

_____, and CANT, D.J., 1984, Sandy fluvial system: in Walker, R.G., ed., Facies Models, Geological Association of Canada, Geoscience Canada Reprint Series, v.1, p. 71-89.

_____, and MIDDLETON, G.V., 1979, Eolian sands: in Walker, R.G., ed., Facies Models, Geological Association of Canada, Geoscience Canada Reprint Series, v.1, p. 33-41.

WALKER, T.R., and HARMS, J.C., 1972, Eolian origin of flagstone beds, Lyons Sandstone (Permian), type area, Boulder County, Colarado: The Mountain Geologist, v.9, p. 279-288.

ZINGERNAGEL, U., 1978, Cathodoluminescence of quartz and its application to sandstone petrology: Contributions to Sedimentology, No. 8, E. Schweizerbartsche Verlagsbuchhandlung, Stuttgart, 69p.